

---

SYSTEMATIC REVISION OF THE ARBOREAL  
NEOTROPICAL "*THORELLII*" CLADE OF  
*CENTRUROIDES* MARX, 1890, BARK SCORPIONS  
(BUTHIDAE C.L. KOCH, 1837) WITH  
DESCRIPTIONS OF SIX NEW SPECIES

---

AARON M. GOODMAN, LORENZO PRENDINI,  
OSCAR F. FRANCKE AND LAUREN A. ESPOSITO



BULLETIN OF THE AMERICAN MUSEUM OF NATURAL HISTORY

SYSTEMATIC REVISION OF THE ARBOREAL  
NEOTROPICAL “THORELLII” CLADE OF  
*CENTRUROIDES* MARX, 1890, BARK SCORPIONS  
(BUTHIDAE C.L. KOCH, 1837) WITH  
DESCRIPTIONS OF SIX NEW SPECIES

AARON M. GOODMAN

*Graduate School and University Center, City University of New York;  
Division of Invertebrate Zoology, American Museum of Natural History;  
Institute for Biodiversity Science and Sustainability, California Academy of Sciences*

LORENZO PRENDINI

*Arachnology Lab and Scorpion Systematics Research Group,  
Division of Invertebrate Zoology, American Museum of Natural History*

OSCAR F. FRANCKE

*Colección Nacional de Arácnidos, Departamento de Zoología,  
Instituto de Biología, Universidad Nacional Autónoma de México*

LAUREN A. ESPOSITO

*Graduate School and University Center, City University of New York;  
Division of Invertebrate Zoology, American Museum of Natural History;  
Institute for Biodiversity Science and Sustainability, California Academy of Sciences*

BULLETIN OF THE AMERICAN MUSEUM OF NATURAL HISTORY

Number 452, 92 pp., 43 figures, 10 tables

Issued September 16, 2021

## CONTENTS

Abstract .....	3
Introduction .....	3
Materials and Methods .....	4
Systematics .....	6
Family Buthidae C.L. Koch, 1837 .....	6
Subfamily Centruroidinae Kraus, 1955 .....	6
<i>Centruroides</i> Marx, 1890 .....	6
Key to Identification of the Species of the “ <i>thorellii</i> ” clade of <i>Centruroides</i> Marx, 1890 ..	7
<i>Centruroides berstoni</i> , sp. nov.....	8
<i>Centruroides catemacoensis</i> , sp. nov.....	15
<i>Centruroides chanae</i> , sp. nov.....	22
<i>Centruroides cuauhmapan</i> , sp. nov.....	33
<i>Centruroides hamadryas</i> , sp. nov.....	41
<i>Centruroides hoffmanni</i> Armas, 1996 .....	53
<i>Centruroides rileyi</i> Sissom, 1995 .....	56
<i>Centruroides schmidti</i> Sissom, 1995.....	61
<i>Centruroides yucatanensis</i> , sp. nov.....	70
Acknowledgments.....	76
References.....	77
Appendix 1.....	84
Appendix 2.....	86
Appendix 3.....	91

## ABSTRACT

The arboreal Neotropical “*thorellii*” clade of *Centruroides* Marx, 1890, bark scorpions (Buthidae C.L. Koch, 1837) is revised, using a novel approach to species delimitation. A phylogenetic analysis, based on 112 morphological characters and 1078 aligned DNA nucleotides from the mitochondrial Cytochrome c Oxidase Subunit I (COI) gene, provided the framework for placing singletons from geographically disparate localities (and often with suboptimal preservation) using COI minibarcodes, thereby enlarging the taxon sample for diagnosis and delimitation of morphological species. Six new species are described, tripling the known diversity in the clade to nine: *Centruroides berstoni*, sp. nov.; *Centruroides catemacoensis*, sp. nov.; *Centruroides chanae*, sp. nov.; *Centruroides cuauhapan*, sp. nov.; *Centruroides hamadryas*, sp. nov.; *Centruroides yucatanensis*, sp. nov. Revised diagnoses are presented for *Centruroides hoffmanni* Armas, 1996, *Centruroides rileyi* Sissom, 1995, and *Centruroides schmidti* Sissom, 1995. Comparative images, a key and distribution maps for all species of the clade are provided, along with a summary of available data for their ecology.

## INTRODUCTION

The Yucatan/Chortis “*thorellii*” clade is one of three clades recently identified in the diverse Neotropical bark scorpion genus *Centruroides* Marx, 1890 (Buthidae C.L. Koch, 1837), based on a phylogenetic analysis of morphological characters and DNA sequences from two nuclear and three mitochondrial gene loci (Esposito and Prendini, 2019). All species of the clade are arboreal and corticolous (Prendini, 2001a), some having been collected 3–15 m above ground in the forest canopy (Goodman and Esposito, 2020; fig. 1). These cryptic scorpions are characterized by relatively small size, mottled coloration and an elongated metasoma and telson, more pronounced in the adult male.

Three species of the clade, i.e., *Centruroides hoffmanni* Armas, 1996, *Centruroides rileyi* Sissom, 1995, and *Centruroides schmidti* Sissom, 1995, were originally assigned together with *Centruroides thorellii* (Kraepelin, 1891) and three other species, *Centruroides chamulaensis* Hoffmann, 1932, *Centruroides tuxtla* Armas, 1996, and *Centruroides sissomi* Armas, 1996, to the informal *thorellii* species group of *Centruroides* based on their similar morphology, habitat and distribution in the forests of southern Mexico and northern Central America (Armas, 1996; Hoffmann, 1932; Martin-Frías et al., 2005; Sissom, 1995; Ponce-Saavedra and Moreno-

Barajas, 2005). Esposito and Prendini (2019) demonstrated that the *thorellii* species group was a paraphyletic assemblage, however. Members of the former *thorellii* group dissociated into three clades, in two cases grouping with morphologically disparate species, suggesting the apparent morphological similarity among species of the *thorellii* group is convergent. *Centruroides tuxtla* grouped with a clade of predominantly striped species, including the type species of *Centruroides*, *Centruroides exilicauda* Wood, 1863, whereas *C. chamulaensis* and *C. “thorellii”* grouped with a clade of large, dark species, e.g., *Centruroides gracilis* Latreille, 1804. The remaining species of the *thorellii* group formed a distinct clade.

The limits of several species formerly assigned to the *thorellii* group of *Centruroides* are similarly confused. For example, the redescription of *C. hoffmanni* by Martin-Frías et al. (2005) appears to be based on specimens that are not conspecific with the types but rather with a sympatric species of *Centruroides* (Esposito, 2011), whereas most reports of *C. sissoyi* that appeared after the original description (Vázquez, 1999; Teruel et al., 2015a; Ponce-Saavedra and Francke, 2019) are misidentifications of a hitherto undescribed, sympatric species of the “*thorellii*” clade, described herein.

Problems concerning the taxonomy of these scorpions may, in part, be explained by the com-

parative scarcity of material in collections. Many collection records are represented by singletons, often females or immatures, and the difficulty of collecting these canopy-dwelling scorpions appears to have resulted in severe undersampling of their known diversity and distribution.

Six operational taxonomic units (OTUs) were previously identified within the “*thorellii*” clade on the basis of DNA sequence data (Esposito, 2011). However, insufficient material prevented a decision as to whether the OTUs were distinct species or variable populations of more widespread species. A larger sample of specimens from across the geographical distribution, needed for a robust assessment of species limits within the genus, was hampered by degraded genetic material within museum specimens. In order to overcome this limitation, a novel approach to species delimitation was applied by Goodman et al. (2021). A phylogenetic analysis, based on 112 morphological characters and 1078 aligned DNA nucleotides from the mitochondrial cytochrome *c* oxidase subunit I (COI) gene, provided the framework for placing singletons from geographically disparate localities (and often suboptimally preserved) using COI minibarcodes, thereby enlarging the taxon sample for adequate diagnosis and delimitation of morphological species.

The present contribution implements the taxonomic discoveries of Goodman et al. (2021). The six OTUs originally identified by Esposito (2011) are described as new species, tripling the known diversity in the clade to nine (table 1): *Centruroides berstoni*, sp. nov.; *Centruroides catemacoensis*, sp. nov.; *Centruroides chanae*, sp. nov.; *Centruroides cuauhmapan*, sp. nov.; *Centruroides hamadryas*, sp. nov.; *Centruroides yucatanensis*, sp. nov. Revised diagnoses are presented for *Centruroides hoffmanni* Armas, 1996, *Centruroides rileyi* Sissom, 1995, and *Centruroides schmidti* Sissom, 1995. Comparative images, a key and distribution maps for all species of the clade are provided, along with a summary of available data for their ecology.

## MATERIAL AND METHODS

Specimens collected by the authors were located at night using ultraviolet (UV) light detection, preserved by submersion in 95% ethanol and subsequently injected with ethanol to improve internal preservation. Additional material, in most cases singletons, was sourced from natural history collections. Material is deposited in the American Museum of Natural History (AMNH), New York; the California Academy of Sciences (CAS), San Francisco; the Colección Nacional de Arácnidos (CNAN), Instituto de Biología, Universidad Nacional Autónoma de México, Mexico City; the Field Museum of Natural History (FMNH), Chicago; the Florida State Collection of Arthropods (FSCA), Gainesville; Northern Arizona University (NAU), Flagstaff; the Oxford University Museum of Natural History (OUMNH), U.K.; and the United States National Museum of Natural History (USNM), Smithsonian Institution, Washington, DC. Tissue samples used for DNA isolation are stored (in the vapor phase of liquid nitrogen at -150°C) in the Ambrose Monell Collection for Molecular and Microbial Research (AMCC) at the AMNH, and the Center for Comparative Genomics at the CAS (appendix 1).

Specimen provenance data from the material examined were digitized. All records of sufficient accuracy were isolated from the material examined and published literature to create a point-locality geographical dataset for mapping distributional ranges. Distribution maps were produced using ArcView GIS Version 10.4 (Environmental Systems Research Institute, Redlands, CA). Raster-based elevational maps, and vector-based political boundaries of countries were acquired from DIVA-GIS v1.4.

Morphological examination of specimens was conducted using a Leica M125 stereomicroscope. Measurements (in millimeters) were recorded using an ocular micrometer calibrated at 10× magnification. Measurements follow Stahnke (1970), Lamoral (1979), and Prendini (2001b). Nomenclature of general anatomy follows Hjelle (1990) and Sissom (1990), except for carination of the carapace, ter-

TABLE 1

**Species of the arboreal Neotropical scorpion “*thorellii*” clade of *Centruroides* Marx, 1890, bark scorpions, with countries, and departments or states in which recorded**

Species	Country	State/Department
<i>Centruroides berstoni</i> , sp. nov.	Guatemala	Izabal
<i>Centruroides catemacoensis</i> , sp. nov.	Mexico	Veracruz
<i>Centruroides chanae</i> , sp. nov.	Mexico	Guerrero, Michoacán
<i>Centruroides cuauhmapan</i> , sp. nov.	Mexico	Oaxaca, Veracruz
<i>Centruroides hamadryas</i> , sp. nov.	Mexico	Chiapas
<i>Centruroides hoffmanni</i> Armas, 1996	Mexico	Chiapas
<i>Centruroides rileyi</i> Sissom, 1996	Mexico	Puebla, Tamaulipas, San Luis Potosí, Veracruz
<i>Centruroides schmidti</i> Sissom, 1995	Guatemala	El Progreso, Zacapa
	Honduras	Atlántida, Cortés, Francisco Morazán, Islas del Bahía
<i>Centruroides yucatanensis</i> , sp. nov.	Mexico	Quintana Roo, Yucatán

gites and metasoma, which follows Vachon (1952), trichobothria, which follows Vachon (1974), pedipalp carination, which follows Prendini (2000a), book lung structure, which follows Kamenz and Prendini (2008), and ovariuterine anatomy, which follows Volschenk et al. (2008).

Photographs were taken in visible light using a Canon EOS Camera with MP-E 65 mm or 100 mm EF macrolenses, and under long wave UV light using a Microptics™ ML-1000 digital imaging system, or Leica SMZ-800 stereomicroscope equipped with a Leica MZ16 A camera, and LED-6WD UV spotlight. Focal planes of image stacks were fused using Leica LAS image stacking program and edited with Adobe Photoshop.

Genomic DNA was extracted from muscle tissue from the fourth leg of the best preserved specimens using the spin column extraction protocol of the Qiagen DNeasy Blood and Tissue Kit (Valencia, CA). PCR amplification of complete mitochondrial and nuclear genes proved impossible for many older museum samples, due to degradation and fragmentation of the DNA. Therefore, a 125 base-pair (bp) hypervariable region of the cytochrome *c* oxidase subunit I (COI) gene was partially amplified (Meusnier et al., 2008). Newly generated sequences were edited, forward and reverse primers removed, and complementary strands assembled into con-

sensus sequences using Geneious v. 11.0.4 (Kearse et al., 2012), by reference to a 1078 bp fragment of COI for *C. rileyi* from GenBank (Esposito and Prendini, 2019). Sequences less than 150 base pairs in length were deposited in the Dryad digital repository (doi: 10.5061/dryad.fttdz08t2), the rest in GenBank (appendix 1).

Adults of specimens from which DNA sequences were generated, were scored using relevant characters from an unpublished morphological character matrix by Esposito (2011), comprising characters from published (Esposito et al., 2017) and unpublished sources (appendix 2). The data matrix comprises 112 characters comprising 43 (35%) from the prosoma, 38 (33%) from the mesosoma, and 30 (29%) from the metasoma; 41% of the characters were derived from carination and surface macrosculpture, 25% from shape and morphometrics, 24% from coloration, and 7% from other character systems, e.g., macrosetae, trichobothria, and internal anatomy (appendix 3). The matrix is deposited in Morphobank (<http://morphobank.org/permalink/?P4047>).

Sequences were aligned using the ClustalW method (Larkin et al., 2007; Thompson et al., 1994) in Mesquite v. 3.51 (Maddison and Maddison, 2018), and checked by eye. Evolutionary relationships were inferred with a simultane-

ous phylogenetic analysis of the molecular and morphological datasets using Bayesian inference (BI) in MrBayes v. 4.3.6 (Ronquist and Huelsenbeck, 2003) and maximum likelihood (ML) using RAxML v. 8.0.0 (Stamatakis, 2014) on the CIPRES supercomputing cluster (Miller et al., 2009).

The limits of putative species were evaluated on the majority-rule consensus tree from the Bayesian 95% posterior probability of the concatenated dataset of morphological characters and aligned DNA sequences using the species delimitation plugin in Geneious (Kearse et al., 2012; Masters et al., 2011). Clusters of sequences were evaluated based on their association with individuals collected at the type locality. Specimens that were monophyletic with those collected at the type locality or within its vicinity with greater than 0.95 posterior probability were considered conspecific and assigned to the species in question. Several metrics were investigated for assessing species delimitation in Geneious, including P (AB) for reciprocal monophyly (Rosenberg, 2007), P (RD) which measures the probability of an observed clade's degree of distinctiveness (Rodrigo et al., 2008), and values for the probability of population identification of a hypothetical sample based on the groups being tested, P ID (Strict), and P ID (Liberal).

Phylogenetic analysis with BI and ML produced almost identical tree topologies with terminal nodes well supported, but basal and internal nodes weakly supported. Nine well-supported, reciprocally monophyletic species-level clades were recovered in both analyses, but relationships within each clade received low support. *Centruroides hoffmanni*, *C. rileyi*, and *C. schmidti* were each monophyletic and received high posterior probabilities and likelihood values (0.99/100, 0.95/1.00, and 0.99/100 respectively). *Centruroides thorelli* and *C. tuxtla* were not monophyletic with the rest of the “*thorelli*” clade (fig. 2), confirming the results of Esposito and Prendini (2019). The six new species described herein were monophyletic and well supported: *C. berstoni* (0.99/99); *C. catemacoensis* (1.00/100); *C. chanae* (1.00/100); *C. cuauh-*

*mapan* (0.99/100), *C. hamadryas* (0.98/82); *C. yucatanensis* (1.00/100). Species-delimitation analysis identified nine distinct species, all of which received values for Rosenberg's P (AB) less than 0.01, supporting the results of the BI and ML analyses. A more detailed explanation of the methods and results of the phylogenetic analyses is provided by Goodman et al. (2021).

## SYSTEMATICS

Family Buthidae C.L. Koch, 1837

Subfamily Centruroidinae Kraus, 1955

*Centruroides* Marx, 1890

Figures 1–43; tables 1–10

*Centrurus* (nec Ehrenberg, 1829): Thorell, 1876a: 9; 1876b: 83; Karsch, 1879a: 18; Pocock, 1890: 120, 121, 127; Kraepelin, 1891: 119–124 (part); Pocock, 1893: 375, 385, 386; Laurie, 1896: 131; Lönnberg, 1897: 196, 197, 208; Kraepelin, 1899: 87 (part); Banks, 1900: 425; Borelli, 1909: 222; Comstock, 1912: 25, 27, fig. 31; Birula, 1917a: 164; 1917b: 54, 107; Ochoterena, 1920: 223; Mello-Campos, 1924a: 246; 1924b: 312; Comstock, 1940: 27, fig. 31 (lapsus calami); Millot and Vachon, 1949: 427; Díaz Nájera, 1966: 110, 111, pl. 1; 1970: 113.

*Centruro*: Karsch, 1879b: 120 (lapsus calami).

*Centruroides* Marx, 1890: 211, type species *Buthus exilicauda* Wood, 1863 (= *Centruroides exilicauda* (Wood, 1863), by monotypy; Pocock, 1902a: 19, 20; 1902b: 365; Kraepelin, 1912: 69–71; 1914: 22; Hoffmann, 1932: 244, 245; Mello-Leitão, 1932: 27; 1934: 4, 5; Franganillo, 1936: 158; Hoffmann, 1937: 201–203; Moreno, 1939: 63; Comstock, 1940: 25, 27; Moreno, 1940: 164; Mello-Leitão, 1942: 126; 1945: 240, 250–252; Scorza, 1954: 190; Bücherl, 1964: 59; 1967: 113; Muma, 1967: 2, 4; Bücherl, 1969: 767; Aguilar and Meneses, 1970: 3; Bücherl, 1971: 327; Stahnke, 1971: 282; 1972: 125, fig. 9; Armas, 1974a: 25; Vachon, 1974: 906, 908;

- 1975: 1598; Francke, 1977: 75; Stahnke and Calos, 1977: 111; Vachon, 1977: 294; Lourenço, 1979: 214; Williams, 1980: 2, 4; Armas, 1984: 2; González-Sponga, 1984: 64, 65; Francke, 1985: 7, 15; Francke and Stockwell, 1987: 7; Armas, 1988: 44, 91, 95; Stockwell, 1988: 3; Sissom, 1990: 94, 101; Nenilin and Fet, 1992: 9, 12–14; Stockwell, 1992: 412, 419; González-Sponga, 1996: 118, 119, 124, 125, figs. 285–287, 289, 292; Armas, 1998: 50; Kovařík, 1998: 106; Fet and Lowe, 2000: 98–122; Towler et al., 2001: 161–163; Armas et al., 2004: 167–171, tables 1–3; Prendini and Wheeler, 2005: 481, table 10; Kamenz and Prendini, 2008: 6, 8, 22, 40, tables 1, 2, pl. 13–17; Volschenk et al., 2008: 654, 656, 658, 659, 663, 664, 674, fig. 1C, tables 1, 2; Armas et al., 2012: 106, 112; Cupitra Vergara et al., 2014: 207–215, figs. 1–4, tables 1, 2; Kovařík and Teruel, 2014: 1, 7, 15, 25, 26; Loria and Prendini, 2014: 3, 9, 10, 24, 25, fig. 2D, table 5; Lourenço, 2014: 60, 63; Miller et al., 2014: 301, 306, 307, table 1; Ponce-Saavedra and Francke, 2014: 54, figs. 11, 14; Quintero Arias and Esposito, 2014: 373–382, figs. 1–6, table 1; Teruel and Rodríguez-Cabrera, 2014: 131; Armas and Ávila, 2015: 66, 67, 69, 70, 71; Ponce-Saavedra et al., 2015: 81–89, figs. 1–5, tables 1, 2; Quijano-Ravell and Ponce-Saavedra, 2015: 35–44, figs. 1–5, tables 1–3; Riquelme et al., 2015: 2, 16, 18, 19; Teruel et al., 2015a: 3–14, figs. 1–37, table 1; 2015b: 1–18, figs. 1–35, tables 1–5; 2015c: 13–33, figs. 1–75, tables 1–4; Baldazo-Monsivaiz et al., 2016: 76–79, fig. 2A, table 1; de los Santos et al., 2016: 1–7, 14, 16–19, 22, figs. 2A–G, 3A, table 1; Kovařík et al., 2016a: 1, 11, 18, 19; Lourenço and Velten, 2016: 61, 65; Quijano-Ravell and Ponce-Saavedra, 2016a: 49–61, figs. 1–9, tables 1–4; 2016b: 85–90, figs. 1–4; Teruel, 2016: 91–93, figs. 1–3; Baldazo-Monsivaiz, 2017: 21–27, fig. 2A; Esposito et al., 2017: 2–15, 29, 30, 35–37, 41, 61, 71, 81, 85, 101, 116, 122, 124, 126, 128–130, fig. 13; McWest et al., 2015: 3, 9, 10, 25, 28, 30–34, 38, figs. 2A, 3A, 4A; Teruel and Myers, 2017: 1–14, figs. 1–11, table 1; Teruel et al., 2017: 6; Ubinski et al., 2018: 475–486, figs. 1–8, tables 1, 2; Esposito and Prendini, 2019: 1–10, figs. 1, 2, 3, tables 1–4; Crews and Esposito, 2020: 8, 9, 12, 17, 18; Fet and Kovařík, 2020: 8, 10, 12, 14, 18, 19, 22–26, 28, 29, 31; Howard et al., 2019: 74, 84, fig. 3, table 1; Miranda and Armas, 2020: 5, 7; Ponce-Saavedra and Francke, 2019: 1–17, figs. 1–11, tables 1–4; Quijano-Ravell et al., 2019: 31–48, figs. 1–32, tables 1–5; Teruel and Questel, 2020: 12, 14; Trujillo and Armas, 2020: 1–8, figs. 1–4, table 1; Wendluff et al., 2020: 2, 5, 6, fig. 2B.
- Centruroides* (*Centruroides*): Werner, 1934: 273.
- Centruoroides*: Díaz Nájera, 1970: 117 (lapsus calami).
- Centrurioides*: Lourenço and Eickstedt, 1988: 7 (lapsus calami).
- Key to Identification of the Species of the “thorellii” Clade of *Centruroides* Marx, 1890
1. Carapace posterosubmedian carinae .....2
  - Carapace posterosubmedian carinae absent ...6
  2. Pedipalp chela manus, retrodorsal carina smooth, dorsomedian carina weakly granular; mesosomal sternite VII, ventrolateral and ventrosubmedian carinae obsolete to absent; metasomal segments I–III, ventrosubmedian and ventrolateral carinae vestigial, smooth (figs. 18, 19D); telson vesicle surfaces smooth (♀) (figs. 23–25D).....  
.....*Centruroides rileyi* Sissom, 1995
  - Pedipalp chela manus, retrodorsal carinae present and dorsomedian carinae present or restricted to proximal third or half; mesosomal sternite VII, ventrolateral and ventrosubmedian carinae distinct; metasomal segments I–III, ventrolateral and ventrosubmedian carinae complete, granular (figs. 18L, R, 19L, R); telson vesicle surfaces granular (♀) (figs. 23L, R, 24L, R, 25L, R) .....3

3. Pedipalp chela manus, prodorsal carina absent.....4
- Pedipalp chela manus, prodorsal carina present.....5
4. Pectinal tooth counts, 15–17 ( $\delta$ ), 14 ( $\varphi$ ) (table 9); mesosomal tergites I–VII, dorsomedian carinae present on I–III, absent on IV–VII; mesosomal sternite VII, ventrolateral and ventrosubmedian carinae distinct; metasoma length greater than 3 $\times$  mesosoma length; metasomal segments I–IV, ventrolateral and ventrosubmedian carinae finely granular on segments I–III (figs. 18I, L, 19I, L), smooth on IV.....  
.....*Centruroides chanae*, sp. nov.
- Pectinal tooth counts, 14 ( $\delta$ ), 12–14 ( $\varphi$ ) (table 10); mesosomal tergites I–VII, dorsomedian carinae absent on I and II, vestigial on III–VI, absent on VII; mesosomal sternite VII, ventrolateral and ventrosubmedian carinae weakly developed; metasoma length less than 3 $\times$  mesosoma length; metasomal segments I–IV, ventrolateral and ventrosubmedian carinae present on segments I–IV (figs. 18O, R, 19O, R).....*Centruroides yucatanensis*, sp. nov.
5. Mesosomal tergites I–VII, dorsomedian carinae distinct, complete; total length ( $\delta$ ,  $\varphi$ ), 44–60 mm (table 8); pectinal tooth counts, 13–15 ( $\delta$ ), 13 ( $\varphi$ ).....  
...*Centruroides hoffmanni* Armas, 1996
- Mesosomal tergites I–VII, dorsomedian carinae restricted to posterior two-thirds of segments I–VI, absent on VII; total length ( $\delta$ ,  $\varphi$ ), 38–52 mm (table 7); pectinal tooth counts, 14–16 ( $\delta$ ), 12–14 ( $\varphi$ ).....  
.....*Centruroides schmidtii* Sissom, 1995
6. Pedipalp chela manus, prodorsal carina complete, granular.....  
.....*Centruroides cuauhmapan*, sp. nov.
- Pedipalp chela manus, prodorsal carina absent.....7
7. Pedipalp chela manus, retrodorsal carina complete, granular; mesosomal sternite VII, ventrolateral and ventrosubmedian carinae obsolete to absent (figs. 13, 14A); telson vesicle surfaces ( $\varphi$ ) smooth (figs. 23–25E).....  
.....*Centruroides hamadryas*, sp. nov.
- Pedipalp chela manus, retrodorsal carina weakly granular; mesosomal sternite VII, ventrolateral and ventrosubmedian carinae weakly developed; telson vesicle surfaces ( $\varphi$ ) granular.....8
8. Total length, 39–51 mm (table 6); pedipalp chela manus, dorsomedian carina weakly granular, restricted to distal half; pectinal tooth counts, 13–14 ( $\delta$ ,  $\varphi$ ); mesosomal tergites I–VII, dorsomedian carinae vestigial; metasoma length less than 3.2 $\times$  greater than mesosoma length; metasomal segments I–IV, ventrolateral and ventrosubmedian carinae absent (figs. 18M, P, 19M, P).....  
.....*Centruroides catemacoensis*, sp. nov.
- Total length, 48–55 mm (table 5); pedipalp chela manus, dorsomedian carina absent; pectinal tooth counts, 14–16 ( $\delta$ ), 13–15 ( $\varphi$ ); mesosomal tergites I–VII, dorsomedian carinae weakly granular, restricted to posterior half; metasoma length greater than 3.2 $\times$  mesosoma length; metasomal segments I–IV, ventrolateral and ventrosubmedian carinae present (figs. 18H, K, 19H, K).....  
.....*Centruroides berstoni*, sp. nov.

#### *Centruroides berstoni*, sp. nov.

Figures 1B, D, 2, 4, 6C, D, 9C, D, 13B, 14B, 17H, K, 18H, K, 19H, K, 20H, K, 21H, K, 22H, K, 23H, K, 24H, K, 25H, K, 34, 35, tables 1, 5, 10

*Centruroides schmidtii*: Sissom, 1995: 94–96; figs. 10–18, table 1 (misidentification: paratypes from Escobas, Izabal, Guatemala).

**TYPE MATERIAL:** GUATEMALA: Departamento Izabal: Municipio Livingston: Holotype  $\delta$  (CASENT 9073325), paratype  $\delta$  (CASENT 9073298), Río Dulce, Hotel Tijax, 15°39'51.2"N 89°00'14.6"W, 17 m, 24.ix.2019, A.M. Goodman, collected along gravel road of Hacienda Tijax Parking Lot, flanked by bamboo groves, and live fencing; 2  $\delta$  paratypes (CASENT 9073312, 9073326), 4  $\varphi$  paratypes (CASENT 9073297, 9073313, 9073324, 9073368), Biotopo Chocón



FIGURE 1. Representative species of the arboreal Neotropical “*thorellii*” clade of *Centruroides* Marx, 1890, bark scorpions (Buthidae C.L. Koch, 1837), habitus in life. A, C. *C. schmidti* Sissom, 1995, A. ♀, El Progreso, Finca El Olvido, Las Minas, Guatemala, C. ♂, Zacapa, Guatemala. B, D. *C. berstoni*, sp. nov., B. ♀, D. ♂, Izabal, Rio Dulce, Hotel Tijax, Guatemala. Note elongated metasoma in males. Both species were collected in vegetation, 3–4 m above ground level.

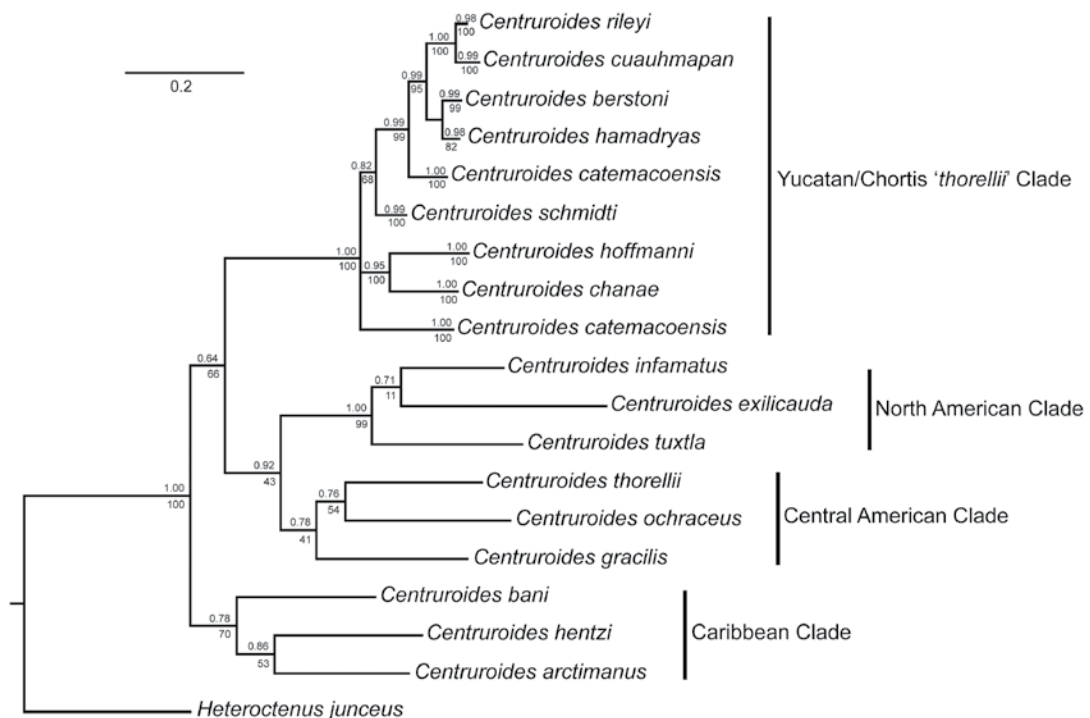


FIGURE 2. Phylogeny of the arboreal Neotropical “*thorellii*” clade of *Centruroides* Marx, 1890, bark scorpions (Buthidae C.L. Koch, 1837), obtained by simultaneous phylogenetic analysis of 112 morphological characters and DNA sequences of the mitochondrial cytochrome oxidase c subunit I gene. Posterior probabilities, obtained with Bayesian inference, and nonparametric bootstraps, obtained with maximum likelihood, indicated above and below branches for corresponding nodes.

Machacas, 15°44'05.3"N 88°54'57.2"W, 15 m, 25.ix.2019, A.M. Goodman.

**ETYMOLOGY:** The species name is a patronym honoring the late Hyman Maxwell Berston, the first author’s grandfather (1930–2021), who inspired his interest in natural history during childhood visits to the California Academy of Sciences.

**DIAGNOSIS:** *Centruroides berstoni* is most closely related to *C. hamadryas*, from which it differs as follows. The carapace is sparsely granular, more densely so on the interocular triangle, in the female of *C. berstoni* but densely granular, with distinct lateral ocular carinae, in the female of *C. hamadryas* (fig. 6B, D). The pedipalp chela manus of the male is proportionally less incrassate in *C. berstoni* (figs. 13–15B) than *C. hamadryas* (fig. 13–15A, tables 4, 5). The retrodorsal carina of the chela manus is weakly granular and the dorsomedian

carina absent in the male of *C. berstoni* (fig. 13B), whereas the retrodorsal carina is complete and the dorsomedian carina weakly developed and restricted to the distal half in the male of *C. hamadryas* (fig. 13A). The retrodorsal carina of the manus is finely granular and the prodorsal carina absent in the female of *C. berstoni* (fig. 14B), whereas the retrodorsal carina is complete and the prodorsal carina restricted to the distal third in the female of *C. hamadryas* (fig. 14A). The first leg of the male is greater than 2× the length of the carapace in *C. berstoni* but less than 2× its length in *C. hamadryas* (table 10). The dorsomedian carinae of the mesosomal tergites are weakly developed and restricted to the posterior half in *C. berstoni* but distinct and complete in *C. hamadryas*. The ventrolateral carinae of mesosomal sternite VII are weakly developed and the ventrosubmedian carinae absent

in *C. berstoni*, whereas the ventrolateral and ventro-submedian carinae are weakly developed to absent in *C. hamadryas*. The telson vesicle is sparsely setose in *C. berstoni* (figs. 23H, K, 24H, K, 25H, K), but densely setose in *C. hamadryas* (figs. 23B, E, 24B, E, 25B, E).

Additional differences between *C. berstoni* and other species of the clade are as follows. The ventro-submedian and ventrolateral carinae of metasomal segments I–IV in the male are weakly developed, smooth in *C. berstoni* (figs. 18H, 19H) but absent in *C. catemacoensis* (figs. 18, 19M), well developed in *C. cuauhmapan* (figs. 18, 19G), weakly developed on segments I–III, absent on IV in *C. hamadryas* (figs. 18–19B, 21–22B), and vestigial, smooth in *C. rileyi* (figs. 18, 19A, 21–22A). The metasomal carinae of the female are finely granular in *C. berstoni* (figs. 17–22K) but well developed, granular in *C. catemacoensis* (figs. 17–22P). The telson vesicle is short and not posteriorly bilobed in the male of *C. berstoni* (figs. 23–25H), unlike in *C. cuauhmapan* (figs. 23–25G) and *C. rileyi* (figs 23–25A), and with surfaces sparsely granular in the female of *C. berstoni* (figs. 23–25K), but smooth in the female of *C. hamadryas* (figs. 23–25E) and densely granular in the female of *C. catemacoensis* (figs. 23–25P), *C. cuauhmapan* (figs. 23–25J), and *C. rileyi* (figs. 23–25D).

**DESCRIPTION:** The following description is based on the holotype male, with differences among other material noted in the section on variation.

**Coloration:** Base color pale yellow, with extensive infuscation, creating mottled or marbled pattern. Carapace with uniformly infuscate marbling, more densely infuscate medially. Pedipalp chela fingers and manus, dorsal and retrolateral intercarinal surfaces with moderately infuscate marbling; prolateral and ventral intercarinal surfaces mostly immaculate. Legs retrolateral surfaces with infuscate marbling; prolateral surfaces pale, immaculate. Tergites with uniformly infuscate mottling, pale stripe medially, blackish spots submedially, and faint, narrow bands laterally. Sternites pale, with faintly infuscate triangular to trapezoidal marking at posterior margin of III, fading to infuscate mot-

ting on VII. Metasomal segments uniformly, faintly marbled; segment V and telson markedly infuscate, noticeably darker than preceding segments.

**Carapace:** Shape trapezoidal; anterior width four-fifths of posterior width (table 5); anteromedian sulcus moderately deep, oval; posteromedian sulcus shallow anteriorly, deeper posteriorly; median ocular tubercle weakly granular; carinae moderately developed, comprising small to medium-sized granules (fig. 6C).

**Pedipalps:** Orthobothrioxic, Type A; femur dorsal trichobothria with α configuration; pedipalp chela fixed finger, trichobothrium *db* situated slightly distal to *et*. Femoral carinae serrate; retromedian carinae comprising spiniform granules; dorsal intercarinal surface moderately granular; prolateral intercarinal surface with series of large spiniform granules. Patella carinae strongly developed, granular; prolateral intercarinal surface with five or six large, subspiniform granules. Chela manus prodorsal and dorsomedian carinae absent; retrodorsal carina weakly developed, granular. Fixed finger, median denticle row comprising eight oblique subrows, each flanked by pro- and retrolateral supernumerary denticles. Movable finger, median denticle row with short terminal row comprising four denticles preceded by eight oblique subrows, each flanked by pro- and retrolateral supernumerary denticles.

**Legs:** Leg I length 2× carapace length (table 10). Telotarsi ventral surfaces densely covered with short setae; unguis markedly curved.

**Pectines:** Pectinal plate 1.65× wider than long; posterior margin distinctly rounded; pectinal tooth count 16/15 (♂) (fig. 9C, table 5).

**Mesosoma:** Tergites width similar to carapace posterior width; I and II slightly narrower (table 5). Pretergites surfaces smooth to finely granular. Posttergites surfaces weakly granular; I–VI with dorsomedian carinae weakly granular, restricted to posterior half of each segment; VII surface weakly granular, dorsomedian carinae moderately granular, dorsosubmedian carinae weakly granular, dorsolateral carinae absent. Sternites III–VI, surfaces smooth; VII surface smooth, ventrolateral carinae reduced to few granules.

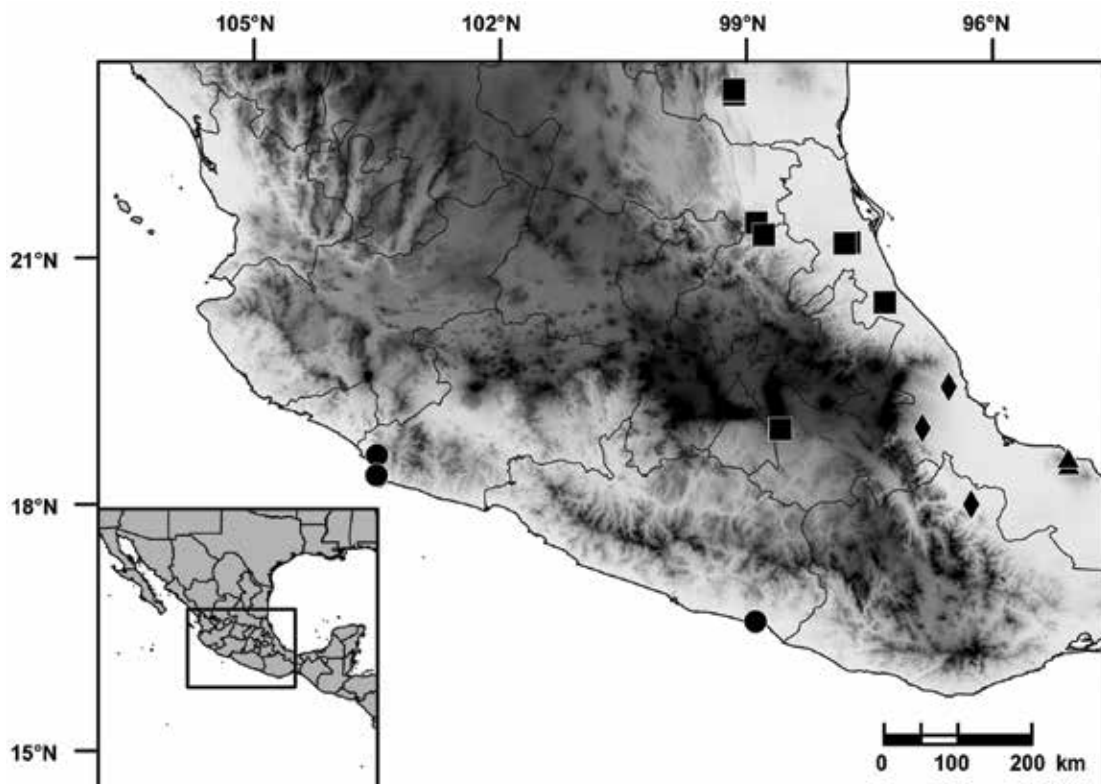


FIGURE 3. Map of central Mexico, plotting known locality records of four species of the arboreal Neotropical "thorelli" clade of *Centruroides* Marx, 1890, bark scorpions (Buthidae C.L. Koch, 1837): *C. catemacoensis*, sp. nov. (triangles); *C. chanae*, sp. nov. (circles); *C. cuauhmapan*, sp. nov. (diamonds); *C. rileyi* Sissom, 1995 (squares).

**Metasoma:** Metasoma length  $3.23 \times$  mesosoma length (table 10). Segments longer than wide; increasing in length posteriorly, segment V  $2 \times$  length of I; carinae weakly developed, smooth on segments I–IV (figs. 17–21H), absent or obsolete on V (figs. 20–22H); intercarinal surfaces sparsely granular.

**Telson:** Vesicle elongate, ovoid; ventral surface shallowly convex; subaculear tubercle narrow and angular in lateral aspect, directed toward midpoint of aculeus. Aculeus angled ventrally at slightly less than  $90^\circ$  (figs. 23–25H).

**Variation:** Base color varies from pale yellow to light orange with considerable variation in infuscation of the carapace and mesosoma, despite localities being less than 50 km apart. Adult males

and females differ as follows. The mesosoma is proportionally longer and slenderer, the metasoma up to  $3 \times$  longer, with segment V markedly longer, and the telson more elongate, with the vesicle more rounded and bilobed posteriorly, in males (figs. 20H, K, 21H, K, 22H, K, table 5). The tegument is more densely infuscate, the pectinal plate produced into a rounded lobe posteriorly, which is punctate and slightly infuscate, and the telson shorter and narrower with the vesicle surfaces less granular, in females (figs. 9C, D, 23H, K, 24H, K, 25H, K, 34–35A, B).

**DISTRIBUTION:** *Centruroides berstoni* is endemic to the Izabal Department of Guatemala and has been recorded from several localities around Morales and Río Dulce (figs. 1B, D, 4).

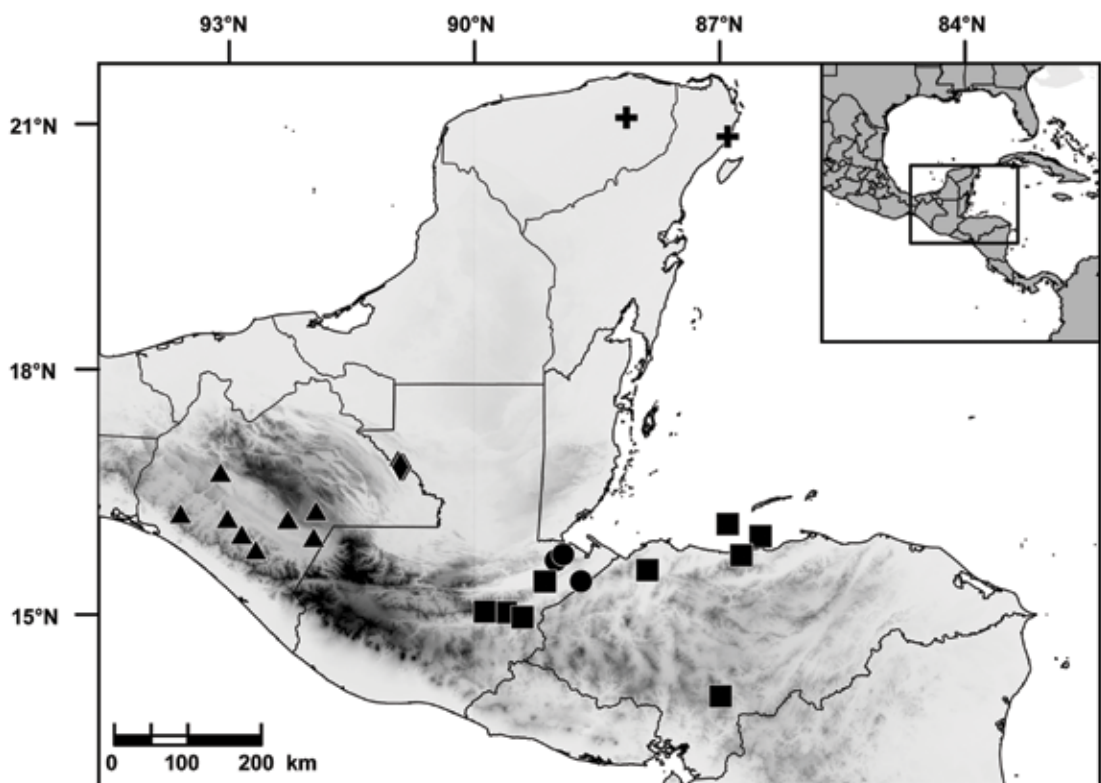


FIGURE 4. Map of southeastern Mexico and northwestern Central America, plotting known locality records of five species of the arboreal Neotropical “*thorellii*” clade of *Centruroides* Marx, 1890, bark scorpions (Buthidae C.L. Koch, 1837): *C. berstoni*, sp. nov. (circles); *C. hamadryas*, sp. nov. (diamonds); *C. hoffmanni* Armas, 1996 (triangles); *C. schmidti* Sissom, 1995 (squares); *C. yucatanensis*, sp. nov. (crosses).

**ECOLOGY:** The localities at which *C. berstoni* was recorded range in altitude from 15–17 m and occur in a region of humid tropical lowland rainforest. Specimens were collected at night with UV light detection, mostly on trees, sitting on bark or branches, and large shoots of bamboo. The habitat and habitus are consistent with the arboreal, corticolous ecomorphotype (Prendini, 2001a).

**REMARKS:** The paratype female of *C. schmidti*, from Morales, Guatemala, was misidentified by Sissom (1995). Differences between the paratype and other females of this species, evident from the illustrations (Sissom, 1995: 94–95 figs. 16–18), include faint reticulate infuscation on the chelicerae, less infuscation of the carapace and tergites, less granulation and

setation of the metasomal segments, and a bilobed telson vesicle.

**MATERIAL EXAMINED: GUATEMALA:** Departamento Izabal: Municipio Livingston: Biotope Chocón Machacas, 15°44'05.3"N 88°54'57.2"W, 15 m, 25.ix.2019, A.M. Goodman, 8 ♂, 1 ♀, 1 juv. ♂ (CASENT 9073271); Río Dulce, Hotel Tijax, 15°40'12.2"N 89°00'27"W, 49 m, 8.vii.2006, J. Huff, C. Víquez, and D. Ortiz, collected along trails through old secondary growth tropical forest using UV at night, 1 ♂ (AMNH [LP 5984]), 15°39'51.2"N 89°00'14.6"W, 17 m, 24.ix.2019, A.M. Goodman, collected along gravel road of Hacienda Tijax Parking Lot, flanked by bamboo groves and live fencing, 1 ♂ (CASENT 9073272), 15°44'05.3"N 88°54'57.2"W, 15 m, 25.ix.2019, A.M. Goodman, 8

TABLE 2

**Meristic data for *Centruroides rileyi* Sissom, 1995**

Material deposited in the Colección Nacional de Arácnidos (CNAN), Universidad Nacional Autónoma de México, Mexico City. Measurements follow Stahnke (1970), Lamoral (1979), and Prendini (2001b).

		♂				♀	
		CNAN				CNAN	
		SC4002	SC4003	SC3999	SC4003	SC3999	SC4003
Total length <sup>1</sup>		35.1	30	32.5	31.4	37.2	33.3
Carapace	length	2.8	2.6	2.9	2.7	3.5	3.4
	ant. width	1.5	1.3	1.4	1.1	1.6	1.7
	post. width	3.1	2.9	3.0	2.9	3.7	3.7
Median ocelli	diameter	0.3	0.2	0.3	0.2	0.3	0.3
Interocular	length <sup>2</sup>	0.3	0.3	0.3	0.3	0.4	0.4
Pedipalp	length <sup>3</sup>	17.4	14.3	15.1	14.9	18.3	17.6
Trochanter	length	1.3	1.1	1.3	1.3	1.3	1.4
Femur	length	3.2	2.6	2.8	2.6	3.3	3.2
	width	0.5	0.5	0.5	0.5	0.7	0.7
	height	0.8	0.6	0.8	0.7	1.0	1.0
Patella	length	3.5	3.0	3.1	3.0	3.7	3.7
	width	0.7	0.7	0.7	0.7	1.0	0.9
	height	1.3	1.1	1.2	1.1	1.6	1.5
Chela	length <sup>4</sup>	5.7	4.6	4.8	4.8	5.8	5.7
Manus	length	2.4	2.0	1.8	2.2	2.2	2.1
	width	1.1	1.0	1.0	1.1	1.2	1.2
	height	1.1	0.9	1.0	1.1	1.3	1.1
Mov. finger	length	3.7	3.0	3.1	3.2	4.2	3.6
Leg I	length	5.8	5.0	5.3	5.1	6.3	6.6
Pectines	length	4.7	4.1	4.3	4.0	4.5	4.6
	tooth count	13/13	14/13	13/14	13/14	12/13	13/13
Mesosoma	length <sup>5</sup>	7.8	9.0	9.0	8.9	12.5	9.6
Sternite VII	length	2.2	2.4	2.6	2.5	3.0	2.5
	width	2.6	2.5	2.9	2.8	4.0	3.7
Metasoma	length <sup>6</sup>	24.5	18.4	20.6	19.8	21.2	20.3
Metasoma I	length	3.0	2.2	2.3	2.4	2.5	2.4
	width	1.1	1.1	1.2	1.2	1.6	1.6
	height	1.2	1.2	1.3	1.3	1.5	1.6
Metasoma II	length	3.8	2.8	3.1	3.0	3.2	3.1
	width	1.1	1.1	1.2	1.2	1.4	1.5
	height	1.1	1.1	1.2	1.2	1.4	1.3

TABLE 2 *continued*

		♂				♀		
		CNAN				CNAN		
		SC4002	SC4003	SC3999	SC4003			
Metasoma III	length	4.2	3.2	3.5	3.4	3.5	3.4	3.3
	width	1.1	1.2	1.2	1.3	1.5	1.4	1.4
	height	1.0	1.1	1.1	1.1	1.4	1.4	1.4
Metasoma IV	length	4.8	3.6	4.0	3.7	3.9	3.6	3.6
	width	1.1	1.1	1.2	1.2	1.4	1.4	1.4
	height	1.0	1.0	1.0	1.1	1.4	1.3	1.3
Metasoma V	length	5.1	3.8	4.6	4.3	4.5	4.2	4.0
	width	1.2	1.1	1.2	1.3	1.5	1.5	1.5
	height	1.1	1.0	1.1	1.2	1.4	1.4	1.5
Telson	length	3.6	2.8	3.1	3.0	3.6	3.6	3.5
Vesicle	length	2.5	1.8	2.1	2.0	2.4	2.1	2.3
	width	1.1	0.8	1.0	1.0	1.2	1.2	1.2
	height	1.0	0.8	0.9	0.9	1.2	1.0	1.1
Aculeus	length	1.3	1.1	1.1	1.0	1.5	1.6	1.5

<sup>1</sup> Sum of carapace, tergites I–VII, metasomal segments I–V, and telson; <sup>2</sup> distance between median ocelli; <sup>3</sup> sum of trochanter, femur, patella, and chela; <sup>4</sup> measured from base of condyle to tip of fixed finger; <sup>5</sup> sum of tergites I–VII; <sup>6</sup> sum of metasomal segments I–V and telson.

♂, 1 ♀, 1 juv. ♂ (CASENT 9073271). Municipio Morales: Morales, Finca Fiymeza, Sendero Anfibio, 15°24'24.1"N 88°41'46.8"W, 595 m, 17.viii.2017, D. Barrales and R. Monjaraz, 1 juv. ♀ (CNAN SC3968).

Estacion Biología Los Tuxtlas, UNAM, Cerro El Vigia Reserva de la Biosfera Los Tuxtlas, 18°34'47.9"N 95°04'29.2"W, 421–429 m, 27. vii.2005, O.F. Francke, M. Cordóva, A. Jaimes, A. Valdez, and H. Montaño.

**ETYMOLOGY:** The species name refers to the town of Catemaco, nearby the type locality, in the state of Veracruz, Mexico.

**DIAGNOSIS:** *Centruroides catemacoensis* differs from the closely related species, *C. berstoni*, *C. cuauhmapan*, *C. hamadryas, and *C. rileyi* as follows. The base coloration of *C. catemacoensis* varies from dark yellow to orange, with considerable infuscation on the pedipalps and metasoma whereas the base coloration of *C. berstoni*, *C. cuauhmapan*, and *C. hamadryas* is pale yellow and of *C. rileyi*, yellowish orange. The carapace posteromedian carinae are reduced or absent in *C. catemacoensis* (fig. 5E, F), absent in *C. berstoni* (fig. 6C, D), *C. cuauhmapan* (fig. 5C, D), and *C. hamadryas* (fig. 6A, B), and present in *C. rileyi* (fig. 5A, B). The pedipalps are longer, and the*

#### *Centruroides catemacoensis*, sp. nov.

Figures 2, 3, 5E, F, 8E, F, 11C, 12C, 17M, P, 18M, P, 19M, P, 20M, P, 21M, P, 22M, P, 23M, P, 24M, P, 25M, P, 30, 31, tables 1, 6, 10

**TYPE MATERIAL:** MEXICO: Veracruz: Municipio Catemaco: Holotype ♂ (CNAN T01424), 4 ♂ paratypes (CASENT 9073286, 9073287, 9073366, CNAN T01421), 4 ♀ paratypes (CASENT 9073309, 9073314, CNAN T01422, T01423), Estacion Biología Los Tuxtlas, Universidad Nacional Autónoma de México (UNAM), 18°34'54"N 95°04'54.6"W, 74–416 m, 17.vii–25.vii.2018, A.M. Goodman, J. Gorneau, and M.K. Lippey; paratype ♂ (CNAN T01420),

chela manus dorsoventrally compressed, in the male, whereas the manus is shorter and slenderer in the female of *C. catemacoensis* than the other species (fig. 11C). Additionally, the chela movable finger is 2.5–3× (male) or 2.5× (female) the length of the manus in *C. catemacoensis* (figs. 11, 12C, table 6) but 1.5–1.7× (male) or 1.3× (female) the length of the manus in *C. berstoni* (figs. 13, 14B, table 5), *C. cuauhmapan* (figs. 11, 12B, table 3), *C. hamadryas* (figs. 13, 14A, table 4), and *C. rileyi* (figs. 11, 12A, table 2). The pedipalp chela manus is two-thirds the length of the patella in *C. catemacoensis* (figs. 11, 12C, table 6), but half its length in *C. berstoni* (figs. 13, 14B, table 5), *C. cuauhmapan* (figs. 11, 12B, table 3), *C. hamadryas* (figs. 13, 14A, table 4), and *C. rileyi* (figs. 11, 12A, table 2). The prodorsal carina is restricted to the distal half of the chela manus in *C. catemacoensis* (figs. 11, 12C), whereas it is complete in *C. cuauhmapan* (figs. 11, 12B), *C. hamadryas* (figs. 13, 14A), and *C. rileyi* (figs. 11, 12A) and absent in *C. chanae* (figs. 15, 16B) and *C. yucatanensis* (figs. 15, 16C). The first leg is less than 2× the length of the carapace in the male of *C. catemacoensis* but greater than 2× its length in *C. cuauhmapan*, *C. hamadryas*, and *C. rileyi* (table 10). The ventro-submedian and ventrolateral carinae of sternite VII of the male are weakly developed in *C. catemacoensis* but well developed, granular in *C. cuauhmapan* and obsolete to absent in *C. berstoni* and *C. rileyi*. The metasoma of the male is greater than 3× the length of the mesosoma in *C. cuauhmapan* but less than 3× its length in *C. berstoni*, *C. hamadryas*, and *C. rileyi* (table 10). The ventrolateral and ventrosubmedian carinae of metasomal segments I–IV in the male are absent in *C. catemacoensis* (figs. 18, 19M), weakly developed, smooth in *C. berstoni* (figs. 18H, K, 19H, K, 21H, K, 22H, K), well developed in *C. cuauhmapan* (figs. 18G, J, 19G, J, 21G, J, 22G, J), weakly developed on segments I–III and absent on IV in *C. hamadryas* (figs. 18B, E, 19B, E), and vestigial, smooth in *C. rileyi* (figs. 18A, D, 19A, D). The metasomal carinae of the female are well developed, granular in *C. catemacoensis* (figs. 17–22P), but finely granular in *C. berstoni* (figs. 17–22K), *C.*

*cuauhmapan* (figs. 17–22J), *C. hamadryas* (figs. 17–22E), and *C. rileyi* (figs. 17–22D).

**DESCRIPTION:** The following description is based on the holotype male, with differences among other material noted in the section on variation.

**Coloration:** Base color yellow to orange, with extensive infuscation, creating mottled or marbled pattern. Carapace with uniformly infuscate marbling, more densely infuscate medially. Pedipalp chela fingers and manus, dorsal and retro-lateral intercarinal surfaces with moderately infuscate marbling; prolateral and ventral intercarinal surfaces mostly immaculate. Legs retro-lateral surfaces with infuscate marbling; prolateral surfaces pale, immaculate. Tergites with uniformly infuscate mottling, pale stripe medially, blackish spots submedially, and distinct, narrow bands laterally. Sternites moderately infuscate, with faintly infuscate triangular marking at posterior margin of III, fading to infuscate mottling on VII. Metasomal segments uniformly, faintly marbled; segment V and telson markedly infuscate, noticeably darker than preceding segments.

**Carapace:** Shape trapezoidal; anterior width four-fifths of posterior width (table 6); anteromedian sulcus moderately deep, narrow; postero-median sulcus shallow anteriorly, deep, narrow posteriorly; carinae moderately developed, comprising small to medium-sized granules (fig. 5E).

**Pedipalps:** Orthobothrioxic, Type A; femur dorsal trichobothria with a configuration; pedipalp chela fixed finger, trichobothrium *db* situated slightly distal to *et*. Femoral carinae moderately to strongly developed, serrate; retromedian carinae comprising spiniform granules; dorsal intercarinal surface moderately granular; prolateral intercarinal surface with series of large spiniform granules. Patella dorsomedian, retrodorsal, prodorsal, and proventral carinae moderately developed, serrate; retromedian carina strongly developed, serrate; retroventral carina incomplete, serrate; prolateral intercarinal surface with five or six large, subspiniform granules. Chela

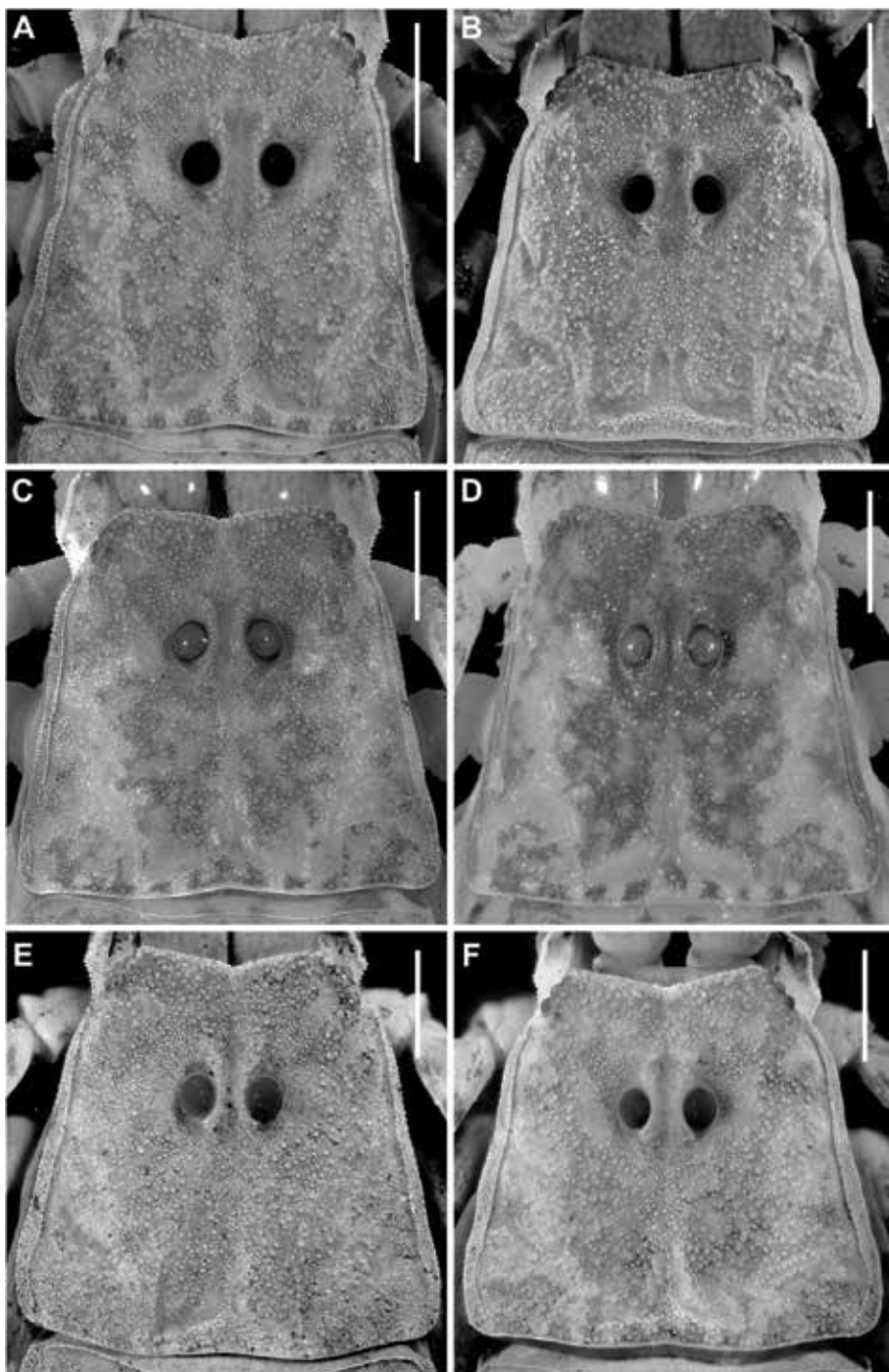


FIGURE 5. *Centruroides* Marx, 1890, carapace, dorsal aspect. A, B. *C. rileyi* Sissom, 1995, A. ♂ (CNAN SC4002), B. ♀ (CNAN SC4003). C, D. *C. cuauhmapan*, sp. nov., C. holotype ♂ (CNAN T01396), D. paratype ♀ (CNAN T01399). E, F. *C. catemacoensis*, sp. nov., E. holotype ♂ (CNAN T01424), F. paratype ♀ (CNAN T01423). Scale bars = 1 mm.

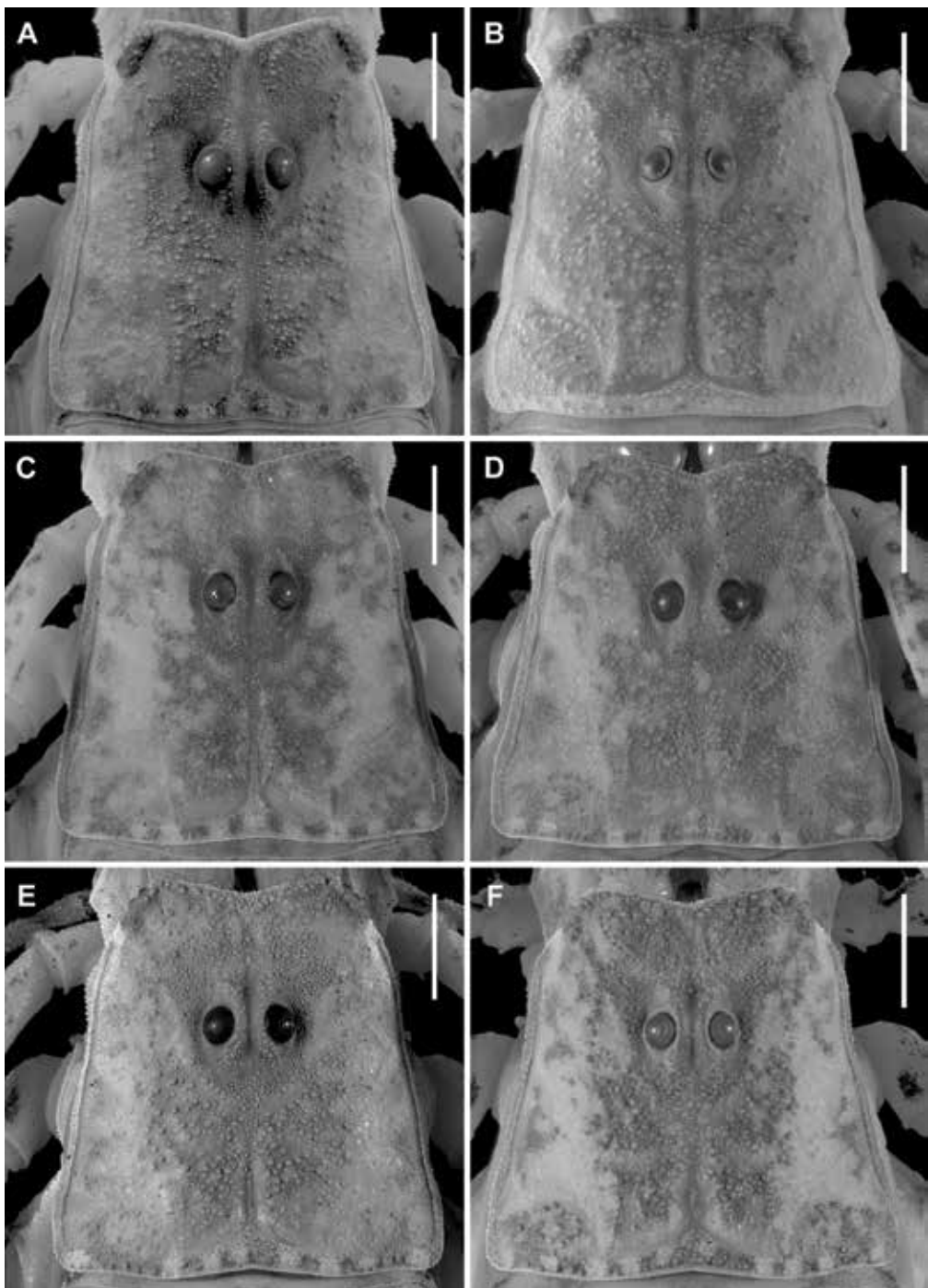


FIGURE 6. *Centruroides* Marx, 1890, carapace, dorsal aspect. A, B. *C. hamadryas*, sp. nov., A. holotype ♂ (CNAN T01408), B. paratype ♀ (CNAN T01415). C, D. *C. berstoni*, sp. nov., C. holotype ♂ (CASENT 9073325), D. paratype ♀ (CASENT 9073313). E, F. *C. schmidti* Sissom, 1995, E. ♂ (CASENT 9073316), F. ♀ (CASENT 9073317). Scale bars = 1 mm.

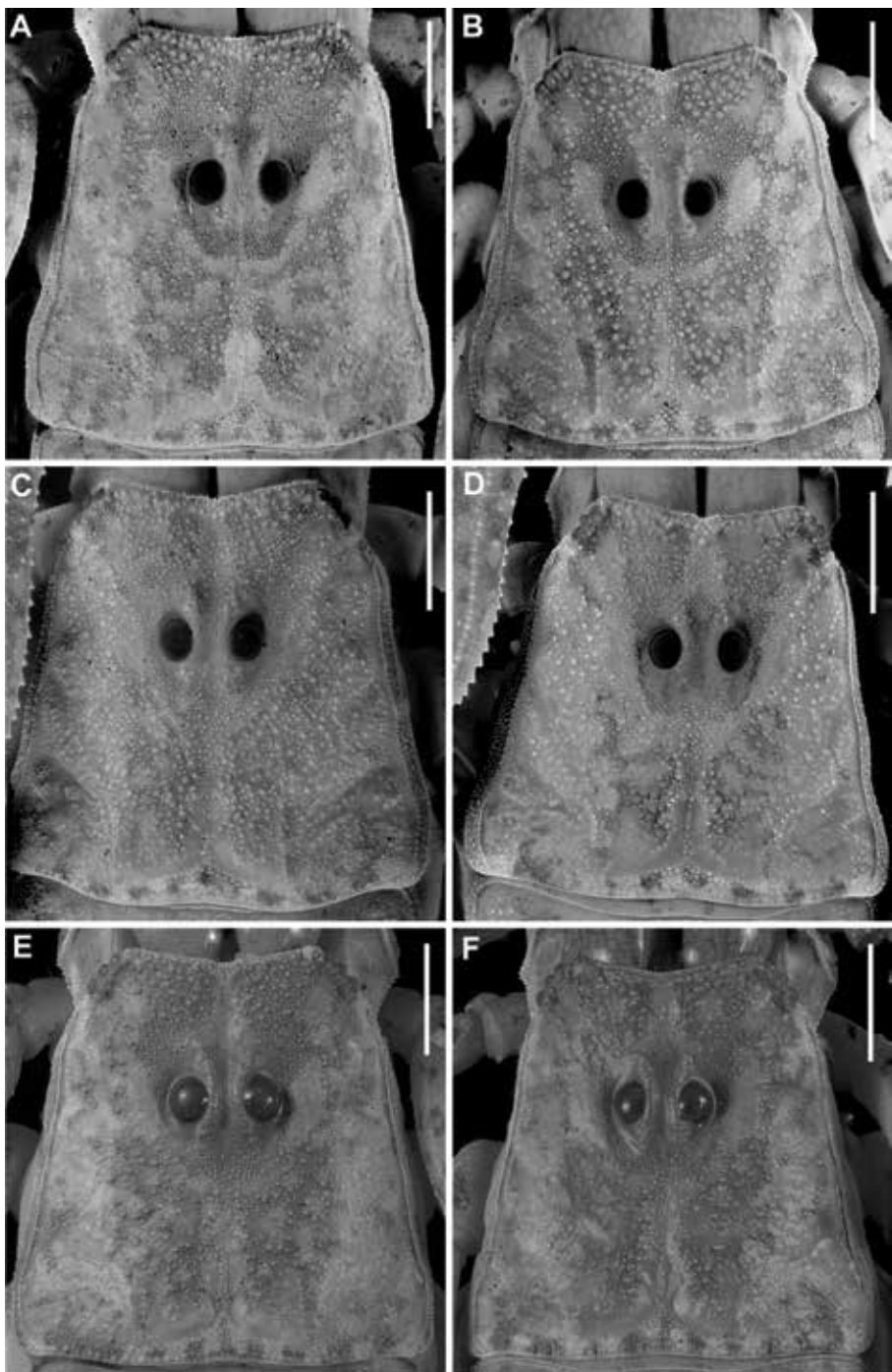


FIGURE 7. *Centruroides* Marx, 1890, carapace, dorsal aspect. A, B. *C. hoffmanni* Armas, 1996, A. ♂ (CNAN SC3996), B. ♀ (CNAN SC3996). C, D. *C. chanae*, sp. nov., C. holotype ♂ (CNAN T01403), D. paratype ♀ (CNAN T01405). E, F. *C. yucatanensis*, sp. nov., E. holotype ♂ (CNAN T01416), F. paratype ♀ (CNAN T01417). Scale bars = 1 mm.

TABLE 3

**Meristic data for type material of *Centruroides cuauhmapan*, sp. nov.**

Material deposited in the Colección Nacional de Arácnidos (CNAN), Universidad Nacional Autónoma de México, Mexico City. Measurements follow Stahnke (1970), Lamoral (1979), and Prendini (2001b).

	Holotype		Paratypes			Paratypes		
	♂	CNAN	♂			♀		
			CNAN		T01402	T01399	CNAN	
		T01396	T01397	T01398		T01400	T01401	
Total length <sup>1</sup>		33.8	31.9	30.9	32.8	32.4	28.2	33.5
Carapace	length	2.9	2.7	2.8	2.8	3.1	2.7	3.1
	ant. width	1.4	1.5	1.4	2.6	1.6	1.5	1.6
	post. width	2.9	3.1	2.9	2.8	3.4	3.0	3.5
Median ocelli	diameter	0.3	0.2	0.3	0.2	0.3	0.2	0.3
Interocular	length <sup>2</sup>	0.3	0.3	0.3	0.3	0.3	0.3	0.4
Pedipalp	length <sup>3</sup>	16.6	15.4	14.9	15.3	16.2	14.7	15.8
Trochanter	length	1.3	1.2	1.1	1.3	1.1	1.3	1.3
Femur	length	3.1	2.9	2.7	2.8	3.0	2.7	2.8
	width	0.5	0.6	0.5	0.5	0.6	0.6	0.6
	height	0.7	0.7	0.7	0.7	0.8	0.7	0.9
Patella	length	3.5	3.2	3.1	3.1	3.3	3.0	3.3
	width	0.7	0.9	0.7	0.7	0.8	0.8	0.9
	height	1.3	1.3	1.2	1.3	1.4	1.2	1.3
Chela	length <sup>4</sup>	5.3	4.9	4.8	4.8	5.2	4.6	4.9
Manus	length	2.1	2.1	1.7	2.2	2.0	1.8	1.9
	width	1.0	1.1	1.0	1.0	1.0	0.9	1.0
	height	2.2	1.1	1.0	1.0	1.0	0.8	1.0
Mov. finger	length	3.4	3.2	3.2	3.3	3.6	3.1	3.5
Leg I	length	5.5	5.0	4.7	5.0	5.8	5.1	5.5
Pectines	length	2.1	2.1	2.1	2.1	2.2	2.1	1.9
	tooth count	13/13	15/14	14/13	14/14	12/12	14/14	10/11
Mesosoma	length <sup>5</sup>	8.0	8.2	8.0	9.6	10.5	9.0	10.6
Sternite VII	length	2.3	2.1	2.3	2.5	2.5	2.2	2.7
	width	2.8	2.7	2.7	2.7	3.6	3.1	3.7
Metasoma	length <sup>6</sup>	22.9	21.0	20.1	20.4	18.8	16.5	19.8
Metasoma I	length	3.0	2.5	2.3	2.6	2.3	2.0	2.2
	width	1.2	1.2	1.2	1.2	1.4	1.2	1.4
	height	1.2	1.3	1.3	1.3	1.5	1.3	1.5
Metasoma II	length	3.4	3.2	3.0	3.2	3.0	2.5	2.8
	width	1.2	1.2	1.2	1.1	1.4	1.2	1.4
	height	1.1	1.2	1.1	1.1	1.4	1.2	1.4

TABLE 3 *continued*

		Holotype		Paratypes			Paratypes	
		$\delta$		$\delta$		$\delta$		$\varphi$
		CNAN	CNAN	T01397	T01398	T01402	T01399	T01400
				T01396			T01399	T01401
Metasoma III	length	3.8	3.7	3.4	3.5	3.5	3.2	2.6
	width	1.2	1.2	1.2	1.1	1.1	1.4	1.2
	height	1.1	1.2	1.1	1.1	1.1	1.3	1.3
Metasoma IV	length	4.5	4.1	4.0	3.8	3.8	3.6	3.0
	width	1.2	1.2	1.1	1.1	1.1	1.4	1.2
	height	1.1	1.2	1.1	1.1	1.1	1.3	1.3
Metasoma V	length	4.8	4.7	4.4	4.3	4.3	3.7	3.6
	width	1.2	1.3	1.2	1.2	1.2	1.4	1.2
	height	1.1	1.2	1.1	1.1	1.1	1.3	1.3
Telson	length	3.4	2.8	3.0	3.0	3.0	3.0	2.8
Vesicle	length	2.2	1.7	2.0	2.0	2.0	2.0	1.6
	width	0.9	0.9	1.0	1.1	1.1	1.0	0.8
	height	0.9	0.9	0.8	1.0	1.0	1.0	0.7
Aculeus	length	1.3	1.2	1.2	0.9	0.9	1.4	1.2

<sup>1</sup> Sum of carapace, tergites I–VII, metasomal segments I–V, and telson; <sup>2</sup> distance between median ocelli; <sup>3</sup> sum of trochanter, femur, patella, and chela; <sup>4</sup> measured from base of condyle to tip of fixed finger; <sup>5</sup> sum of tergites I–VII; <sup>6</sup> sum of metasomal segments I–V and telson.

manus proventral carina moderately developed, comprising few rounded granules; other carinae weakly developed, granular. Fixed finger, median denticle row comprising eight oblique subrows, each flanked by pro- and retrolateral supernumerary denticles. Movable finger, median denticle row with short terminal row comprising four denticles preceded by eight oblique subrows, each flanked by pro- and retrolateral supernumerary denticles.

**Legs:** Leg I length 1.94× greater than carapace length (table 10). Telotarsi ventral surfaces densely covered with short setae; unguis markedly curved.

**Pectines:** Pectinal plate 1.9× wider than long; posterior margin distinctly rounded; pectinal tooth count 14/14 ( $\delta$ ) (fig. 8E, table 6).

**Mesosoma:** Tergites width similar to carapace posterior width; I and II slightly narrower (table 6). Pretergites surfaces smooth to finely granular.

Posttergites surfaces weakly granular; I–VI with dorsomedian carinae vestigial, reduced to several small granules; VII surface weakly granular, dorsomedian carina vestigial, reduced to several small granules, dorsosubmedian and dorsolateral carinae finely serrate. Sternites III–VI, surfaces smooth; VII surface weakly granular, ventrolateral carinae serrate.

**Metasoma:** Metasoma length 2.83× mesosoma length (table 6). Segments longer than wide; increasing in length posteriorly, segment V 2× length of I; dorsolateral and dorsosubmedian carinae weakly serrate on segments I–III, other carinae absent or obsolete; intercarinal surfaces sparsely granular (figs. 17–22M).

**Telson:** Vesicle elongate, ovoid, length 1.5× width (table 6); ventral surface shallowly convex; ventromedian carina granular, terminating at subaculear tubercle; subaculear tubercle narrow and angular in lateral aspect, directed toward

midpoint of aculeus. Aculeus angled ventrally at slightly less than 90° (fig. 25M).

**Variation:** Base coloration varies from light yellow to orange with considerable variation in infuscation of the carapace and mesosoma (figs. 30, 31A, B). Adult males and females differ as follows. The mesosoma is proportionally longer and slenderer, the metasoma up to 3× longer, with segment V markedly longer, and the telson more elongate, with the vesicle more rounded and bilobed posteriorly, in males (figs. 17–22M, table 6). The tegument is more densely infuscate, the pectinal plate is produced into a rounded lobe posteriorly, which is punctate and slightly infuscate, and the telson is shorter and narrower, with the vesicle surfaces less granular, in females (figs. 23–25P). The pectinal tooth count is similar in both sexes (fig. 8E, F, table 6).

**DISTRIBUTION:** *Centruroides catemacoensis* is endemic to the Los Tuxtlas Biosphere Reserve in the state of Veracruz, eastern Mexico. Most of the known material was collected in the vicinity of the Estación Biológica Los Tuxtlas, UNAM (fig. 3).

**ECOLOGY:** The localities at which *C. catemacoensis* has been recorded range in altitude from 74 to 493, in an area of tropical moist broadleaf forest, dominated by thorny palms, *Astrocaryum mexicanum* Leibm. (Arecaceae Berch and J. Presl), and buttress trees including *Siparuna andina* Tul. (Sipuranaeae A. DC.) and *Vochysia guatemalensis* Donn. Sm. (Vochysiaceae A. St.-Hil). This arboreal scorpion has been collected from 3 to 15 m above ground in the forest canopy, often in bromeliads, *Aechmea bracteata* Grisebach (Bromeliaceae Juss). A few individuals were collected in the leaf litter. The habitat and habitus are consistent with the arboreal, corticolous ecomorphotype (Prendini, 2001a).

**MATERIAL EXAMINED: MEXICO:** Veracruz: Municipio Catemaco: Estacion Biología Los Tuxtlas, UNAM, 18°35'05.6"N 95°04'29.9"W, 162 m, 27.vi.1968, C.R.B., in *A. bracteata* at 15 m, 2 ♂, 1 ♀ (CNAN SC3975), 25.i.1969, C.R.B., 15 m above ground in *A. bracteata*, 1 ♀, 1 juv.

♀ (CNAN SC3976), 22.v.1969, C.R.B., *A. bracteata* at 12 m, 1 juv. ♂ (CNAN SC3972), 14.vi.1969, C.R.B., in *A. bracteata* at 10 m, 1 ♂ (CNAN SC3974), 15.viii.1997, G. Pérez II, 1 ♂ (CNAN SC3971), 134 m, 18.iii.1998, D.E. González Manuel, habitación, 1 ♀ (CNAN SC3969), 162 m, 16.iv.1998, in leaf litter, 1 ♀, 2 juv. ♀ (CNAN SC3970), iii.2001, M. López, 15 m above ground in *A. bracteata*, 1 ♀ (CNAN SC3977), 134 m, 26.viii.2005. O.F. Francke, M. Córdova, A. Jaimes, A. Valdez, and H. Montaño, 1 ♂ (AMNH [LP 5231]), 18°34'54"N 95°04'54.6"W, 134 m, 19.vii.2002, J. Ponce and O.F. Francke, 1 ♀ (AMNH [LP 2070]), 74–416 m, 17.vii–25.vii.2018, A.M. Goodman, J. Gorneau, and M.K. Lippey, 2 ♂ (CASENT 9073270, 9073427), 2 juv. ♂ (CASENT 9073315, 9073409), 4 juv. ♀ (CASENT 9073408, 9073410, 9073426, 9073428); surroundings of Estacion Biología, Reserva de la Biosfera Los Tuxtlas, 18°30'03.5"N 95°04'29.5"W, 134–493 m, 26.viii.2005, O.F. Francke, M. Cordova, A. Jaimes, A. Valdez, H. Montaño, 2 ♀, 1 juv. ♀ (CNAN SC3973).

#### *Centruroides chanae*, sp. nov.

Figures 2, 3, 7C, D, 10C, D, 15B, 16B, 17I, L, 18I, L, 19I, L, 20I, L, 21I, L, 22I, L, 23I, L, 24I, L, 25I, L, 40,41, tables 1, 9, 10

**TYPE MATERIAL: MEXICO:** Guerrero: Municipio Copala: Holotype ♂ (CNAN T01407), Microondas Fogos, 16°33'59.5"N 98°53'18.1"W, 14 m, 2.xi.2007, O.F. Francke, H. Montaño, and A. Ballesteros; 2 ♂ paratypes (CNAN T01403, T01404), 2 ♀ paratypes (CNAN T01405, T01406), same data except: 103 m, 22.vi.2007, O.F. Francke, M. Escalante, H. Montaño, and J. Ballesteros.

**ETYMOLOGY:** The species name honors Kendra Chan, a friend of the first author, who passed away in 2018.

**DIAGNOSIS:** *Centruroides chanae* is most closely related to *C. hoffmanni*, from which it differs as follows. A dark line along the lateral margins of the

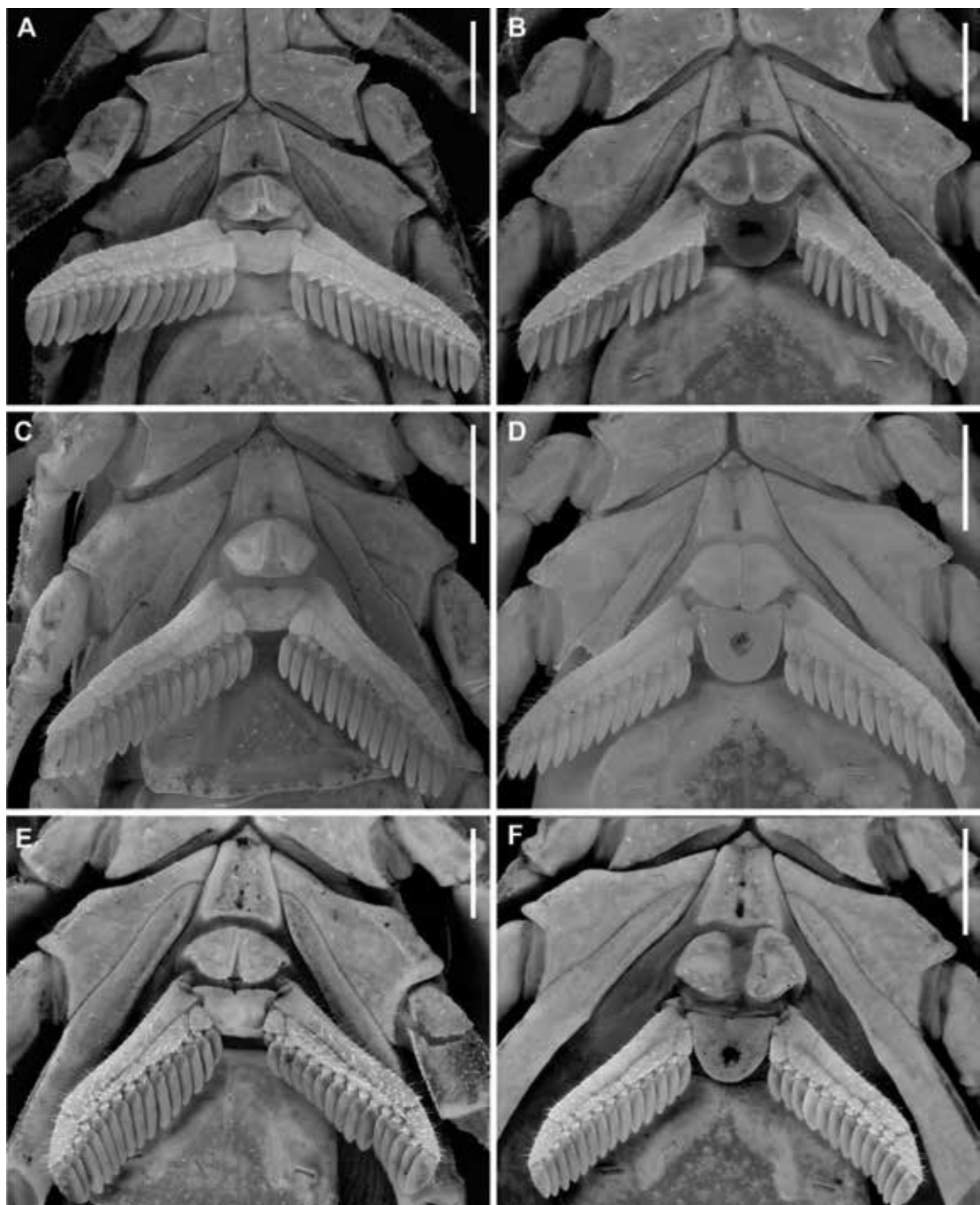


FIGURE 8. *Centruroides* Marx, 1890, pectines and sternum, ventral aspect. A, B. *C. rileyi* Sissom, 1995, A. ♂ (CNAN SC4002), B. ♀ (CNAN SC4003). C, D. *C. cuauhmapan*, sp. nov., C. holotype ♂ (CNAN T01396), D. paratype ♀ (CNAN T01399). E, F. *C. catemacoensis*, sp. nov., E. holotype ♂ (CNAN T01424), F. paratype ♀ (CNAN T01423). Scale bars = 1 mm.

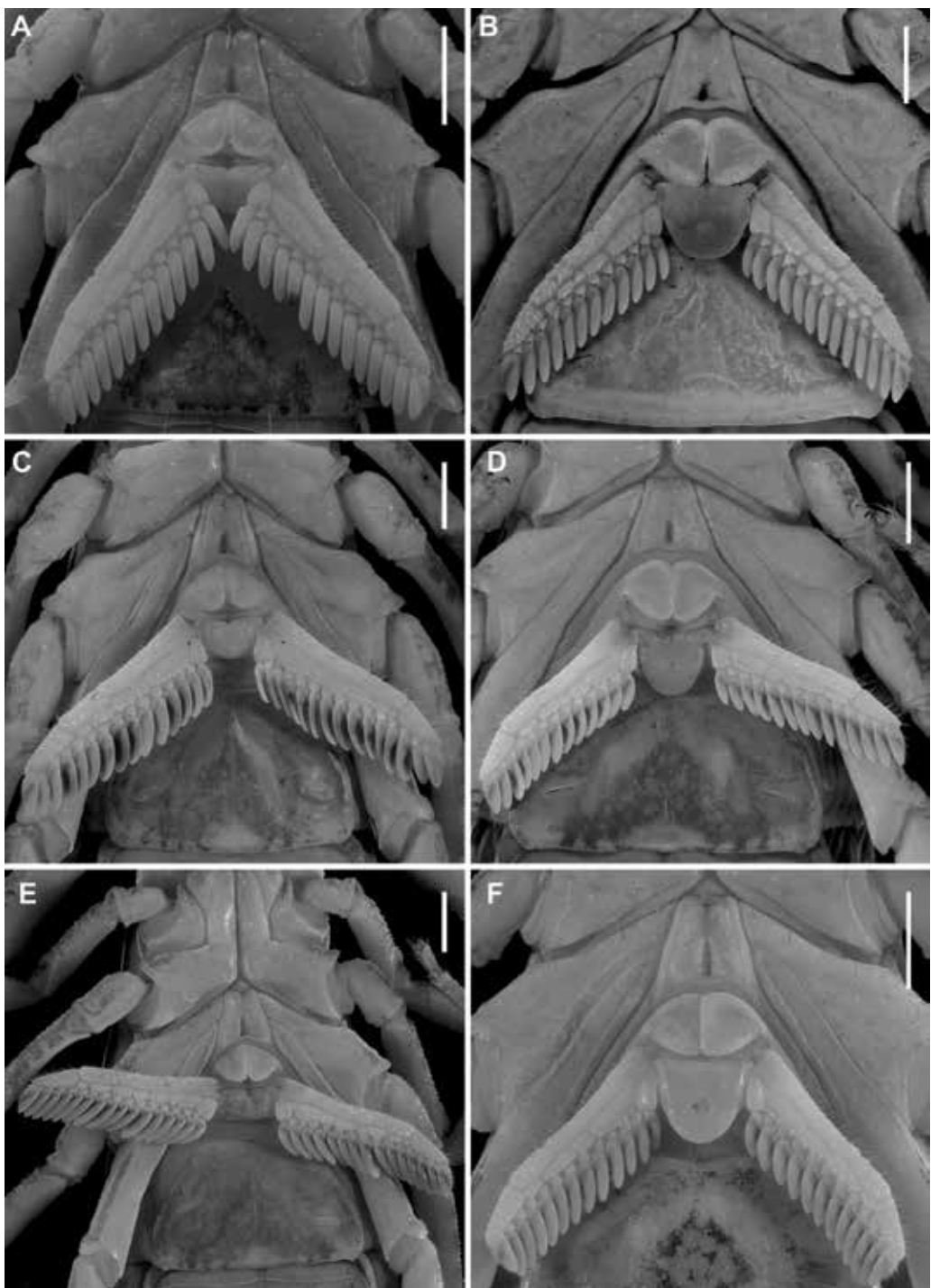


FIGURE 9. *Centruroides* Marx, 1890, pectines and sternum, ventral aspect. A, B. *C. hamadryas*, sp. nov., A. holotype ♂ (CNAN T01408), B. paratype ♀ (CNAN T01415). C, D. *C. berstoni*, sp. nov., C. holotype ♂ (CASENT 9073325), D. paratype ♀ (CASENT 9073313). E, F. *C. schmidti* Sissom, 1995, E. ♂ (CASENT 9073316), F. ♀ (CASENT 9073317). Scale bars = 1 mm.

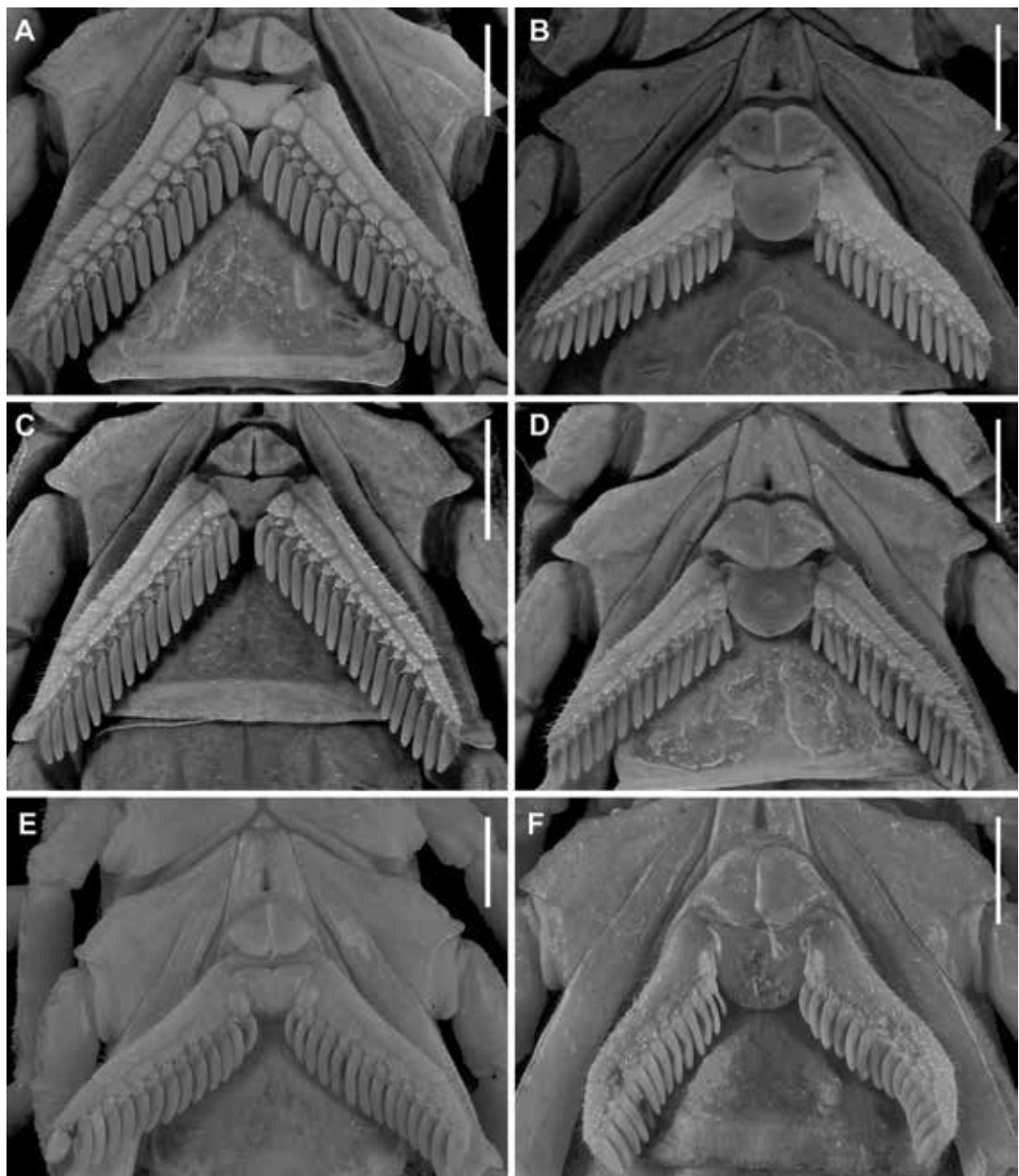


FIGURE 10. *Centruroides* Marx, 1890, pectines and sternum, ventral aspect. A, B. *C. hoffmanni* Armas, 1996, A. ♂ (CNAN SC3996), B. ♀ (CNAN SC3996). C, D. *C. chanae*, sp. nov., C. holotype ♂ (CNAN T01403), D. paratype ♀ (CNAN T01405). E, F. *C. yucatanensis*, sp. nov., E. holotype ♂ (CNAN T01416), F. paratype ♀ (CNAN T01417). Scale bars = 1 mm.

TABLE 4

**Meristic data for type material of *Centruroides hamadryas*, sp. nov.**

Material deposited in the Colección Nacional de Arácnidos (CNAN), Universidad Nacional Autónoma de México, Mexico City. Measurements follow Stahnke (1970), Lamoral (1979), and Prendini (2001b).

	Holotype		Paratypes				Paratypes		
	♂	CNAN	♂				♀	CNAN	
			CNAN		CNAN				
		T01408	T01409	T01411	T01412	T01414		T01410	T01413
Total length <sup>1</sup>		44.5	35.9	35	39	37.7	29.1	31.2	34.8
Carapace	length	3.5	2.9	3.0	3.3	3.1	3.0	3.2	3.3
	ant. width	1.8	1.5	1.5	1.7	1.5	1.5	1.6	1.8
	post. width	3.6	3.2	3.2	3.5	3.3	3.3	3.4	3.6
Median ocelli	diameter	0.3	0.3	0.3	0.3	0.3	0.3	0.3	0.3
Interocular	length <sup>2</sup>	0.4	0.3	0.3	0.3	0.3	0.3	0.3	0.3
Pedipalp	length <sup>3</sup>	20.6	16.7	16.6	18.7	16.7	15.3	14.0	17.2
Trochanter	length	1.6	1.3	1.3	1.2	1.1	1.2	1.3	1.4
Femur	length	4.0	3.2	3.1	3.6	3.3	2.8	3.0	3.0
	width	0.6	0.6	0.5	0.6	0.5	0.6	0.6	0.7
	height	1.0	0.8	0.8	0.8	0.7	0.8	0.9	0.8
Patella	length	4.5	3.5	3.5	3.9	3.6	3.2	3.5	3.4
	width	0.8	0.7	0.8	0.8	0.8	0.9	0.9	1.0
	height	1.6	1.3	1.3	1.4	1.3	1.3	1.4	1.5
Chela	length <sup>4</sup>	6.5	5.4	5.3	6.2	5.4	4.8	5.2	5.6
Manus	length	2.9	2.4	2.5	2.8	2.3	2.0	2.0	2.1
	width	1.3	1.2	1.1	1.2	1.2	1.1	1.2	1.1
	height	1.1	1.1	1.0	1.1	1.1	1.1	1.1	1.1
Mov. finger	length	4.0	3.3	3.4	3.8	3.3	3.3	1.0	3.8
Leg I	length	6.6	5.5	5.5	5.8	5.8	5.4	6.0	5.6
Pectines	length	5.2	4.6	4.5	5.0	4.5	4.2	3.8	5.8
	tooth count	13/14	15/16	14/15	14/13	14/14	13/13	12/12	14/14
Mesosoma	length <sup>5</sup>	10.2	8.6	8.4	8.5	8.7	8.5	8.8	10.2
Sternite VII	length	3.0	2.6	2.6	2.5	2.4	2.9	2.4	2.4
	width	3.3	2.8	2.7	2.8	2.8	3.3	3.3	3.4
Metasoma	length <sup>6</sup>	30.8	24.4	23.6	27.2	25.9	17.6	19.2	21.3
Metasoma I	length	3.9	3.0	3.1	3.6	3.2	2.3	2.5	2.8
	width	1.4	1.2	1.2	1.3	1.3	1.3	1.4	1.4
	height	1.4	1.2	1.3	1.3	1.3	1.4	1.6	1.6
Metasoma II	length	4.9	3.8	3.3	4.3	3.9	2.7	3.0	3.2
	width	1.3	1.3	1.2	1.3	1.3	1.3	1.4	1.4
	height	1.3	1.2	1.2	1.2	1.2	1.3	1.4	1.4

TABLE 4 *continued*

		Holotype		Paratypes				Paratypes	
		♂		♂				♀	
		CNAN	T01408	CNAN				CNAN	
			T01409	T01411	T01412	T01414	T01410	T01413	T01415
Metasoma III	length	5.5	4.5	4.2	4.8	4.5	2.9	3.2	3.5
	width	1.3	1.3	1.3	1.3	1.3	1.4	1.4	1.4
	height	1.2	1.1	1.2	1.1	1.2	1.3	1.3	1.3
Metasoma IV	length	6.2	4.7	4.8	5.2	5.0	3.3	3.5	3.9
	width	1.3	1.3	1.2	1.2	1.3	1.3	1.4	1.3
	height	1.2	1.2	1.2	1.2	1.2	1.3	1.3	1.3
Metasoma V	length	6.5	5.3	5.1	5.7	5.6	3.7	4.0	4.4
	width	1.4	1.3	1.3	1.3	1.4	1.4	1.5	1.4
	height	1.3	1.2	1.3	1.3	1.3	1.3	1.3	1.3
Telson	length	3.8	3.1	3.1	3.6	3.7	2.7	3.0	3.5
Vesicle	length	2.7	2.2	2.0	2.6	2.5	1.4	1.6	2.2
	width	1.2	1.0	1.0	1.1	1.1	1.0	1.5	1.0
	height	1.2	1.0	1.0	1.1	1.3	0.9	1.0	1.0
Aculeus	length	1.3	1.1	1.2	1.2	1.3	1.4	0.9	1.5

<sup>1</sup> Sum of carapace, tergites I–VII, metasomal segments I–V, and telson; <sup>2</sup> distance between median ocelli; <sup>3</sup> sum of trochanter, femur, patella, and chela; <sup>4</sup> measured from base of condyle to tip of fixed finger; <sup>5</sup> sum of tergites I–VII; <sup>6</sup> sum of metasomal segments I–V and telson.

carapace and mesosomal tergites I–III, and pale stripe medially on the carapace and tergites, present in *C. chanae*, are absent in *C. hoffmanni* (fig. 7A, D). The carapace, pedipalps, tergites, and metasoma are less infuscate, creating a less mottled appearance, in *C. chanae* than *C. hoffmanni*. More reticulate infuscation is present on the chelicerae of *C. chanae* than those of *C. hoffmanni*. The interocular triangle is less darkly infuscate in *C. chanae* than *C. hoffmanni*. The marbled infuscation of the mesosomal sternites is faint or absent in *C. chanae* but pronounced in *C. hoffmanni*. The carapace is shorter, its length and width similar, in *C. chanae*, but longer, its length greater than its width, in *C. hoffmanni*. The carapace surfaces are more finely granular, the carinae less developed and the sulci broader and shallower in *C. chanae* than *C. hoffmanni*. The pedipalp chela manus of the male is less incrassate in *C. chanae* (figs. 15, 16A) than *C. hoff-*

*manni* (figs. 15, 16B). The ventral surfaces of the telotarsi of leg I are more coarsely and densely setose in *C. chanae* than *C. hoffmanni*. The pectinal tooth count of the male is higher in *C. chanae*, usually 17 (fig. 10A) than *C. hoffmanni*, usually 15 (fig. 10C, tables 8, 9). The ventrolateral carinae of mesosomal sternite VII are distinct, granular and the ventrosubmedian carinae weakly developed, granular in *C. chanae*, whereas the ventrolateral carinae are granular, and the ventrosubmedian carinae weakly granular and restricted to the posterior half of the segment in *C. hoffmanni*. Although the metasomal segments of the male are shorter and broader in *C. chanae* than *C. hoffmanni*, the metasoma is more than 3× (up to 3.3×) the length of the mesosoma in *C. chanae*, but less than 3× its length in *C. hoffmanni* (table 10). The ventrolateral and ventrosubmedian carinae of metasomal segments I–IV are less pronounced in *C. chanae*, being finely

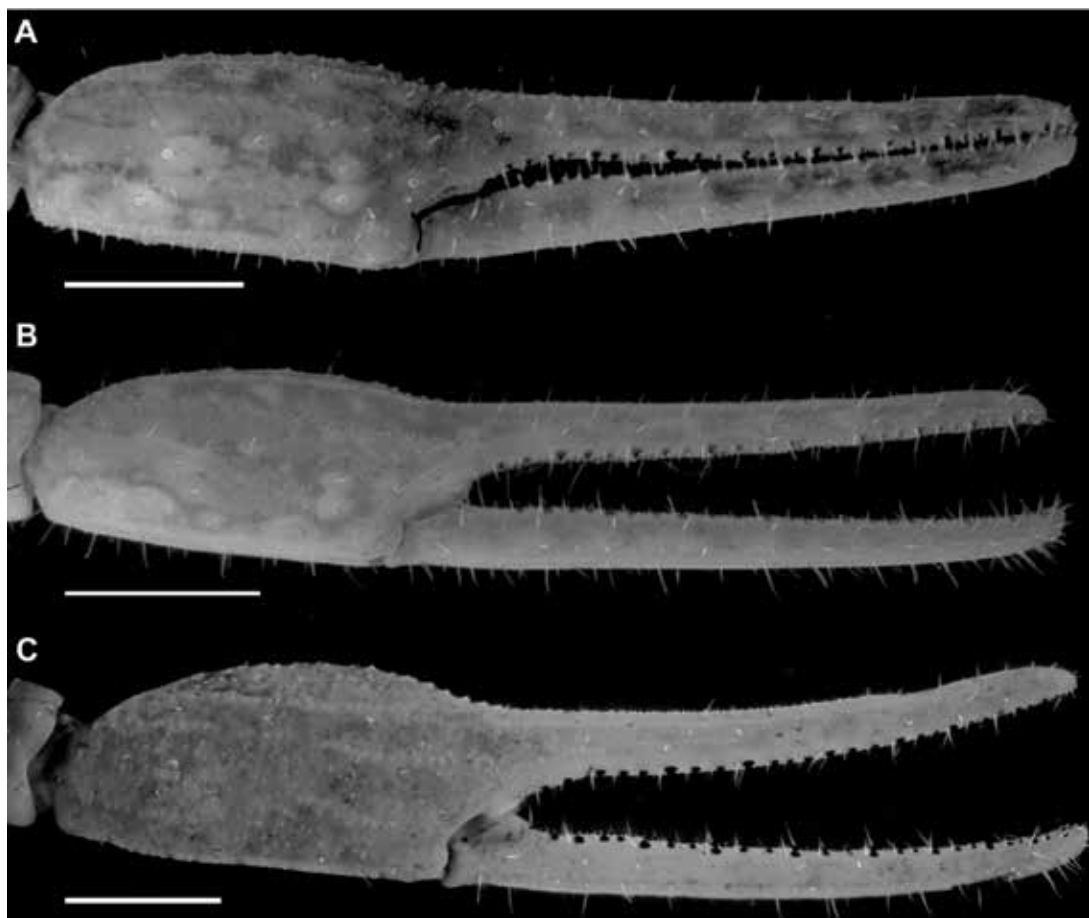


FIGURE 11. *Centruroides* Marx, 1890, pedipalp chela, retrolateral aspect. A. *C. rileyi* Sissom, 1995, ♂ (CNAN SC4002). B. *C. cuauhmapan*, sp. nov., holotype ♂ (CNAN T01396). C. *C. catemacoensis*, sp. nov., holotype ♂ (CNAN T01424). Scale bars = 1 mm.

granular to subserrate on I–III and obsolete, smooth on IV (figs. 18I, L, 19I, L), compared with slightly serrate on I–IV in *C. hoffmanni* (fig. 18C, F, 19C, F). The ventrosubmedian carinae of metasomal segments I and II are absent or obsolete in *C. chanae* but very pronounced in *C. hoffmanni*. The telson of the male is shorter, the vesicle rounded posteriorly, in *C. chanae* (figs. 23–25I) whereas the telson is elongate and the vesicle bilobed posteriorly in *C. hoffmanni* (figs. 23–25C).

**DESCRIPTION:** The following description is based on the holotype male, with differences among other material noted in the section on variation.

**Coloration:** Base color light yellow, with extensive infuscation, creating mottled or marbled pattern. Carapace with uniformly infuscate marbling, more densely infuscate medially. Pedipalp chela fingers and manus, dorsal and retrolateral intercarinal surfaces with moderately infuscate marbling; prolateral and ventral intercarinal surfaces mostly immaculate. Legs retrolateral surfaces with infuscate marbling; prolateral surfaces pale, immaculate. Tergites with uniformly infuscate mottling, pale stripe medially, blackish spots submedially, and faint, narrow bands laterally. Sternites pale, mostly immaculate. Metasomal

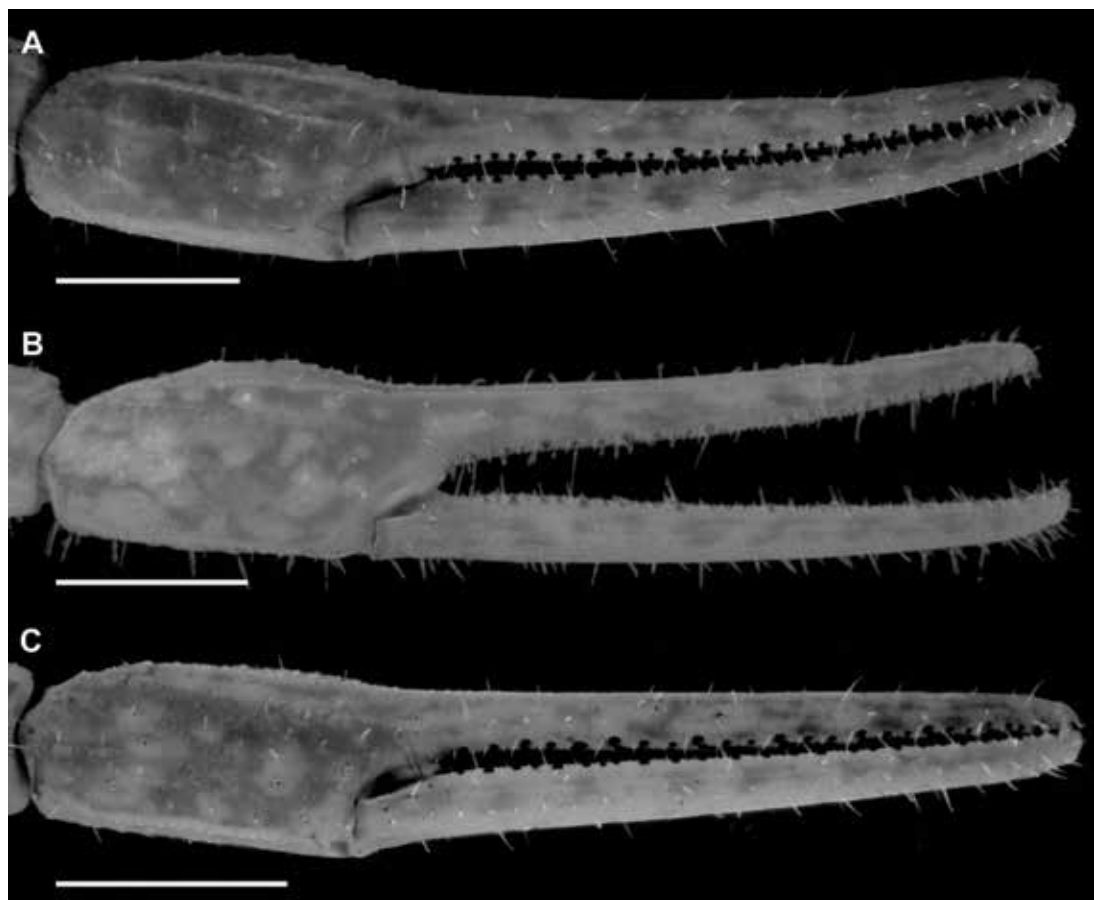


FIGURE 12. *Centruroides* Marx, 1890, pedipalp chela, retrolateral aspect. A. *C. rileyi* Sissom, 1995, ♀ (CNAN SC4003). B. *C. cuauhmapan*, sp. nov., paratype ♀ (CNAN T01399). C. *C. catemacoensis*, sp. nov., paratype ♀ (CNAN T01418). Scale bars = 1 mm.

segments uniformly marbled; segment V and telson markedly infuscate, noticeably darker than preceding segments.

**Carapace:** Shape trapezoidal; anterior width four-fifths of posterior width (table 9); anteromedian sulcus moderately deep, oval; posteromedian sulcus shallow anteriorly, deep posteriorly; median ocular tubercle weakly granular; carinae moderately developed, comprising small to medium-sized granules; lateral ocular and posterosubmedian carinae distinct; intercarinal surfaces finely and evenly granular (fig. 7D).

**Pedipalps:** Orthobothriotaxic, Type A; femur dorsal trichobothria with α configuration; pedi-

palp chela fixed finger, trichobothrium *db* situated slightly distal to *et*. Femoral carinae strongly developed, serrate; retromedian carinae comprising spiniform granules; prolateral intercarinal surface with series of large spiniform granules. Patella carinae strongly developed, granular; prolateral intercarinal surface with five or six large, subspiniform granules. Chela manus dorsomedian and retrodorsal carinae complete, granular; prodorsal carina absent. Fixed finger, median denticle row comprising eight oblique subrows, each flanked by pro- and retrolateral supernumerary denticles. Movable finger, median denticle row with short terminal row comprising four denticles preceded

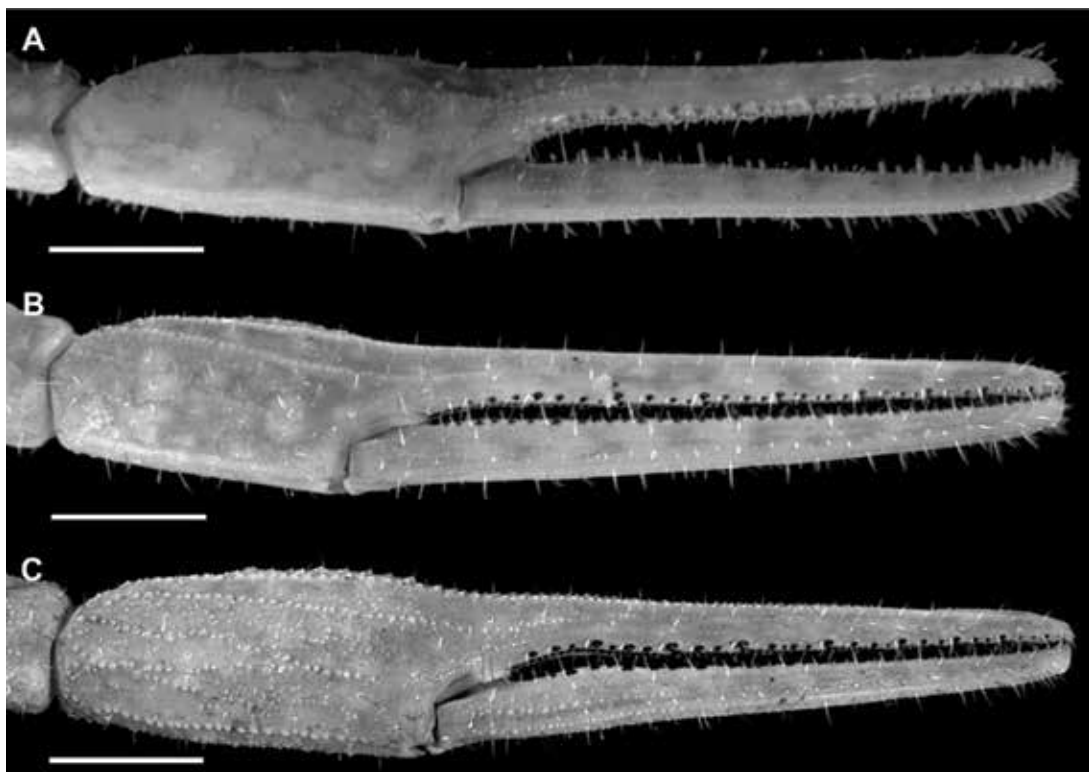


FIGURE 13. *Centruroides* Marx, 1890, pedipalp chela, retrolateral aspect. **A.** *C. hamadryas*, sp. nov., holotype ♂ (CNAN T01408). **B.** *C. berstoni*, sp. nov., holotype ♂ (CASENT 9073325). **C.** *C. schmidti* Sissom, 1995, ♂ (CASENT 9073316). Scale bars = 1 mm.

by eight oblique subrows, each flanked by pro- and retrolateral supernumerary denticles.

**Legs:** Leg I length 1.79× greater than carapace length (table 10). Telotarsi ventral surfaces densely covered with short setae; unguis markedly curved.

**Pectines:** Pectinal plate 1.65× wider than long; posterior margin distinctly rounded; pectinal tooth count 17/17 (♂) (fig. 10C, table 9).

**Mesosoma:** Tergites width similar to carapace posterior width; I and II slightly narrower (table 9). Pretergites surfaces smooth to finely granular. Posttergites surfaces weakly granular; I–VI with dorsomedian carinae finely granular on I–III, absent on IV–VI; VII surface weakly granular, dorsomedian carina absent, dorsosubmedian and dorsolateral carinae smooth. Sternites III–VI, surfaces smooth; VII surface, ventrolateral and ventrosubmedian carinae smooth.

**Metasoma:** Metasoma length 3.1× mesosoma length (table 9). Segments longer than wide; increasing in length posteriorly, segment V 2× length of I; carinae finely granular on segments I–III, smooth on IV, absent on V; intercarinal surfaces sparsely granular (figs. 17–22I).

**Telson:** Vesicle elongate, ovoid; ventral surface shallowly convex; ventromedian carina granular, terminating at subaculeolar tubercle; subaculeolar tubercle narrow and angular in lateral aspect, directed toward midpoint of aculeus. Aculeus angled ventrally at slightly less than 90° (fig. 25I).

**Variation:** Base coloration varies from light yellow to orange with considerable variation in infuscation of the carapace and mesosoma (figs. 40, 41A, B). Adult males and females differ as follows. The prodorsal carina of the pedipalp chela manus is absent, the pectinal tooth count

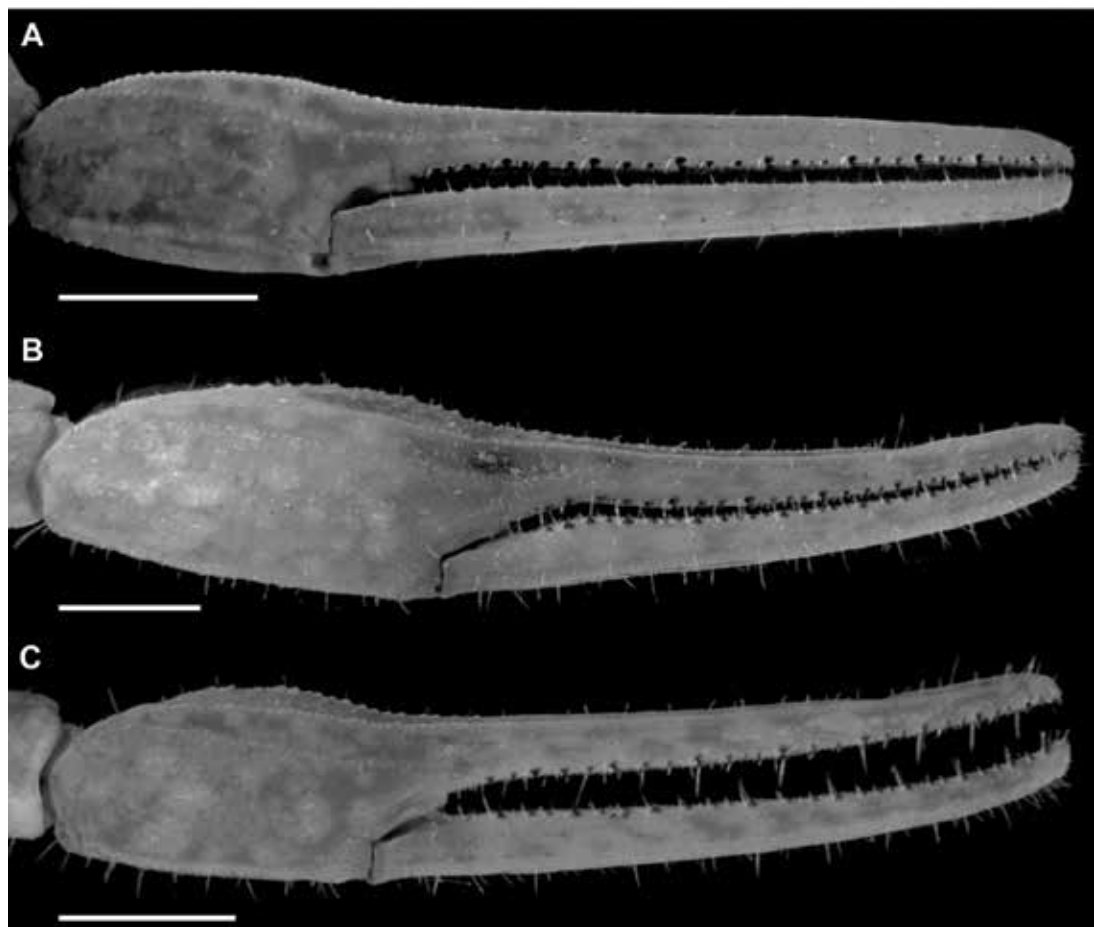


FIGURE 14. *Centruroides* Marx, 1890, pedipalp chela, retrolateral aspect. A. *C. hamadryas*, sp. nov., paratype ♀ (CNAN T01415). B. *C. berstoni*, sp. nov., paratype ♀ (CASENT 9073313). C. *C. schmidti* Sissom, 1995, ♀ (CASENT 9073317). Scale bars = 1 mm.

higher (16 or 17), the mesosoma proportionally longer and slenderer, the metasoma up to 3× longer, with segment V markedly longer, and the telson more elongate, with the vesicle more rounded and smoother, in males (figs. 23I, L, 24I, L, 25I, L, table 9). The prodorsal carina is granular and restricted to the distal half of the chela manus, the tegument more densely infuscate, the pectinal plate produced into a rounded lobe posteriorly, which is punctate and slightly infuscate, the pectinal tooth count lower (13 or 14), and the telson shorter and narrower, with the vesicle surfaces weakly granular, in females (figs. 10C,

D, 12B, C, 15–16B, 20I, L, 22I, L, 23I, L, 24I, L, 25I, L, table 9).

**DISTRIBUTION:** *Centruroides chanae* is endemic to the states of Guerrero and Michoacán, in southwestern Mexico. The known records extend from eastern Michoacán, near the border of Colima, to western Guerrero, south of the Sierra Madre del Sur and east of the Sierra Madre Occidental (fig. 3).

**ECOLOGY:** The localities at which *C. chanae* has been recorded range in altitude from 8 to 221 m. The habitat at these localities varies from low to medium-height deciduous tropical forest and

TABLE 5

**Meristic data for type material of *Centruroides berstoni*, sp. nov.**

Material deposited in the California Academy of Sciences (CASENT), San Francisco. Measurements follow Stahnke (1970), Lamoral (1979), and Prendini (2001b).

	Holotype		Paratypes				Paratypes		
	♂	CASENT	♂		♀			CASENT	
			CASENT		CASENT			CASENT	
		9073325	9073312	9073326	9073298	9073313	9073324	9073368	9073297
Total length <sup>1</sup>	49.9	50	43.7	48.6	37.7	32.7	36.6	36.3	
Carapace	length	3.9	3.7	3.4	3.6	3.4	3.1	3.4	3.4
	ant. width	1.9	1.8	1.7	1.9	1.8	1.5	1.8	1.7
	post. width	3.9	3.9	3.5	3.9	3.9	3.3	3.7	3.8
Median ocelli	diameter	0.3	0.3	0.3	0.3	0.3	0.3	0.3	0.3
Interocular	length <sup>2</sup>	0.4	0.3	0.3	0.4	0.4	0.3	0.4	0.3
Pedipalp	length <sup>3</sup>	23.6	22.8	20.5	22.7	19.9	16.9	19.7	19.1
Trochanter	length	1.9	1.8	1.6	1.7	1.5	1.3	1.5	1.5
Femur	length	4.5	4.4	4.0	4.3	3.4	2.8	3.5	3.5
	width	0.7	0.7	0.7	0.8	0.6	0.5	0.7	0.7
	height	1.0	1.0	1.0	1.0	1.0	0.9	1.0	1.0
Patella	length	5.1	4.7	4.3	4.7	4.0	3.2	4.1	3.8
	width	1.0	1.0	0.9	1.0	1.0	0.9	1.0	1.0
	height	1.5	1.6	1.5	1.5	1.6	1.4	1.6	1.5
Chela	length <sup>4</sup>	7.5	7.3	6.4	7.5	6.5	5.1	6.3	6.0
Manus	length	3.5	3.2	2.8	3.3	2.4	1.9	2.4	2.2
	width	1.6	1.6	1.5	1.6	1.2	1.0	1.2	1.2
	height	1.4	1.4	1.4	1.5	1.1	1.0	1.1	1.0
Mov. finger	length	4.6	4.6	4.2	4.5	4.5	4.5	4.3	4.3
Leg I	length	7.7	7.6	6.5	7.2	6.5	5.3	6.4	6.6
Pectines	length	6.6	6.0	6.0	6.0	5.2	4.8	5.1	4.8
	tooth count	16/15	14/14	16/16	15/15	13/14	15/14	13/13	13/13
Mesosoma	length <sup>5</sup>	10.7	12.5	10.4	12.0	11.3	10.0	10.5	11.3
Sternite VII	length	3.2	3.4	3.0	3.3	2.9	3.2	2.7	2.7
	width	3.3	3.3	3.3	3.4	4.2	2.5	3.8	3.8
Metasoma	length <sup>6</sup>	35.3	33.8	29.9	33.0	23.0	19.6	22.7	21.6
Metasoma I	length	4.5	4.2	3.7	4.2	3.1	2.3	2.6	2.6
	width	1.4	1.4	1.5	1.6	1.5	1.3	1.4	1.5
	height	1.4	1.4	1.4	1.5	1.7	1.5	1.6	1.7
Metasoma II	length	5.6	5.3	4.6	5.2	3.4	2.9	3.3	3.2
	width	1.4	1.4	1.4	1.5	1.5	1.4	1.5	1.5
	height	1.3	1.3	1.3	1.4	1.4	1.3	1.5	1.4

TABLE 5 *continued*

		Holotype		Paratypes				Paratypes			
		$\delta$		$\delta$				$\varphi$			
		CASENT		CASENT				CASENT			
		9073325	9073312	9073326	9073298	9073313	9073324	9073368	9073297		
Metasoma III	length	6.5	6.0	5.2	5.8	3.7	3.1	3.7	3.5		
	width	1.4	1.4	1.3	1.5	1.6	1.4	1.5	1.7		
	height	1.4	1.3	1.4	1.4	1.4	1.3	1.4	1.5		
Metasoma IV	length	7.1	6.5	5.7	6.5	4.2	3.5	4.2	3.9		
	width	1.4	1.4	1.4	1.5	1.5	1.4	1.5	1.6		
	height	1.4	1.3	1.5	1.4	1.4	1.2	1.4	1.4		
Metasoma V	length	7.1	7.1	6.2	6.7	4.6	4.2	4.8	4.6		
	width	1.5	1.5	1.5	1.6	1.6	1.3	1.6	1.6		
	height	1.5	1.5	1.4	1.6	1.4	1.2	1.5	1.4		
Telson	length	4.5	4.7	4.5	4.6	4.0	3.6	4.1	3.8		
Vesicle	length	3.3	3.3	3.1	3.1	2.4	2.0	2.4	2.8		
	width	1.3	1.6	1.3	1.3	1.2	1.6	1.2	1.1		
	height	1.4	1.4	1.2	1.4	1.1	1.0	1.0	1.1		
Aculeus	length	1.6	1.3	1.7	1.6	1.8	1.9	1.9	1.6		

<sup>1</sup> Sum of carapace, tergites I–VII, metasomal segments I–V, and telson; <sup>2</sup> distance between median ocelli; <sup>3</sup> sum of trochanter, femur, patella, and chela; <sup>4</sup> measured from base of condyle to tip of fixed finger; <sup>5</sup> sum of tergites I–VII; <sup>6</sup> sum of metasomal segments I–V and telson.

savanna to mangroves and oaks near the coastline. Specimens from Microondas Fogos were collected on fence poles in rangeland at night. The habitat and habitus are consistent with the arboreal, corticolous ecomorphotype (Prendini, 2001a).

MATERIAL EXAMINED: MEXICO: Guerrero: Municipio Copala: Microondas Fogos, 16°33'59.5"N 98°53'18.1"W, 103 m, 22.vi.2007, O.F. Francke, M. Escalante, H. Montaño, and A. Ballesteros, 1 ♂ (AMNH [LP 7032]), 1 juv. ♂ (CNAN SC3983), 14 m, 2.xi.2007, O.F. Francke, H. Montaño, and A. Ballesteros, 3 ♂ (CNAN SC3978), 1 ♀ (AMNH [LP 8582]). Michoacán: Municipio Aquila: Faro de Bucerias, 18°21'08.3"N 103°30'20.9"W, 13 m, 10.iii.2002, J. Ponce, low deciduous forest, 1 juv. ♀ (CNAN SC3982), 13.iv.2002, J. Ponce, low deciduous forest, 2 ♂ (CNAN SC3979, SC3980), 3 ♂ (CNAN SC4005), 18°35'50.5"N 103°30'04.3"W, 221 m, 14.iv.2002, J. Ponce and E. González, low deciduous forest, 1 ♂ (AMNH [LP 2009]). Municipio Aquila: La Llorona, el Faro, 18°20'17.2"N

103°29'49.2"W, 8 m, 6.v.2000, E. Miranda, beach gap, 1 ♂ (CNAN SC3981).

#### *Centruroides cuauhmapan*, sp. nov.

Figures 2, 3, 5A, B, 8A, B, 11A, 12A, 17A, D, 18A, D, 19A, D, 20A, D, 21A, D, 22A, D, 23A, D, 24A, D, 25A, D, 28, 29, tables 1, 3, 10

*Centruroides schmidti*: Francke, 2007: 69, 71, 72, fig. 1 (misidentification); Armas and Martín-Frías, 2008: 7–10, 12, 17, 19, 20, figs. 2–4, table XIV (misidentification).

TYPE MATERIAL: MEXICO: Oaxaca: Municipio San Juan Bautista Tuxtepec: Holotype ♂ (CNAN T01396), 4 ♀ paratypes (CNAN T01399–T01402), 17 km from San Juan Bautista Tuxtepec, Cerro del Oro Dam, 17°59'55"N 96°15'47.2"W, 74 m, 23.v.1990, E. Barrera and A. Cadena. Veracruz: Municipio Actopan: 2 ♂ para-

TABLE 6

**Meristic data for type material of *Centruroides catemacoensis*, sp. nov.**

Material deposited in the California Academy of Sciences (CASENT), San Francisco and the Colección Nacional de Arácnidos (CNAN), Universidad Nacional Autónoma de México, Mexico City. Measurements follow Stahnke (1970), Lamoral (1979), and Prendini (2001b).

		Holotype		Paratypes				Paratypes			
		♂	CNAN	♂		CNAN		♀		CNAN	
				CASENT	T01420	T01421	9073309	9073314	9073366	T01422	T01423
		T01424	9073286	9073287							
Total length <sup>1</sup>		46.6	36.4	35.7	41.8	40.7	31.8	33.1	30.1	29.6	32.4
Carapace	length	3.6	2.9	2.8	3.4	3.3	3.0	3.0	3.0	2.7	3.2
	ant. width	1.8	1.4	1.4	1.8	1.6	1.6	1.7	1.5	1.5	1.7
	post. width	3.9	3.3	3.1	3.8	3.5	3.6	3.5	3.5	3.1	3.9
Median ocelli	diameter	0.3	0.3	0.3	0.3	0.4	0.3	0.3	0.3	3.0	0.3
Interocular	length <sup>2</sup>	0.3	0.3	0.3	0.3	0.3	0.3	0.3	0.3	2.9	0.3
Pedipalp	length <sup>3</sup>	16.8	11.3	12.3	15.9	14.0	12.0	12.2	12.0	11.4	12.8
Trochanter	length	1.5	1.1	1.2	1.6	1.3	1.3	1.3	1.3	1.2	1.3
Femur	length	4.0	2.8	3.0	3.8	3.5	2.8	2.7	2.7	2.6	3.0
	width	0.7	0.5	0.5	0.7	0.6	0.5	0.6	0.6	0.6	0.6
	height	1.0	0.7	0.7	1.0	0.8	0.9	0.9	0.9	0.7	0.9
Patella	length	4.6	3.3	3.3	4.2	3.7	3.2	3.2	3.2	3.0	3.5
	width	1.0	0.7	0.7	0.8	0.7	0.8	0.8	0.8	0.8	0.9
	height	1.6	1.1	1.1	1.3	1.3	1.4	1.3	1.3	1.3	1.4
Chela	length <sup>4</sup>	6.7	4.1	4.8	6.3	5.5	4.7	5.0	4.8	4.6	5.0
Manus	length	3.0	2.0	2.0	2.8	2.5	1.9	1.7	1.8	1.6	2.0
	width	1.4	1.0	1.0	1.3	1.2	1.0	0.9	1.0	0.9	1.0
	height	1.2	0.9	1.0	1.1	1.0	0.9	1.0	0.9	0.8	1.0
Mov. finger	length	4.1	2.9	3.2	4.0	3.5	3.2	3.5	3.2	3.3	3.4
Leg I	length	7.0	5.3	5.0	6.6	6.0	5.5	5.8	5.2	5.2	5.6
Pectines	length	5.7	4.5	4.5	5.1	4.5	4.1	4.5	4.2	3.8	4.6
	tooth count	14/13	14/14	14/14	13/14	14/14	14/13	14/14	13/13	13/13	14/14
Mesosoma	length <sup>5</sup>	11.2	10.4	9.7	9.5	11.0	10.1	11.3	8.6	9.6	9.1
Sternite VII	length	3.0	2.8	3.0	2.7	3.1	2.7	2.8	2.3	2.6	2.5
	width	3.6	2.9	3.0	3.2	3.0	3.4	3.6	3.4	3.4	3.4
Metasoma	length <sup>6</sup>	31.8	23.1	23.2	28.9	26.4	18.7	18.8	18.5	17.3	20.1
Metasoma I	length	4.0	3.0	3.1	3.6	3.3	2.5	2.2	2.5	2.3	2.5
	width	1.4	1.2	1.2	1.4	1.3	1.4	1.4	1.3	1.4	1.5
	height	1.4	1.2	1.3	1.3	1.3	1.5	1.5	1.5	1.4	1.7
Metasoma II	length	5.1	3.5	3.5	4.6	4.2	2.8	2.8	2.9	2.5	3.0
	width	1.4	1.2	1.3	1.4	1.3	1.4	1.5	1.5	1.3	1.6
	height	1.3	1.2	1.2	1.2	1.2	1.4	1.3	1.3	1.4	1.5

TABLE 6 *continued*

		Holotype		Paratypes				Paratypes			
		♂	♂				♀				
			CNAN	CASENT		CNAN	CASENT	CNAN	CASENT	CNAN	
			T01424	9073286	9073287	T01420	T01421	9073309	9073314	9073366	T01422
Metasoma III	length	5.5	4.0	4.1	5.1	4.7	3.1	3.1	3.0	2.8	3.4
	width	1.4	1.2	1.2	1.4	1.3	1.5	1.5	1.5	1.4	1.7
	height	1.3	1.2	1.2	1.3	1.2	1.3	1.4	1.3	1.2	1.6
Metasoma IV	length	6.2	4.5	4.4	5.5	5.3	3.4	3.6	3.4	3.0	3.7
	width	1.4	1.2	1.2	1.3	1.3	1.4	1.5	1.4	1.3	1.7
	height	1.4	1.1	1.2	1.2	1.3	1.4	1.4	1.3	1.2	1.6
Metasoma V	length	6.7	4.7	4.6	5.9	5.3	3.7	3.7	3.7	3.6	4.0
	width	1.5	1.3	1.2	1.4	1.3	1.4	1.5	1.4	1.3	1.6
	height	1.4	1.2	1.2	1.3	1.2	1.3	1.4	1.3	1.2	1.6
Telson	length	4.3	3.4	3.5	4.2	3.6	3.2	3.4	3.0	3.1	3.5
Vesicle	length	3.1	2.3	2.3	2.9	2.5	1.9	2.0	1.9	1.8	2.2
	width	1.4	1.0	1.0	1.1	1.1	1.4	1.0	1.0	1.0	1.0
	height	1.3	1.0	0.9	1.1	1.0	1.0	1.0	1.1	0.9	1.2
Aculeus	length	1.2	1.2	1.0	1.3	1.2	1.0	1.5	1.3	1.3	1.5

<sup>1</sup> Sum of carapace, tergites I–VII, metasomal segments I–V, and telson; <sup>2</sup> distance between median ocelli; <sup>3</sup> sum of trochanter, femur, patella, and chela; <sup>4</sup> measured from base of condyle to tip of fixed finger; <sup>5</sup> sum of tergites I–VII; <sup>6</sup> sum of metasomal segments I–V and telson.

types (CNAN T01397, T01398), Los Idolos, 19°25'44.9"N 96°32'12.4"W, 112 m, 5.v.2006, O.F. Francke, P. Berea, and J. Ballesteros, collected with UV detection.

**ETYMOLOGY:** The species name is a noun in apposition, taken from the Nahuatl word meaning “up in a tree” and alludes to the arboreal habitat of species in the genus.

**DIAGNOSIS:** *Centruroides cuauhmapan* is most closely related to *C. rileyi*, from which it differs as follows. The posterosubmedian carinae on the carapace are absent in *C. cuauhmapan* (fig. 5D) but weakly developed in *C. rileyi* (fig. 5A). The retrodorsal carina of the pedipalp chela manus is finely granular, the dorsomedian carina distinct, granular, and the prodorsal carina distinct, granular and complete in the male of *C. cuauhmapan* (figs. 11, 12B), whereas the retrodorsal carina is smooth, the dorsomedian carina weakly granular, and the prodorsal carina weakly granular and

restricted to the distal half of the segment in the male of *C. rileyi* (figs. 11, 12A). The ventrolateral and ventrosubmedian carinae of mesosomal sternite VII are distinct, granular and the intercarinal surfaces finely granular in *C. cuauhmapan*, whereas the ventrolateral and ventrosubmedian carinae are obsolete to absent and the intercarinal surfaces smooth in *C. rileyi*. The metasoma and telson are longer in the male and more robust, proportionally longer and broader, in the female of *C. cuauhmapan* than *C. rileyi*. The ventrolateral and ventrosubmedian carinae are distinct, granular on metasomal segments I–V in the male and female of *C. cuauhmapan* (figs. 18G, J, 19G, J, 21G, J, 22G, J), but granular on segment I in the female, vestigial on I–III, and smooth on IV and V in the male of *C. rileyi* (figs. 18A, D, 19A, D, 21A, D, 22A, D). The surfaces of the telson vesicle of the female are granular in *C. cuauhmapan* (figs. 23–25J), but smooth in *C. rileyi* (figs. 23–25D).

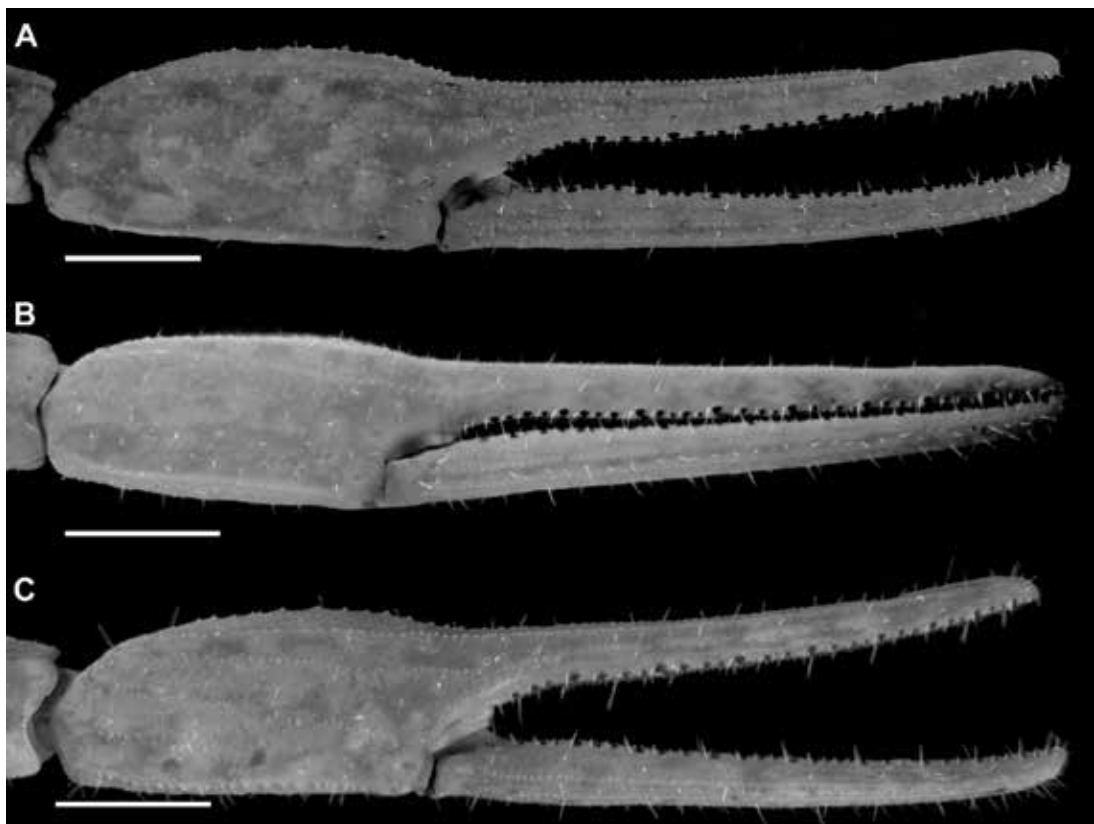


FIGURE 15. *Centruroides* Marx, 1890, pedipalp chela, retrolateral aspect. A. *C. hoffmanni* Armas, 1996, ♂ (CNAN SC3996). B. *C. chanae*, sp. nov., holotype ♂ (CNAN T01403). C. *C. yucatanensis*, sp. nov., holotype ♂ (CNAN T01416). Scale bars = 2 mm.

**DESCRIPTION:** The following description is based on the holotype male, with differences among other material noted in the section on variation.

**Coloration:** Base color pale yellow, with extensive infuscation, creating mottled or marbled pattern. Carapace with uniformly infuscate marbling, more densely infuscate medially. Pedipalp chela fingers and manus, dorsal and retrolateral intercarinal surfaces with moderately infuscate marbling; prolateral and ventral intercarinal surfaces immaculate. Legs retrolateral surfaces with infuscate marbling; prolateral surfaces pale, immaculate. Tergites with uniformly infuscate mottling, pale stripe medially, blackish spots submedially, and distinct, narrow bands laterally. Sternites slightly infuscate posteriorly, with

faintly infuscate triangular marking at posterior margin of sternite III, fading to infuscate mottling on sternite VII. Metasomal segments uniformly, faintly marbled; segment V and telson markedly infuscate, noticeably darker than preceding segments.

**Carapace:** Shape trapezoidal; anterior width four-fifths of posterior width (table 3); anteromedian sulcus moderately deep, oval; posteromedian sulcus shallow anteriorly, deeper posteriorly; carinae moderately developed, comprising small to medium-sized granules (fig. 5C).

**Pedipalps:** Orthobothriotic, Type A; femur dorsal trichobothria with  $\alpha$  configuration; pedipalp chela fixed finger, trichobothrium *db* situated slightly distal to *et*. Femoral carinae granular; dorsal intercarinal surface moderately

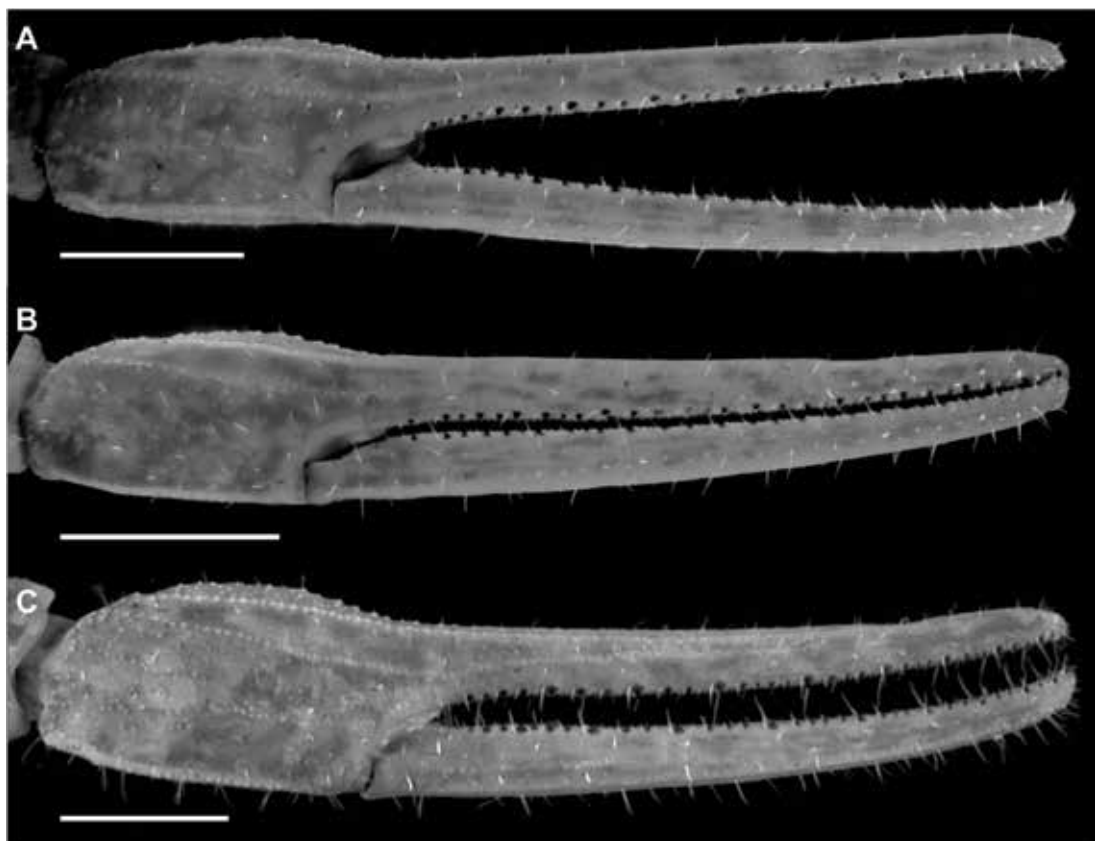


FIGURE 16. *Centruroides* Marx, 1890, pedipalp chela, retrolateral aspect. A. *C. hoffmanni* Armas, 1996, ♀ (CNAN SC3996). B. *C. chanae*, sp. nov., paratype ♀ (CNAN T01405). C. *C. yucatanensis*, sp. nov., paratype ♀ (CNAN T01418). Scale bars = 1 mm.

granular; pro- and retrolateral intercarinal surfaces each with series of large spiniform granules. Patella carinae granular; prolateral intercarinal surface with eight to 10 large subspiniform granules. Chela manus slightly incrassate; dorsal secondary carina well developed, finely serrate; digital and retrolateral secondary carinae moderately developed, finely crenulate; retrodorsal carina well developed, coarsely crenulate; retroventral carina well developed, finely crenulate; proventral carina moderately developed, comprising few rounded granules; prodorsal carina well developed, coarsely serrate. Fixed and movable fingers each shallowly curved proximally. Fixed finger, median denticle row comprising eight oblique subrows, each flanked by pro-

retrolateral supernumerary denticles. Movable finger, median denticle row with short terminal subrow comprising four denticles preceded by eight oblique subrows, each flanked by pro- and retrolateral supernumerary denticles.

*Legs:* Leg I length 1.92× greater than carapace length (table 10). Telotarsi ventral surfaces densely covered with short setae; unguis strongly curved.

*Pectines:* Pectinal plate 1.8× wider than long; posterior margin distinctly rounded; pectinal tooth count 14/14 (♂) (fig. 8C, table 3).

*Mesosoma:* Tergites width similar to carapace posterior width; I and II slightly narrower (table 3). Pretergites surfaces smooth to finely granular. Posttergites surfaces weakly granular; I–VI with dorsomedian carinae vestigial and reduced to

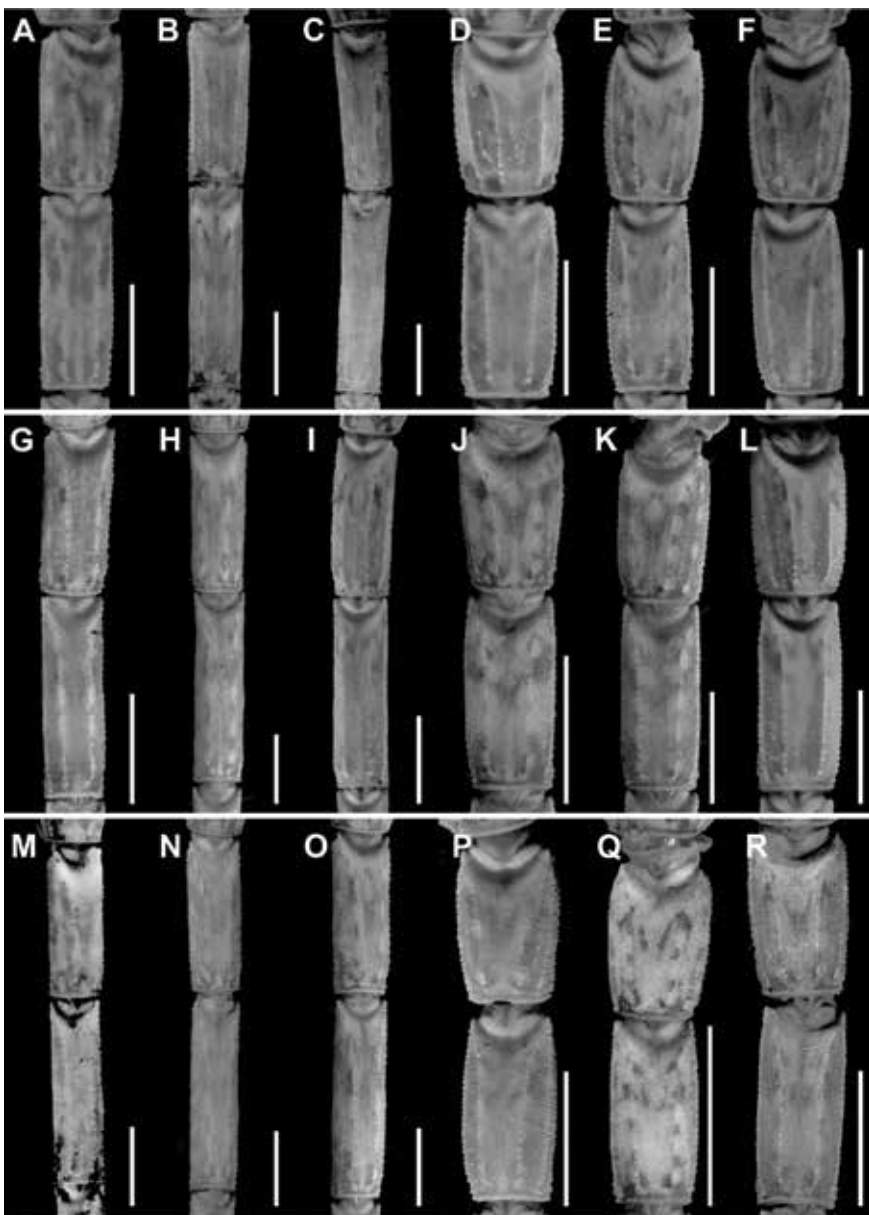


FIGURE 17. *Centruroides* Marx, 1890, metasomal segments I and II, dorsal aspect. A, D. *C. rileyi* Sissom, 1995, A. ♂ (CNAN SC4002), D. ♀ (CNAN SC4003). B, E. *C. hamadryas*, sp. nov., B. holotype ♂ (CNAN T01408), E. paratype ♀ (CNAN T01415). C, F. *C. hoffmanni* Armas, 1996, C. ♂, F. ♀ (CNAN SC3996). G, J. *C. cuauhmapan*, sp. nov., G. holotype ♂ (CNAN T01396), J. paratype ♀ (CNAN T01399). H, K. *C. berstoni*, sp. nov., H. holotype ♂ (CASENT 9073325), K. paratype ♀ (CASENT 9073313). I, L. *C. chanae*, sp. nov., I. holotype ♂ (CNAN T01403), L. paratype ♀ (CNAN T01405). M, P. *C. catemacoensis*, sp. nov., M. holotype ♂ (CNAN T01424), P. paratype ♀ (CNAN T01423). N, Q. *C. schmidti* Sissom, 1995, N. ♂ (CASENT 9073316), Q. ♀ (CASENT 9073317). O, R. *C. yucatanensis*, sp. nov., O. holotype ♂ (CNAN T01416), R. paratype ♀ (CNAN T01417). Scale bars = 2 mm.

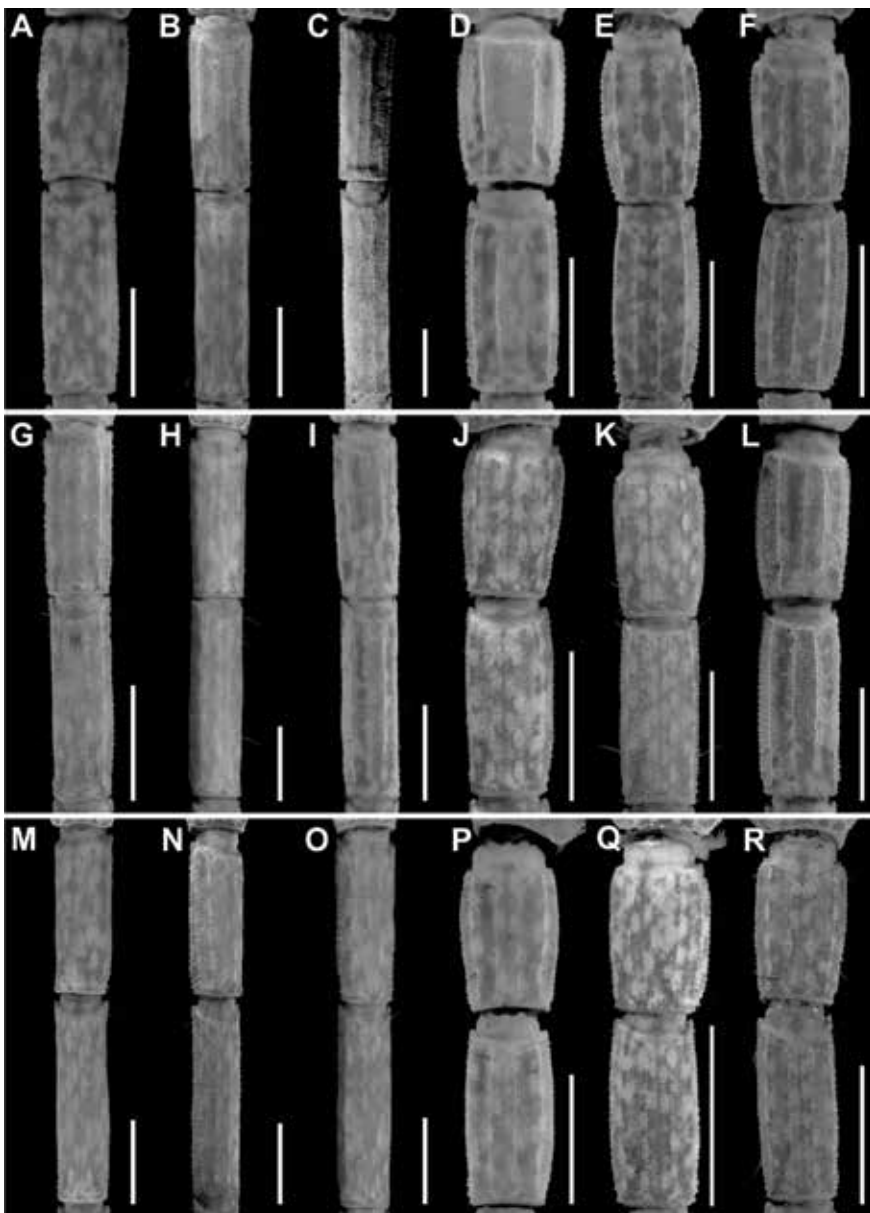


FIGURE 18. *Centruroides* Marx, 1890, metasomal segments I and II, ventral aspect. A, D. *C. rileyi* Sissom, 1995, A. ♂ (CNAN SC4002), D. ♀ (CNAN SC4003). B, E. *C. hamadryas*, sp. nov., B. holotype ♂ (CNAN T01408), E. paratype ♀ (CNAN T01415). C, F. *C. hoffmanni* Armas, 1996, C. ♂, F. ♀ (CNAN SC3996). G, J. *C. cuauhtemapan*, sp. nov., G. holotype ♂ (CNAN T01396), J. paratype ♀ (CNAN T01399). H, K. *C. berstoni*, sp. nov., H. holotype ♂ (CASENT 9073325), K. paratype ♀ (CASENT 9073313). I, L. *C. chanae*, sp. nov., I. holotype ♂ (CNAN T01403), L. paratype ♀ (CNAN T01405). M, P. *C. catemacoensis*, sp. nov., M. holotype ♂ (CNAN T01424), P. paratype ♀ (CNAN T01423). N, Q. *C. schmidti* Sissom, 1995, N. ♂ (CASENT 9073316), Q. ♀ (CASENT 9073317). O, R. *C. yucatanensis*, sp. nov., O. holotype ♂ (CNAN T01416), R. paratype ♀ (CNAN T01417). Scale bars = 2 mm.

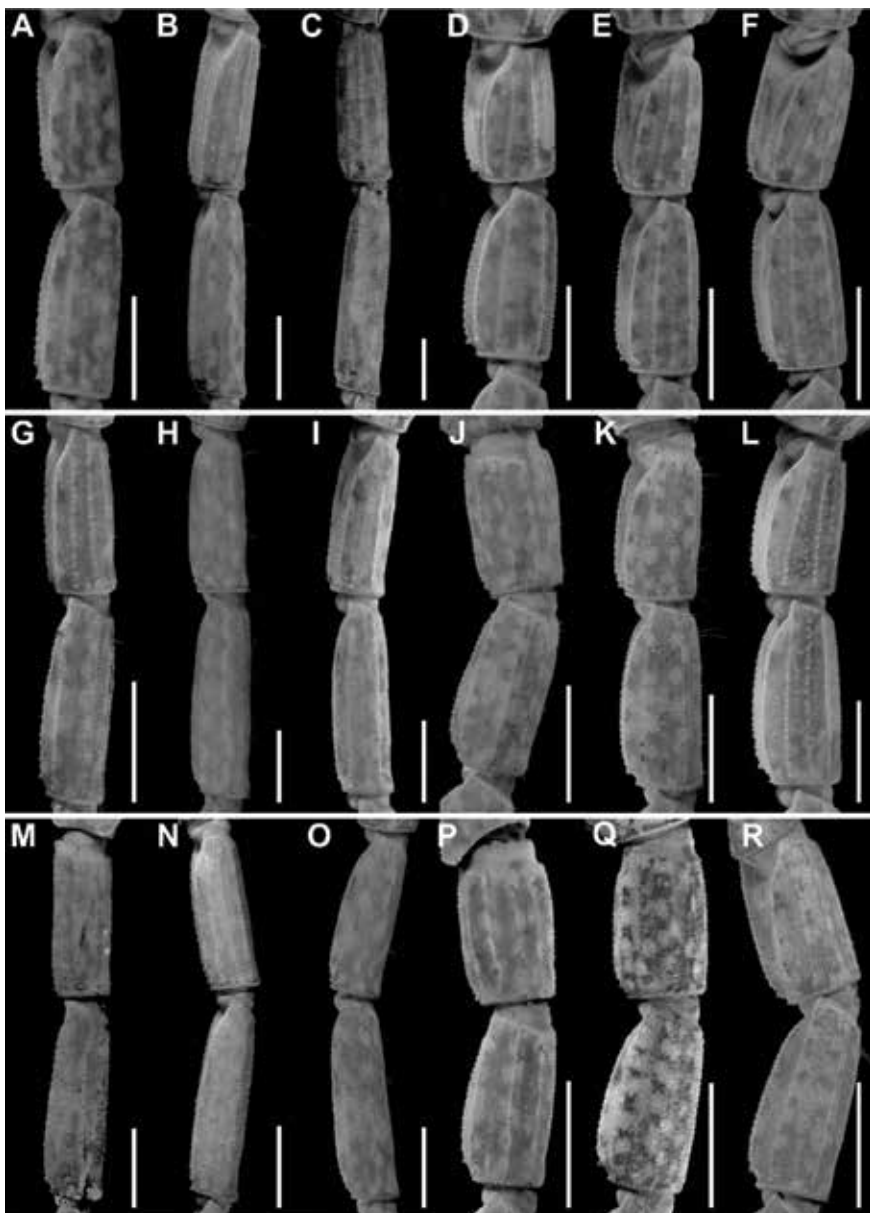


FIGURE 19. *Centruroides* Marx, 1890, metasomal segments I and II, lateral aspect. A, D. *C. rileyi* Sissom, 1995, A. ♂ (CNAN SC4002), D. ♀ (CNAN SC4003). B, E. *C. hamadryas*, sp. nov., B. holotype ♂ (CNAN T01408), E. paratype ♀ (CNAN T01415). C, F. *C. hoffmanni* Armas, 1996, C. ♂, F. ♀ (CNAN SC3996). G, J. *C. cuauhmapan*, sp. nov., G. holotype ♂ (CNAN T01396), J. paratype ♀ (CNAN T01399). H, K. *C. berstoni*, sp. nov., H. holotype ♂ (CASENT 9073325), K. paratype ♀ (CASENT 9073313). I, L. *C. chanae*, sp. nov., I. holotype ♂ (CNAN T01403), L. paratype ♀ (CNAN T01405). M, P. *C. catemacoensis*, sp. nov., M. holotype ♂ (CNAN T01424), P. paratype ♀ (CNAN T01423). N, Q. *C. schmidti* Sissom, 1995, N. ♂ (CASENT 9073316), Q. ♀ (CASENT 9073317). O, R. *C. yucatanensis*, sp. nov., O. holotype ♂ (CNAN T01416), R. paratype ♀ (CNAN T01417). Scale bars = 2 mm.

several small granules; VII surface finely granular, dorsomedian and dorsosubmedian carinae present, dorsolateral carinae finely serrate. Sternites III–VI, surfaces smooth; VII surface weakly granular, ventrolateral carinae serrate.

**Metasoma:** Metasoma length  $2.86 \times$  mesosoma length (table 3). Segments longer than wide; increasing in length posteriorly, segment V  $2 \times$  length of I; carinae distinct, granular; intercarinal surfaces sparsely granular (figs. 20–22G).

**Telson:** Vesicle elongate, ovoid; ventral surface shallowly convex, moderately granular; ventromedian carina granular, terminating at subaculear tubercle; subaculear tubercle narrow and angular in lateral aspect, directed toward midpoint of aculeus. Aculeus angled ventrally at slightly less than  $90^\circ$  (figs. 23–25G).

**Variation:** Adult males and females differ as follows. The dorsomedian carinae of the pedipalp patella are absent, the pectinal tooth count slightly higher (13 or 14), the mesosoma proportionally longer and slenderer, and the metasoma longer, in males (figs. 28A, B, 29A, B, table 3). The first pair of legs are shorter and stouter, the pectinal tooth count slightly lower (11–13), and the metasomal carinae more developed and finely serrate in females (figs. 8C, D, 17G, J, 18G, J, 19G, J, 20G, J, 21G, J, 22G, J, 23G, J, 24G, J, 25G, J, table 3).

**DISTRIBUTION:** *Centruroides cuauhmapan* is endemic to eastern Mexico and recorded from two localities in the state of Veracruz and a third, approximately 200 km south, in the state of Oaxaca (fig. 3).

**ECOLOGY:** The localities at which *C. cuauhmapan* has been recorded range in altitude from 74 to 555 m. The habitat at these localities varies from subtropical highland forest to humid subtropical forest. One individual was collected in a coffee plantation in lowland rainforest. The habitat and habitus are consistent with the arboreal, corticolous ecomorphotype (Prendini, 2001a).

**REMARKS:** Specimens from Córdoba, Veracruz, were misidentified as *C. schmidti* by Armas and Frías (2008). This species has not been recorded from Mexico.

**MATERIAL EXAMINED: MEXICO:** Oaxaca: Municipio San Juan Bautista Tuxtepec: Cerro del Oro Dam, 17 km from San Juan Bautista Tuxtepec,  $17^\circ 59' 55''\text{N}$   $96^\circ 15' 47.2''\text{W}$ , 74 m, 23.v.1990, E. Barrera and A. Cadena, 1 ♂ (CNAN SC4001). Veracruz: Municipio Amatlán de los Reyes: Cañada Blanca,  $18^\circ 55' 43.5''\text{N}$   $96^\circ 51' 26''\text{W}$ , 555 m, 18.vii.2002, E. González, found in coffee plantation in lowland rainforest, collected at night with UV light, 1 ♂ (AMNH [LP 2073]).

### *Centruroides hamadryas*, sp. nov.

Figures 2, 4, 6A, B, 9A, B, 13A, 14A, 17B, E, 18B, E, 19B, E, 20B, E, 21B, E, 22B, E, 23B, E, 24B, E, 25B, E, 32, 33, tables 1, 4, 10

**TYPE MATERIAL: MEXICO:** Chiapas: Municipio Ocosingo: Holotype ♂ (CNAN T01408), paratype ♂ (CNAN T01412), paratype ♀ (CNAN T01413), La Galleta,  $16^\circ 48' 18.5''\text{N}$   $90^\circ 54' 25''\text{W}$ , 103 m, 2.v.2005 A. Valdez, O.F. Francke, and A. Ballesteros, collected with UV light detection; paratype ♂ (CNAN T01414), paratype ♀ (CNAN T01415), same data, except: 2.v.1992, E. Barrera; 2 ♂ paratypes (CNAN T01409, T01411), paratype ♀ (CNAN T01410), same data, except: 114 m, 28.iv.2005, urban area toward blue water bridge.

**ETYMOLOGY:** The species name is noun in apposition, taken from the Greek nymph Hamadryas, mother of the hamadryads, tree-dwelling nymphs with lifelong bonds to the trees.

**DIAGNOSIS:** *Centruroides hamadryas* is most closely related to *C. berstoni*, from which it differs in the following respects. The carapace is densely granular, with distinct lateral ocular carinae, in the female of *C. hamadryas* (fig. 6B) but sparsely granular, more densely so on the interocular triangle, in the female of *C. berstoni* (fig. 6D). The pedipalp chela manus of the male is proportionally more incrassate in *C. hamadryas* (fig. 13A) than *C. berstoni* (fig. 13B). The legs of the male are less than  $2 \times$  the length of the carapace in *C. hamadryas* but greater than  $2 \times$  the length of the carapace in *C. berstoni* (table 10).

TABLE 7

**Meristic data for *Centruroides schmidti* Sissom, 1995**

Material deposited in the California Academy of Sciences (CASENT), San Francisco. Measurements follow Stahnke (1970), Lamoral (1979), and Prendini (2001b).

		♂				♀			
		CASENT 9073316				CASENT 9073317			
Total length <sup>1</sup>		47.9	47.4	35.3	37.7	34.8	33.3	34.9	33.8
Carapace	length	3.6	3.6	3.0	2.9	3.3	3.2	3.3	3.2
	ant. width	1.8	1.8	1.5	1.5	1.7	1.7	1.7	1.7
	post. width	3.9	3.9	3.3	3.2	3.7	3.6	3.8	3.7
Median ocelli	diameter	0.3	0.3	0.3	0.3	0.3	0.3	0.3	0.3
Interocular	length <sup>2</sup>	0.3	0.4	0.3	0.3	0.4	0.4	0.3	0.3
Pedipalp	length <sup>3</sup>	17.0	16.3	13.2	13.3	14.2	13.8	14.1	13.8
Trochanter	length	1.6	1.5	1.3	1.3	1.4	1.3	1.4	1.3
Femur	length	4.1	3.9	3.0	3.1	3.3	3.1	3.2	3.2
	width	0.7	0.7	0.6	0.5	0.7	0.6	0.7	0.7
	height	1.0	1.0	0.9	0.8	1.0	1.0	1.0	1.0
Patella	length	4.5	4.2	3.7	3.5	3.7	3.6	3.7	3.5
	width	1.0	1.0	0.8	0.8	1.0	1.0	0.9	1.0
	height	1.6	1.6	1.3	1.3	1.5	1.5	1.5	1.5
Chela	length <sup>4</sup>	6.8	6.7	5.2	5.4	5.8	5.8	5.8	5.8
Manus	length	2.6	2.7	2.2	2.3	2.2	2.1	2.1	2.3
	width	1.5	1.4	1.0	1.1	1.1	1.2	1.2	1.2
	height	1.3	1.3	1.0	1.1	1.2	1.1	1.2	1.1
Mov. finger	length	4.2	4.3	3.5	3.1	4.0	4.0	4.1	4.0
Leg I	length	7.0	6.8	5.6	5.6	6.1	6.0	6.0	6.1
Pectines	length	6.2	6.2	4.6	4.7	4.3	4.5	5.0	5.0
	tooth count	15/15	16/15	14/14	15/15	12/12	13/13	14/14	14/14
Mesosoma	length <sup>5</sup>	11.8	11.6	8.8	10.1	11.7	10.4	11.2	11.6
Sternite VII	length	3.4	3.3	2.4	2.7	3.0	2.5	3.0	2.6
	width	3.5	3.4	2.9	2.9	4.1	3.8	4.1	4.1
Metasoma	length <sup>6</sup>	32.5	32.2	23.5	24.7	19.8	19.7	20.4	19.0
Metasoma I	length	4.2	4.1	3.0	3.1	2.1	2.4	2.3	2.2
	width	1.4	1.4	1.4	1.2	1.7	1.7	1.8	1.6
	height	1.4	1.5	1.4	1.3	1.5	1.5	1.6	1.5
Metasoma II	length	5.1	5.0	3.7	3.8	3.0	2.9	3.1	3.0
	width	1.4	1.4	1.3	1.2	1.6	1.5	1.6	1.5
	height	1.3	1.3	1.2	1.2	1.5	1.5	1.5	1.3
Metasoma III	length	5.7	5.7	4.2	4.0	3.3	3.2	3.2	3.2
	width	1.3	1.4	1.3	1.2	1.4	1.4	1.6	1.5
	height	1.2	1.3	1.2	1.1	1.6	1.4	1.4	1.4

TABLE 7 *continued*

		♂				♀			
		CASENT 9073316				CASENT 9073317			
Metasoma IV	length	6.5	6.2	4.5	4.7	3.8	3.7	3.8	3.7
	width	1.3	1.3	1.2	1.1	1.4	1.4	1.5	1.4
	height	1.2	1.2	1.1	1.1	1.5	1.4	1.4	1.3
Metasoma V	length	7.0	6.7	4.7	5.5	4.1	4.0	4.4	3.7
	width	1.3	1.3	1.2	1.2	1.4	1.4	1.5	1.4
	height	1.3	1.3	1.2	1.1	1.5	1.5	1.4	1.3
Telson	length	4.0	4.5	3.4	3.6	3.5	3.5	3.6	3.2
Vesicle	length	3.0	3.2	2.3	2.5	2.2	2.1	2.2	2.1
	width	1.3	1.2	0.9	1.0	0.9	1.0	1.1	1.3
	height	1.2	1.3	0.9	0.9	1.0	1.0	1.2	1.1
Aculeus	length	1.3	1.5	1.1	1.3	1.5	1.5	1.4	1.0

<sup>1</sup> Sum of carapace, tergites I–VII, metasomal segments I–V, and telson; <sup>2</sup> distance between median ocelli; <sup>3</sup> sum of trochanter, femur, patella, and chela; <sup>4</sup> measured from base of condyle to tip of fixed finger; <sup>5</sup> sum of tergites I–VII; <sup>6</sup> sum of metasomal segments I–V and telson.

The dorsomedian carinae of the mesosomal tergites are distinct and complete in *C. hamadryas* but weakly developed and restricted to the posterior half of the segments in *C. berstoni*. The ventrolateral and ventrosubmedian carinae of mesosomal sternite VII are weakly developed to absent in *C. hamadryas*, whereas the ventrolateral carinae are weakly developed and the ventrosubmedian carinae absent in *C. berstoni*. The telson vesicle is densely setose in *C. hamadryas* but sparsely setose in *C. berstoni*.

Additional differences between *C. hamadryas* and other species of the clade are as follows. The retrodorsal carina of the chela manus is complete and the dorsomedian carina weakly developed and restricted to the distal half, in the male of *C. hamadryas* (fig. 13A), whereas the retrodorsal carina is weakly granular and the dorsomedian carina absent in the male of *C. berstoni* (fig. 13B), *C. catemacoensis* (fig. 11B), *C. cuauhmapan* (fig. 11C), and *C. rileyi* (fig. 11A). The retrodorsal carina of the manus of the female is complete and the prodorsal carina restricted to the distal third in the female of *C. hamadryas* (fig. 13B), whereas the retrodorsal carina is finely granular and the prodorsal carina absent in the female of

*C. berstoni* (fig. 14B), *C. catemacoensis* (fig. 12B), *C. cuauhmapan* (fig. 12C), and *C. rileyi* (fig. 12A). The pedipalp chela fingers bear short, dense setation in *C. hamadryas* but sparse setation in *C. berstoni*. The dorsosubmedian and dorsolateral carinae of metasomal segments I–III are well developed and granular in the male of *C. hamadryas* (figs. 17–19E) but weakly developed to absent in the male of *C. berstoni* (figs. 17–19K). The telson vesicle of the male is not posteriorly bilobed in *C. hamadryas* (figs. 23–25B), unlike *C. cuauhmapan* (figs. 23–25G) and *C. rileyi* (figs. 23–25A). The vesicle of the female is shorter and more robust, with intercarinal surfaces smooth in *C. hamadryas* (figs. 23–25E), but sparsely granular in *C. berstoni* (figs. 23–25K) and densely granular in *C. catemacoensis* (figs. 23–25P), *C. cuauhmapan* (figs. 23–25J), and *C. rileyi* (figs. 23–25D).

**DESCRIPTION:** The following description is based on the holotype male, with differences among other material noted in the section on variation.

**Coloration:** Base color pale yellow, with extensive infuscation, creating mottled or marbled pattern. Carapace with uniformly infuscate mar-

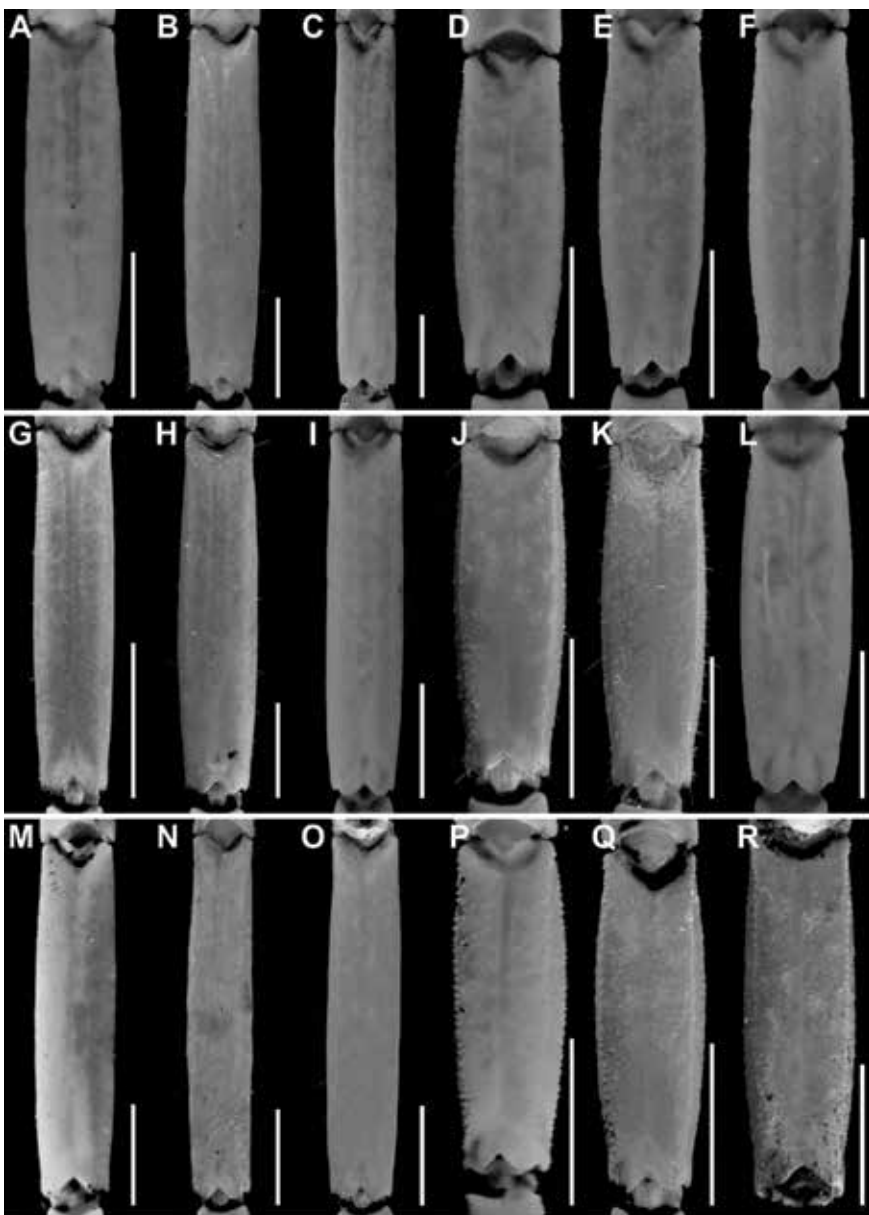


FIGURE 20. *Centruroides* Marx, 1890, metasomal segment V, dorsal aspect. A, D. *C. rileyi* Sissom, 1995, A. ♂ (CNAN SC4002), D. ♀ (CNAN SC4003). B, E. *C. hamadryas*, sp. nov., B. holotype ♂ (CNAN T01408), E. paratype ♀ (CNAN T01415). C, F. *C. hoffmanni* Armas, 1996, C. ♂, F. ♀ (CNAN SC3996). G, J. *C. cuauh-mapan*, sp. nov., G. holotype ♂ (CNAN T01396), J. paratype ♀ (CNAN T01399). H, K. *C. berstoni*, sp. nov., H. holotype ♂ (CASENT 9073325), K. paratype ♀ (CASENT 9073313). I, L. *C. chanae*, sp. nov., I. holotype ♂ (CNAN T01403), L. paratype ♀ (CNAN T01405). M, P. *C. catemacoensis*, sp. nov., M. holotype ♂ (CNAN T01424), P. paratype ♀ (CNAN T01423). N, Q. *C. schmidti* Sissom, 1995, N. ♂ (CASENT 9073316), Q. ♀ (CASENT 9073317). O, R. *C. yucatanensis*, sp. nov., O. holotype ♂ (CNAN T01416), R. paratype ♀ (CNAN T01417). Scale bars = 2 mm.

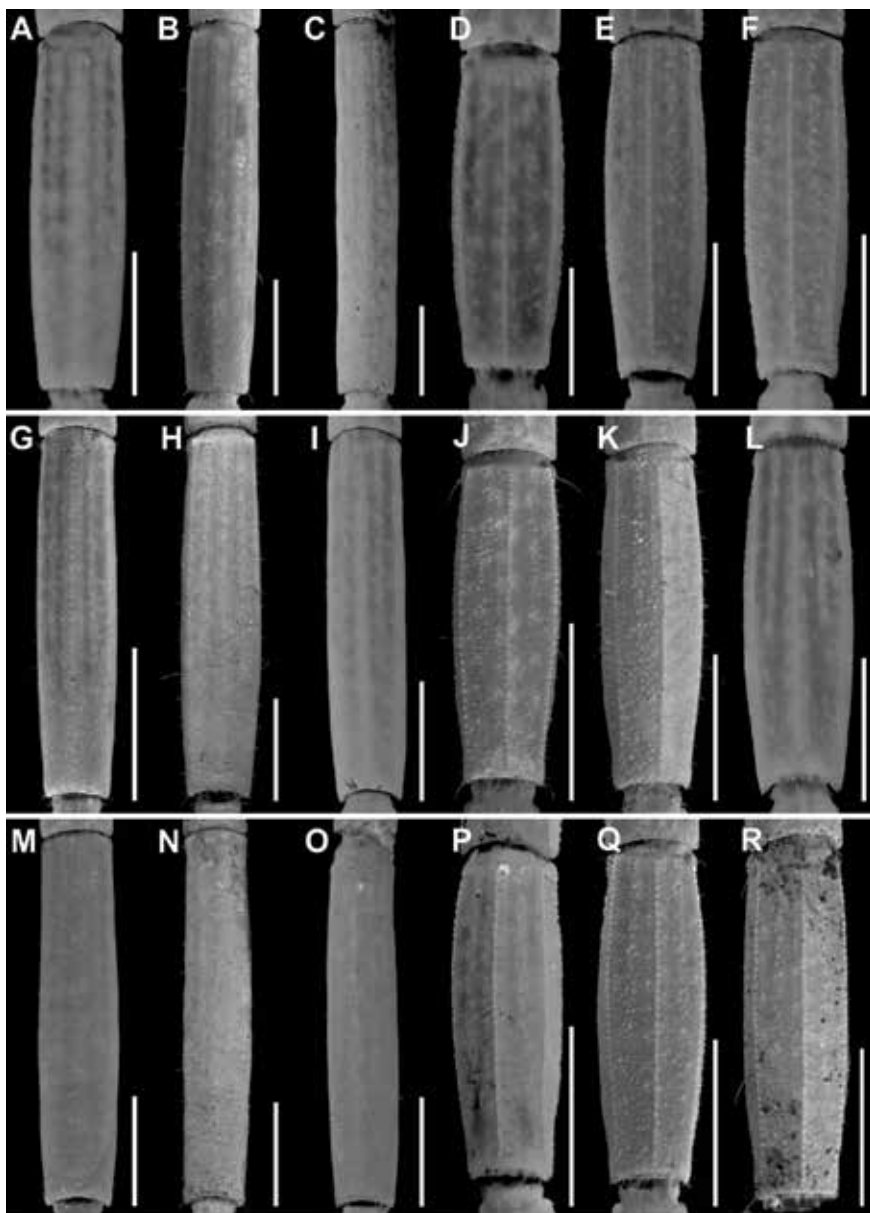


FIGURE 21. *Centruroides* Marx, 1890, metasomal segment V, ventral aspect. A, D. *C. rileyi* Sissom, 1995, A. ♂ (CNAN SC4002), D. ♀ (CNAN SC4003). B, E. *C. hamadryas*, sp. nov., B. holotype ♂ (CNAN T01408), E. paratype ♀ (CNAN T01415). C, F. *C. hoffmanni* Armas, 1996, C. ♂, F. ♀ (CNAN SC3996). G, J. *C. cuauhmapan*, sp. nov. G. holotype ♂ (CNAN T01396), J. paratype ♀ (CNAN T01399). H, K. *C. berstoni*, sp. nov., H. holotype ♂ (CASENT 9073325), K. paratype ♀ (CASENT 9073313). I, L. *C. chanae*, sp. nov., I. holotype ♂ (CNAN T01403), L. paratype ♀ (CNAN T01405). M, P. *C. catemacoensis*, sp. nov., M. holotype ♂ (CNAN T01424), P. paratype ♀ (CNAN T01423). N, Q. *C. schmidti* Sissom, 1995, N. ♂ (CASENT 9073316), Q. ♀ (CASENT 9073317). O, R. *C. yucatanensis*, sp. nov., O. holotype ♂ (CNAN T01416), R. paratype ♀ (CNAN T01417). Scale bars = 2 mm.

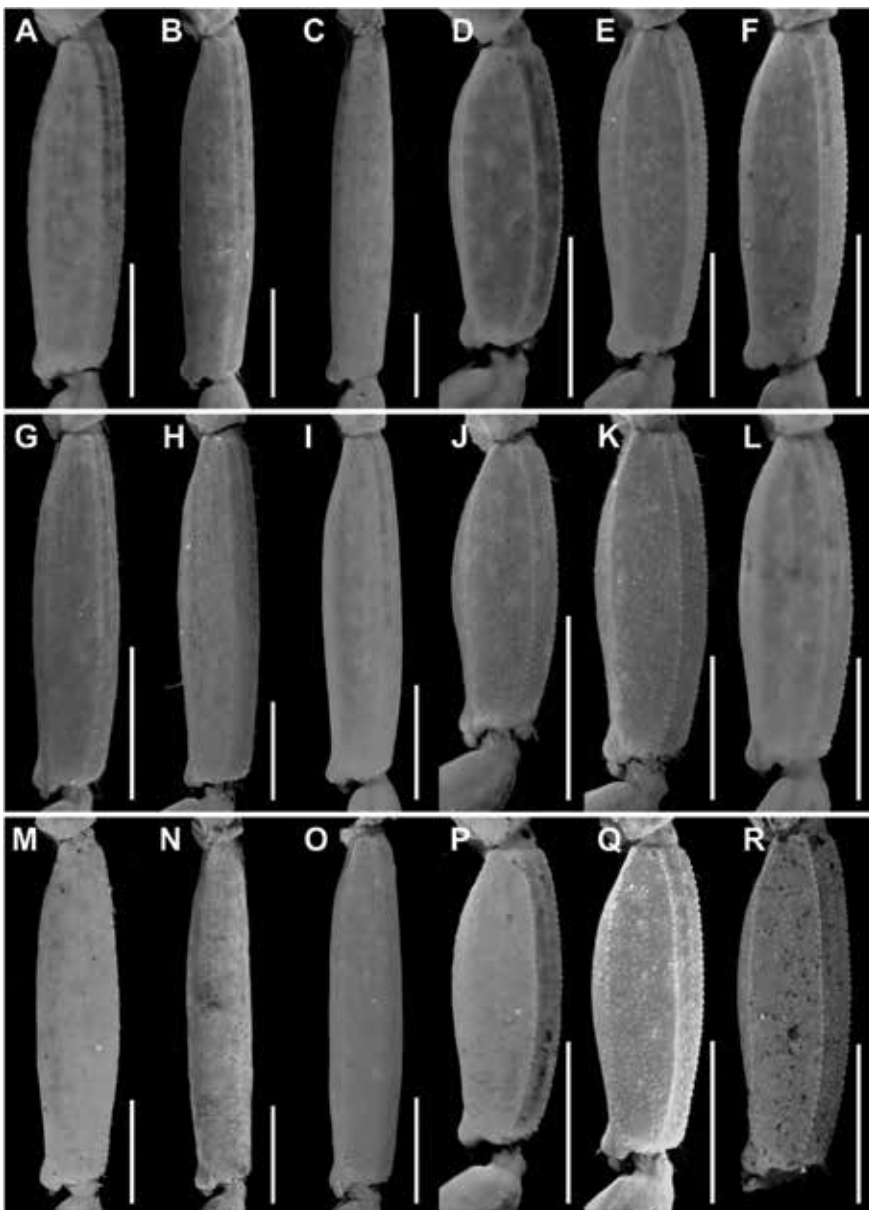


FIGURE 22. *Centruroides* Marx, 1890, metasomal segment V, lateral aspect. A, D. *C. rileyi* Sissom, 1995, A. ♂ (CNAN SC4002), D. ♀ (CNAN SC4003). B, E. *C. hamadryas*, sp. nov., B. holotype ♂ (CNAN T01408), E. paratype ♀ (CNAN T01415). C, F. *C. hoffmanni* Armas, 1996, C. ♂, F. ♀ (CNAN SC3996). G, J. *C. cuauhmapan*, sp. nov., G. holotype ♂ (CNAN T01396), J. paratype ♀ (CNAN T01399). H, K. *C. berstoni*, sp. nov., H. holotype ♂ (CASENT 9073325), K. paratype ♀ (CASENT 9073313). I, L. *C. chanae*, sp. nov., I. holotype ♂ (CNAN T01403), L. paratype ♀ (CNAN T01405). M, P. *C. catemacoensis*, sp. nov., M. holotype ♂ (CNAN T01424), P. paratype ♀ (CNAN T01423). N, Q. *C. schmidti* Sissom, 1995, N. ♂ (CASENT 9073316), Q. ♀ (CASENT 9073317). O, R. *C. yucatanensis*, sp. nov., O. holotype ♂ (CNAN T01416), R. paratype ♀ (CNAN T01417). Scale bars = 2 mm.

bling, more densely infuscate medially. Pedipalp chela fingers and manus, dorsal and retrolateral intercarinal surfaces with moderately infuscate marbling; prolateral and ventral intercarinal surfaces mostly immaculate. Legs retrolateral surfaces with infuscate marbling; prolateral surfaces pale, immaculate. Tergites with uniformly infuscate mottling, pale stripe medially, blackish spots submedially, and faint, narrow bands laterally. Sternites pale, with faintly infuscate triangular to trapezoidal marking at posterior margin of sternite III, fading to infuscate mottling on sternite VII. Metasomal segments uniformly, faintly marbled; segment V and telson markedly infuscate, noticeably darker than preceding segments.

**Carapace:** Shape trapezoidal; anterior width four-fifths of posterior width (table 4); anteromedian sulcus moderately deep, oval; posteromedian sulcus shallow anteriorly, deeper posteriorly; median ocular tubercle moderately granular; carinae weakly developed, comprising small to medium-sized granules (fig. 6A).

**Pedipalps:** Orthobothriotaxic, Type A; femur dorsal trichobothria with a configuration; pedipalp chela fixed finger, trichobothrium *db* situated slightly distal to *et*. Femoral carinae serrate; retromedian carinae comprising spiniform granules; dorsal intercarinal surface moderately granular; prolateral surface with series of large spiniform granules. Patella prodorsal, dorsomedian, retrodorsal and proventral carinae moderately developed, serrate; retromedian carina well developed, serrate; retroventral carina incomplete, serrate; prolateral intercarinal surface with five or six large, subspiniform granules. Chela manus proventral carina moderately developed, comprising few rounded granules; other carinae weakly developed, granular. Fixed finger, median denticle row comprising eight oblique subrows, each flanked by pro- and retrolateral supernumerary denticles. Movable finger, median denticle row with short terminal row comprising four denticles preceded by eight oblique subrows, each flanked by pro- and retrolateral supernumerary denticles.

**Legs:** Leg I length 1.88× greater than carapace length (table 10). Telotarsi ventral surfaces densely covered with short setae; unguis markedly curved.

**Pectines:** Pectinal plate 1.9× wider than long; posterior margin distinctly rounded; pectinal tooth count 14/14 (♂) (fig. 6A, table 4).

**Mesosoma:** Tergites width similar to carapace posterior width; I and II slightly narrower (table 4). Pretergites surfaces smooth to finely granular. Posttergites surfaces weakly granular; I–VI with dorso-median carinae moderately granular; VII surface weakly granular, dorsomedian carina moderately granular, dorsosubmedian carinae serrate, dorsolateral carinae well developed. Sternites III–VI, surfaces smooth; VII surface weakly granular, ventrolateral carinae reduced to few granules.

**Metasoma:** Metasoma length 3.01× mesosoma length (table 4). Segments longer than wide; increasing in length posteriorly, segment V 2× length of I; carinae complete, granular on segments I–III, other carinae absent or obsolete; intercarinal surfaces sparsely granular (figs. 17–22E).

**Telson:** Vesicle elongate, ovoid; ventral surface shallowly convex, sparsely granular posteriorly; ventromedian carina granular, terminating at subaculear tubercle; subaculear tubercle narrow and angular in lateral aspect, directed toward midpoint of aculeus. Aculeus angled ventrally at slightly less than 90° (fig. 25B, E).

**Variation:** Adult males and females differ as follows. The pectinal tooth count is slightly higher (14 or 15), the mesosoma proportionally longer and slenderer, and the metasoma up to 3× longer, with segment V also roughly 1.5 mm longer, in males (figs. 23B, E, 24B, E, 25B, E, table 4). The tegument is more densely infuscate, the pectinal plate produced into a rounded lobe posteriorly, which is punctate and slightly infuscate, the pectinal tooth count slightly lower (12 or 13), and the telson shorter and narrower, in females (figs. 9A, B, 23B, E, 24B, E, 25B, E, 32A, B, 33A, B, table 4).

**DISTRIBUTION:** *Centruroides hamadryas* is known only from the state of Chiapas in southeastern Mexico, but may extend across the Usu-

TABLE 8

**Meristic data for *Centruroides hoffmanni* Armas, 1996**

Material deposited in the Colección Nacional de Arácnidos (CNAN), Universidad Nacional Autónoma de México, Mexico City. Measurements follow Stahnke (1970), Lamoral (1979), and Prendini (2001b).

		♂				♀				
		CNAN				CNAN				
		SC3993	SC3996	SC3997	SC3998	SC3993	SC3996	SC3996	SC3996	
Total length <sup>1</sup>		37.1	55.9	38.4	40.5	42.7	35.5	33.1	34.8	33.7
Carapace	length	3.1	3.9	3.3	3.2	3.3	3.4	3.4	3.3	3.4
	ant. width	1.5	1.9	1.7	1.5	1.6	1.8	1.9	1.8	1.8
	post. width	3.4	4.0	3.6	3.3	3.3	3.8	3.9	3.9	3.7
Median ocelli	diameter	0.3	0.3	0.3	0.3	0.3	0.3	0.3	0.3	0.3
Interocular	length <sup>2</sup>	0.3	0.4	0.4	0.3	0.3	0.3	0.3	0.4	0.4
Pedipalp	length <sup>3</sup>	12.8	18.1	14.0	14.2	15.1	14.0	14.2	14.6	14.3
Trochanter	length	1.1	1.6	1.3	1.4	1.3	1.4	1.4	1.5	1.4
Femur	length	2.6	4.2	3.2	3.4	3.6	3.2	3.3	3.3	3.3
	width	0.5	0.7	0.6	0.6	0.6	0.8	0.8	0.7	0.9
	height	0.9	1.1	0.9	0.9	1.0	1.0	1.0	1.0	1.0
Patella	length	3.6	4.9	3.6	3.8	4.0	3.7	3.7	3.8	3.9
	width	0.8	1.0	0.8	0.9	0.8	1.0	1.0	1.0	1.2
	height	1.2	1.7	1.4	1.4	1.3	1.4	1.5	1.5	1.6
Chela	length <sup>4</sup>	5.5	7.4	6.0	5.7	6.2	5.7	5.8	6.0	5.7
Manus	length	2.4	3.4	2.5	2.5	2.8	2.1	2.3	2.3	2.4
	width	1.1	1.5	1.2	1.1	1.3	1.1	1.3	1.1	1.2
	height	1.0	1.5	1.2	1.1	1.2	1.0	1.1	1.1	1.3
Mov. finger	length	3.5	4.7	3.6	3.4	3.8	4.0	4.0	4.0	4.0
Leg I	length	5.6	7.5	5.8	6.0	6.0	6.1	6.4	6.2	5.8
Pectines	length	4.8	6.5	5.0	4.7	4.8	4.7	4.5	4.5	4.5
	tooth count	14/14	15/15	14/14	15/15	13/13	15/14	13/13	13/14	13/13
Mesosoma	length <sup>5</sup>	10.1	13.1	10.4	9.8	10.6	11.7	9.4	11.4	10.5
Sternite VII	length	2.8	4.0	3.0	3.1	2.9	2.8	2.6	2.9	2.6
	width	3.0	3.9	3.1	3.0	3.1	4.3	4.0	4.3	4.1
Metasoma	length <sup>6</sup>	23.9	38.9	24.7	27.5	28.8	20.4	20.3	20.1	19.8
Metasoma I	length	3.1	4.8	3.1	3.5	3.5	2.5	2.7	2.5	2.3
	width	1.3	1.6	1.3	1.3	1.2	1.7	1.8	1.8	1.8
	height	1.3	1.5	1.3	1.2	1.2	1.5	1.5	1.5	1.5
Metasoma II	length	3.3	6.8	3.9	4.2	4.4	3.3	3.1	3.2	3.2
	width	1.2	1.4	1.2	1.2	1.2	1.5	1.6	1.5	1.6
	height	1.2	1.4	1.2	1.1	1.1	1.5	1.5	1.5	1.7

TABLE 8 *continued*

		$\delta$					$\varphi$			
		CNAN					CNAN			
		SC3993	SC3996	SC3997	SC3998		SC3993	SC3996		
Metasoma III	length	4.2	7.1	4.1	5.0	5.2	3.6	3.4	3.4	3.4
	width	1.2	1.4	1.2	1.1	1.2	1.5	1.5	1.5	1.5
	height	1.2	1.3	1.2	1.1	1.2	1.4	1.5	1.5	1.5
Metasoma IV	length	4.8	7.7	5.1	5.5	5.8	4.0	3.8	3.7	3.8
	width	1.2	1.3	1.2	1.1	1.1	1.4	1.4	1.3	1.6
	height	1.2	1.3	1.1	1.1	1.1	1.3	1.4	1.3	1.5
Metasoma V	length	5.2	8.2	5.4	5.7	6.2	4.1	4.3	4.3	4.3
	width	1.2	1.5	1.2	1.2	1.2	1.5	1.4	1.3	1.5
	height	1.2	1.4	1.2	1.1	1.1	1.3	1.3	1.4	1.4
Telson	length	3.3	4.3	3.1	3.6	3.7	2.9	3.0	3.0	2.8
Vesicle	length	2.3	3.1	2.1	2.6	2.7	1.7	1.8	1.7	1.7
	width	1.0	1.4	1.1	0.9	1.0	1.2	1.1	1.0	1.0
	height	1.0	1.4	1.0	0.9	1.0	1.0	1.0	1.0	1.0
Aculeus	length	1.2	1.3	1.2	1.1	1.0	1.2	1.2	1.3	1.3

<sup>1</sup> Sum of carapace, tergites I–VII, metasomal segments I–V, and telson; <sup>2</sup> distance between median ocelli; <sup>3</sup> sum of trochanter, femur, patella, and chela; <sup>4</sup> measured from base of condyle to tip of fixed finger; <sup>5</sup> sum of tergites I–VII; <sup>6</sup> sum of metasomal segments I–V and telson.

macinta River into Guatemala. The known records occur in the Lacondón Forest, on the northern edge of the Montes Azules Biosphere Reserve (fig. 4).

**ECOLOGY:** The localities at which *C. hamadryas* has been recorded range in altitude from 103 to 153 m, all situated in a lowland tropical rainforest. Most specimens of this strictly arboreal species were located with UV light detection at night and captured by holding an insect net beneath the branch on which they were sitting and tapping the branch with a stick; their escape reaction is to drop immediately to the leaf litter below, where they invariably disappear. The habitat and habitus are consistent with the arboreal, corticolous ecomorphotype (Prendini, 2001a).

**REMARKS:** Specimens from Frontera Corozal, Chiapas, Mexico, were misidentified as *C. schmidti* by Francke (2007). Teruel and Stockwell (2002) and Francke (2007) noted differences among the pectinal counts of specimens from Chiapas, with 13–16 ( $\delta$ ) and 13–14 ( $\varphi$ ), and Honduras, with

12–15 ( $\delta$ ) and 13–15 ( $\varphi$ ). Although this slight variation in pectinal tooth counts does not provide sufficient evidence to distinguish between *C. hamadryas* and *C. schmidti*, additional morphological differences, outlined in their respective diagnoses, together with genetic divergence among samples from the two areas, confirmed the distinction between them.

**MATERIAL EXAMINED: MEXICO: Chiapas:** Município Ocosingo: La Galleta, 2 km SE of Frontera Corozal, 16°48'12.7"N 90°52'11.1"W, 132–150 m, 28.iv.2004, R. Paredes and J.L. Castelo, collected with UV light detection, 2  $\delta$  (AMNH [LP 2948]), 1  $\varphi$  (CNAN SC3987), 16°49'55"N 90°56'08"W, 146 m, 7.iv.2005, A. Valdez, O.F. Francke, and A. Ballesteros, collected at night with UV lamp, 1 juv.  $\delta$  (CNAN SC3986), 16°48'18.5"N 90°54'25"W, 114 m, 28.iv.2005, A. Valdez, O.F. Francke, and A. Ballesteros, urban area toward blue water bridge, collected with UV light detection, 2  $\delta$ , 1  $\varphi$ , 1 juv.  $\delta$ , 1 juv. (CNAN SC3988).

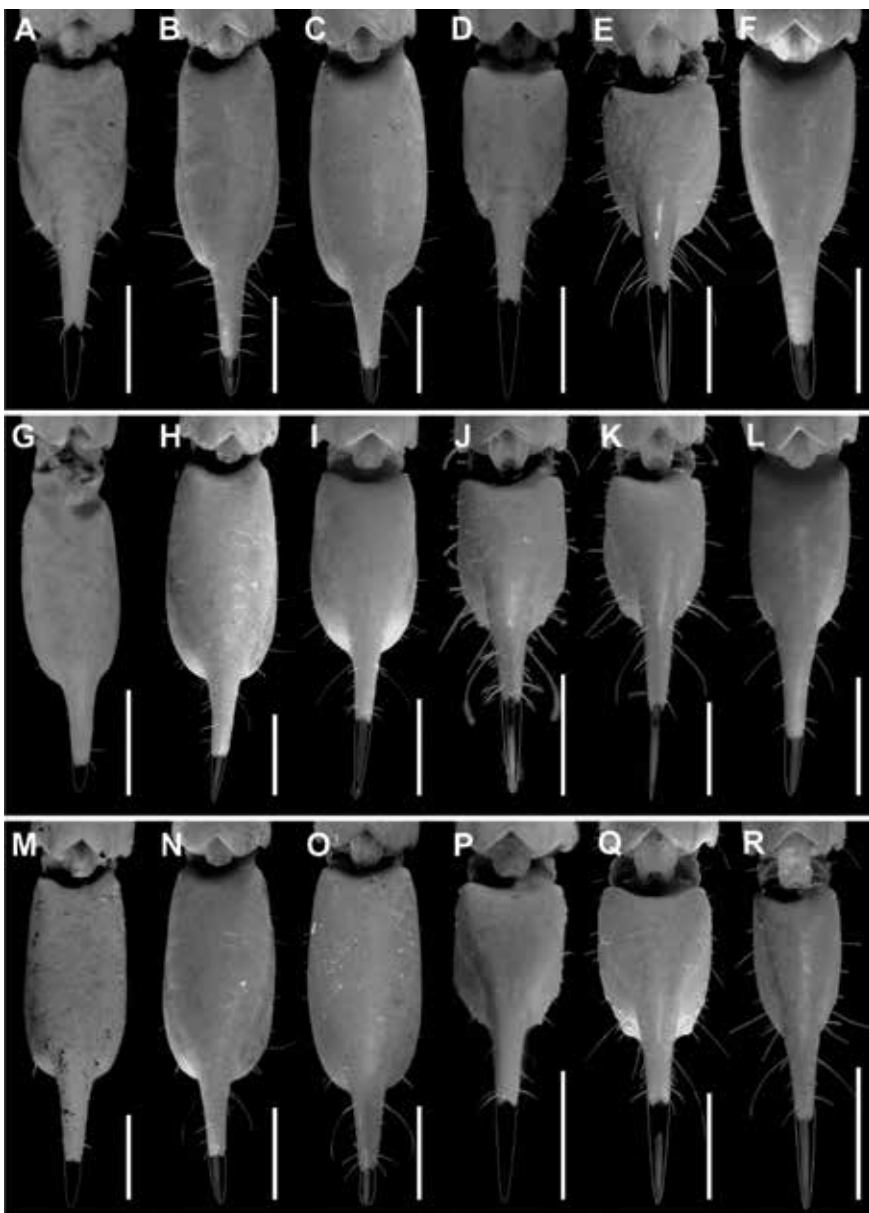


FIGURE 23. *Centruroides* Marx, 1890, telson, dorsal aspect. A, D. *C. rileyi* Sissom, 1995, A. ♂ (CNAN SC4002), D. ♀ (CNAN SC4003). B, E. *C. hamadryas*, sp. nov., B. holotype ♂ (CNAN T01408), E. paratype ♀ (CNAN T01415). C, F. *C. hoffmanni* Armas, 1996, C. ♂, F. ♀ (CNAN SC3996). G, J. *C. cuauhmapan*, sp. nov., G. holotype ♂ (CNAN T01396), J. paratype ♀ (CNAN T01399). H, K. *C. berstoni*, sp. nov., H. holotype ♂ (CASENT 9073325), K. paratype ♀ (CASENT 9073313). I, L. *C. chanae*, sp. nov., I. holotype ♂ (CNAN T01403), L. paratype ♀ (CNAN T01405). M, P. *C. catemacoensis*, sp. nov., M. holotype ♂ (CNAN T01424), P. paratype ♀ (CNAN T01423). N, Q. *C. schmidti* Sissom, 1995, N. ♂ (CASENT 9073316), Q. ♀ (CASENT 9073317). O, R. *C. yucatanensis*, sp. nov., O. holotype ♂ (CNAN T01416), R. paratype ♀ (CNAN T01418). Scale bars = 1 mm.

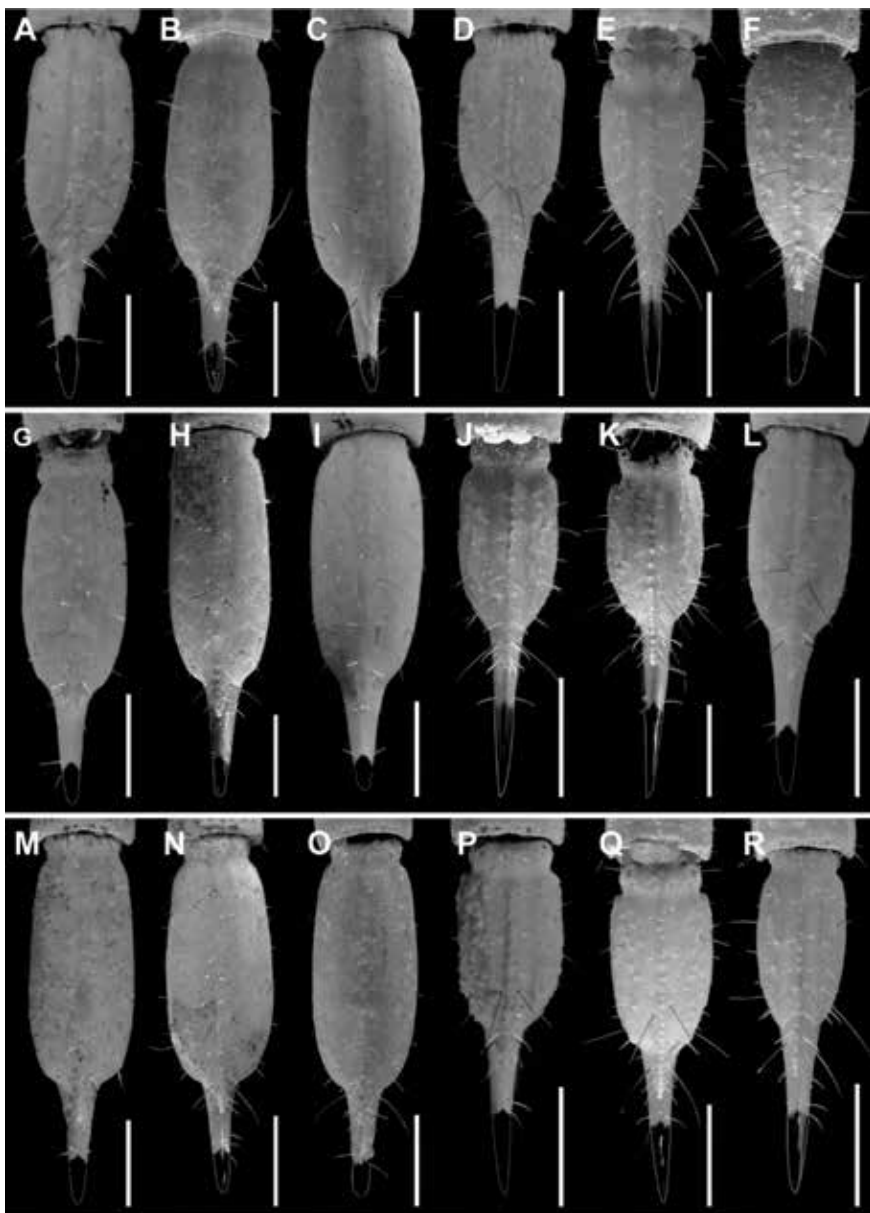


FIGURE 24. *Centruroides* Marx, 1890, telson, ventral aspect. A, D. *C. rileyi* Sissom, 1995, A. ♂ (CNAN SC4002), D. ♀ (CNAN SC4003). B, E. *C. hamadryas*, sp. nov., B. holotype ♂ (CNAN T01408), E. paratype ♀ (CNAN T01415). C, F. *C. hoffmanni* Armas, 1996, C. ♂, F. ♀ (CNAN SC3996). G, J. *C. cuauhmapan*, sp. nov., G. holotype ♂ (CNAN T01396), J. paratype ♀ (CNAN T01399). H, K. *C. berstoni*, sp. nov., H. holotype ♂ (CASENT 9073325), K. paratype ♀ (CASENT 9073313). I, L. *C. chanae*, sp. nov., I. holotype ♂ (CNAN T01403), L. paratype ♀ (CNAN T01405). M, P. *C. catemacoensis*, sp. nov., M. holotype ♂ (CNAN T01424), P. paratype ♀ (CNAN T01423). N, Q. *C. schmidti* Sissom, 1995, N. ♂ (CASENT 9073316), Q. ♀ (CASENT 9073317). O, R. *C. yucatanensis*, sp. nov., O. holotype ♂ (CNAN T01416), R. paratype ♀ (CNAN T01418). Scale bars = 1 mm.

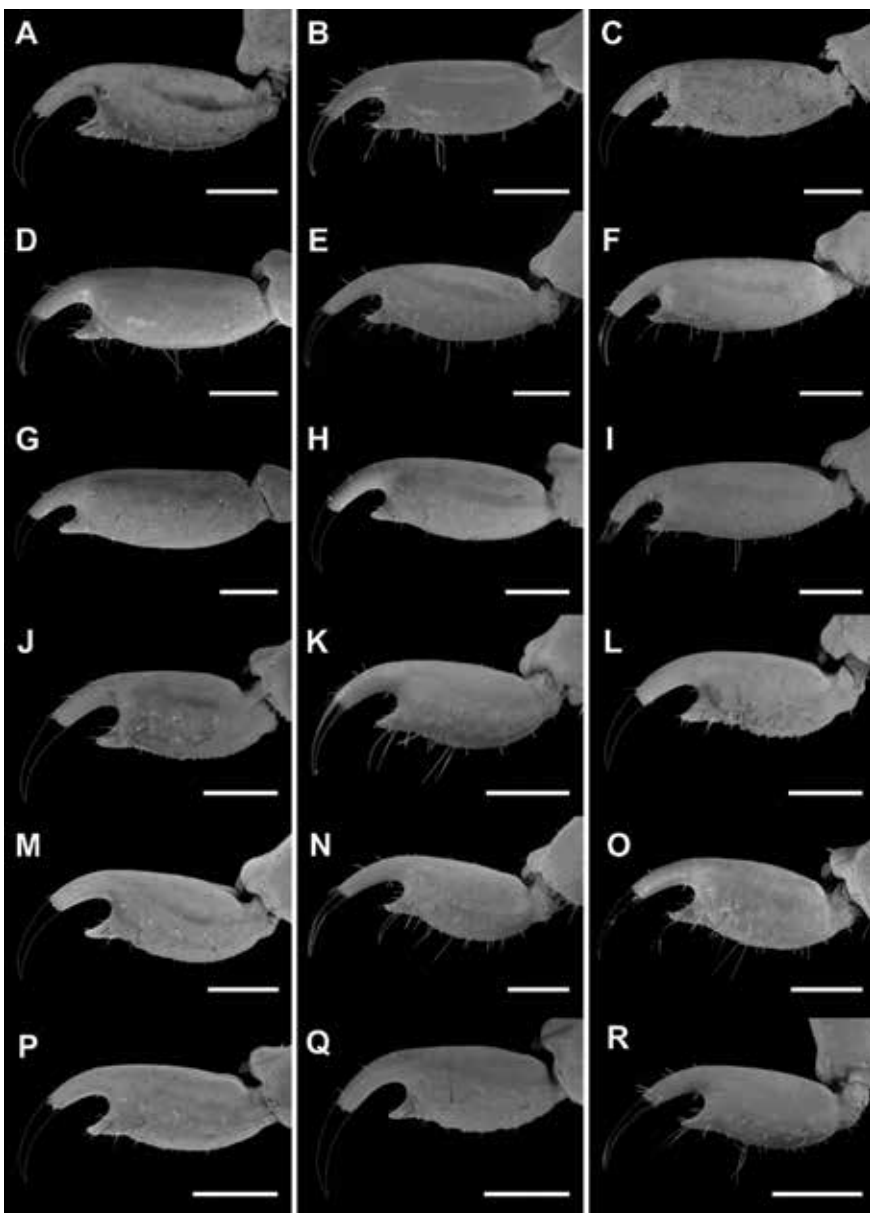


FIGURE 25. *Centruroides* Marx, 1890, telson, lateral aspect. A, D. *C. rileyi* Sissom, 1995, A. ♂ (CNAN SC4002), D. ♀ (CNAN SC4003). B, E. *C. hamadryas*, sp. nov., B. holotype ♂ (CNAN T01408), E. paratype ♀ (CNAN T01415). C, F. *C. hoffmanni* Armas, 1996, C. ♂, F. ♀ (CNAN SC3996). G, J. *C. cuauhmapan*, sp. nov., G. holotype ♂ (CNAN T01396), J. paratype ♀ (CNAN T01399). H, K. *C. berstoni*, sp. nov., H. holotype ♂ (CASENT 9073325), K. paratype ♀ (CASENT 9073313). I, L. *C. chanae*, sp. nov., I. holotype ♂ (CNAN T01403), L. paratype ♀ (CNAN T01405). M, P. *C. catemacoensis*, sp. nov., M. holotype ♂ (CNAN T01424), P. paratype ♀ (CNAN T01423). N, Q. *C. schmidti* Sissom, 1995, N. ♂ (CASENT 9073316), Q. ♀ (CASENT 9073317). O, R. *C. yucatanensis*, sp. nov., O. holotype ♂ (CNAN T01416), R. paratype ♀ (CNAN T01418). Scale bars = 1 mm.

*Centruroides hoffmanni* Armas, 1996

Figures 2, 4, 7A, B, 10A, B, 15A, A, 17C, F, 18C, F, 19C, F, 20C, F, 21C, F, 22C, F, 23C, F, 24C, F, 25C, F, 38, 39 tables 1, 8, 10

*Centruroides hoffmanni* Armas, 1996: 29–32, figs. 5–9; 1999: 47, 51; Beutelspacher-Baigts, 2000: 123, 126, 139, 144, 155, map 106 (in part: records from Arriaga, Chiapas); Kovařík, 1998: 107; Fet and Lowe, 2000: 109; González-Santillán, 2001: 573; Armas et al., 2002: 94, 95; 2003: 94 (misidentification); 2004: 170, table 1 (misidentification); Martín-Frías et al., 2005: 1–6, figs. 1–13 (misidentification); Teruel et al., 2006: 223; Santibáñez-López and Ponce-Saavedra, 2009: 321, 323, 326, 328–321, figs. 12–15, 8–11, 16 (misidentification); Santibáñez-López and Contreras-Felix, 2013: 131, 138, fig. 7 (misidentification); Teruel et al., 2015a: 3, 6, 7, figs. 35–37 (misidentification); Kovařík et al., 2016b: 11 (misidentification); Esposito et al., 2017: 13; Esposito and Prendini, 2019: 4, 7, fig. 2.

**TYPE MATERIAL:** MEXICO: Chiapas: Municipio Arriaga: Holotype ♀, (CNAN 71), La Gloria 16°08'39.4"N 94°06'04.7"W, 11.xii.1974. J.L. Garcia, R. Ruiz, and J. Luis M.G., household collection.

**DIAGNOSIS:** *Centruroides hoffmanni* is most closely related to *C. chanae*, from which it differs as follows. A dark line along the lateral margins of the carapace and mesosomal tergites I–III, and pale stripe medially on the carapace and tergites, absent in *C. hoffmanni* (fig. 7A, B) are present in *C. chanae* (fig. 7C, D). The carapace, pedipalps, tergites, and metasoma are more infuscate, creating a more mottled appearance, in *C. hoffmanni* (figs. 38A, B, 39A, B) than *C. chanae* (figs. 40A, B, 41A, B). Less reticulate infuscation is present on the chelicerae of *C. hoffmanni* than *C. chanae*. The interocular triangle is more darkly infuscate in *C. hoffmanni* than *C. chanae*. The marbled infuscation of the mesosomal sternites is pronounced in

*C. hoffmanni*, but faint or absent in *C. chanae*. The carapace is longer, its length greater than its width, in *C. hoffmanni*, but shorter, its length and width similar, in *C. chanae* (tables 8, 9). The carapace surfaces are more coarsely granular, the carinae more pronounced, and the sulci narrower and deeper in *C. hoffmanni* (fig. 7A, B) than *C. chanae* (fig. 7C, D). The pedipalp chela manus of the male is more incrassate in *C. hoffmanni* than *C. chanae* (fig. 15A, B). The ventral surfaces of the telotarsi of leg I are more finely and sparsely setose in *C. hoffmanni* than *C. chanae*. The pectinal tooth count of the male is lower in *C. hoffmanni*, usually 15, than *C. chanae*, usually 17 (table 8). The ventrolateral carinae of mesosomal sternite VII are granular, and the ventrosubmedian carinae weakly granular and restricted to the posterior half of the segment in *C. hoffmanni*, whereas the ventrolateral carinae are distinct, granular, and the ventro-submedian carinae weakly developed, granular in *C. chanae*. Although the metasomal segments of the male are longer and narrower in *C. hoffmanni* than *C. chanae*, the metasoma is less than 3× the length of the mesosoma in *C. hoffmanni* but greater than 3× (up to 3.3×) its length in *C. chanae* (table 10). The ventrolateral and ventrosubmedian carinae of the metasomal segments are more pronounced in *C. hoffmanni*, being slightly serrate on segments I–IV, compared with finely granular to subserrate on I–III and obsolete, smooth on IV in *C. chanae*. The ventrosubmedian carinae of segments I and II are very pronounced in *C. hoffmanni* (figs. 18C, F, 19C, F) but absent or obsolete in *C. chanae* (figs. 18I, L, 19I, L). The telson of the male is elongate, the vesicle bilobed posteriorly in *C. hoffmanni* (fig. 25C, F), whereas the telson is shorter, the vesicle rounded posteriorly in *C. chanae* (fig. 25I, L).

**DISTRIBUTION:** *Centruroides hoffmanni* is endemic to the state of Chiapas in southeastern Mexico. The known records are restricted to the Central Depression, bounded by the Central Highlands, to the north, and the Sierra Madre de Chiapas, to the south (fig. 4), an area which exhibits high levels of endemism (Reyes-García and Sousa, 1995).

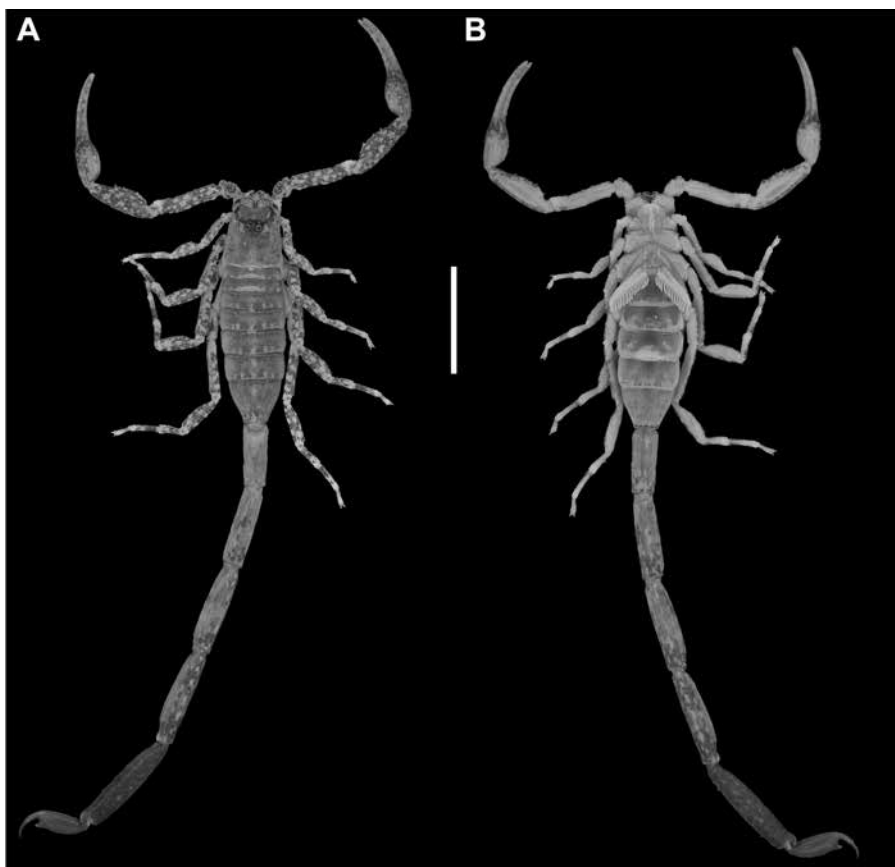


FIGURE 26. *Centruroides rileyi* Sissom, 1995, ♂ (CNAN SC4002), habitus. A. Dorsal aspect. B. Ventral aspect. Scale bars = 5 mm.

**ECOLOGY:** The localities at which *C. hoffmanni* has been recorded range in altitude from 529 to 1513 m and are situated in subtropical dry forest. The habitat and habitus are consistent with the arboreal, corticolous ecomorphotype (Prendini, 2001a).

**REMARKS:** Confusion has surrounded this species since its original description. Armas (1996) described the holotype as an adult female, but later (Armas, 1999; Armas et al. 2003) stated it was immature. Beutelspacher-Baigts (2000) confused *C. hoffmanni* with *Centruroides nigrovariatus* Pocock, 1898, and *C. tuxtla*, erroneously listing the species from the Mexican state of Oaxaca, an error repeated by Armas et al. (2003, 2004). Martín-Frías et al.

(2005) redescribed *C. hoffmanni* from material originating in Oaxaca that is evidently heterospecific with the holotype based on characters of the female: the pectinal plate of the material described is not distinctly lobed or posteriorly rounded, the pectinal tooth count is higher, the metasoma and telson markedly are granular, and the subaculear tubercle is not elongate and angular. Santibáñez-López and Ponce-Saavedra (2009) again misidentified *C. hoffmanni*, presenting photographs of female specimens in which the pectinal plate is not distinctly lobed or posteriorly rounded, along with measurements and pectinal tooth counts inconsistent with the holotype, once more erroneously listing the species from Oaxaca.

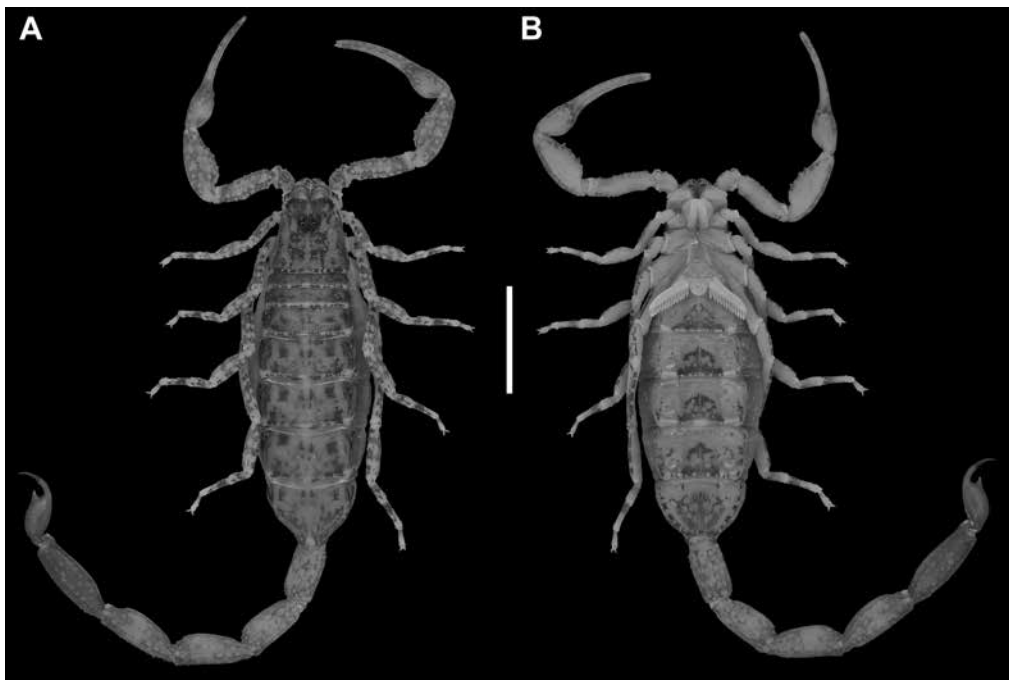


FIGURE 27. *Centruroides rileyi* Sissom, 1995, ♀ (CNAN SC4003), habitus. **A.** Dorsal aspect. **B.** Ventral aspect. Scale bars = 5 mm.

The error was repeated by Santibáñez-López and Contreras-Félix (2013), and yet again by Teruel et al. (2015a), who erroneously associated *C. hoffmanni* with the “*nigrovariatus* group” of *Centruroides*. Kovařík et al. (2016b) followed previous authors in misidentifying material from Guerrero and Oaxaca as *C. hoffmanni*.

**MATERIAL EXAMINED: MEXICO:** Chiapas: Municipio Angel Albino Corzo: 8 km from Siltepec, 18°48'33"N 92°40'30.6"W, 663 m, 17.viii.2007, C. Mayorga, G. Ortega, and L. Cervantes, 1 juv. ♀ (CNAN SC3990). Municipio Comitan: Parque Nacional Lagunas de Montebelo, 16°17'17"N 91°56'16"W, 1473 m, 3.ix.2005, O.F. Francke, M. Córdova, A. Jaimes, A. Valdez, and H. Montaño, 1 juv. ♂ (CNAN SC3992). Municipio La Concordia: Villa Corzo La Tigrilla, San Julián, Revolución Mexicana, 16°00'00"N 92°50'47"W, 544 m, 17.iii.2007, C. Mayorga, G. Ortega, and L. Cervantes. 1 ♂, 1 ♀ (CNAN SC3998).

Municipio Tuxtla Gutiérrez: Las Delicias, 16°45'31.1"N 93°06'26.4"W, 529 m, 2.iii.2005, O.F. Francke, M. Córdova, A. Jaimes, A. Valdez, and H. Montaño, 1 ♀ (AMNH [LP 5224]); Gutiérrez, San Julián, Revolución Mexicana, 16°11'41"N 93°01'16"W, 544 m, 16.iii.2007, G. Ortega and A. Cervantes, 2 ♂, 3 ♀ (CNAN SC3997). Municipio Tzimol: Carretera [Hwy] Comitán-Tzimol Santa Rosa, 16°11'03.4"N 92°16'59.3"W, 632–730 m, 2.ix.2005, O.F. Francke, M. Córdova, A. Jaimes, A. Valdez, and H. Montaño, 1 ♂, 1 ♀ (AMNH [LP 5249]), 1 ♀, first instar juvs (CNAN SC3994), 1 ♀, first instar juvs (CNAN SC3995), 3 ♂, 9 ♀, 2 juv. ♂, 14 juv. ♀ (CNAN SC3996). Municipio Villaflores: Reserva de La Biosfera La Sepultura, 1 km SE of Ejido California, 16°15'14.2"N 93°35'46.4"W, 1009–1132 m, 30.viii.2005, O.F. Francke, M. Córdova, A. Jaimes, A. Valdez, and H. Montaño, 1 ♂ (AMNH [LP 5350]), 1 ♂, 2 ♀, 4 juv. ♂ (CNAN SC3993), 1 ♀, first instar juvs (CNAN SC3991).



FIGURE 28. *Centruroides cuauhmapan*, sp. nov., ♂ (CNAN T01396), habitus. A. Dorsal aspect. B. Ventral aspect. Scale bars = 5 mm.

*Centruroides rileyi* Sissom, 1995

Figures 2, 3, 5C, D, 8C, D, 11B, 12B, 17G, J, 18G, J, 19G, J, 20G, J, 21G, J, 22G, J, 23G, J, 24G, J, 25G, G, 26, 27, tables 1, 2, 10

*Centruroides rileyi* Sissom, 1995: 96–99, figs. 19–27; Armas et al., 2002: 1; 2003: 95; Cancino and Blanco, 2002: 71; Sissom and Hendrixson, 2005: 126, 127, 134, 475; Esposito et al., 2017: 14, 30, fig: 14; 2018: 97, 116; Esposito and Prendini, 2019: 4, fig. 2; Ponce-Saavedra and Francke, 2019: 3;

Crews and Esposito, 2020: 14, fig. 11; Goodman and Esposito, 2020: 1–9, fig. 1C (misidentification).

**TYPE MATERIAL: MEXICO:** *Tamaulipas*: Município Gómez Farías: Holotype ♂, paratype ♀ (USNM), Bocatoma, 7 km SSE of Gómez Farías, 22°56'30.2"N 99°06'19.3"W, 25–30. iii.1978, E.G. Riley; paratype ♀ (FSCA), Gómez Farías, 16.iii.1977, R. Schmidt. *San Luis Potosí*: Município Tamazunchale: Paratype ♀ (NAU), 5 km N of Tamazunchale off Hwy 85, 21°18'13.6"N 98°47'58.7"W, 1.viii.1987, J.A. Nilsson.

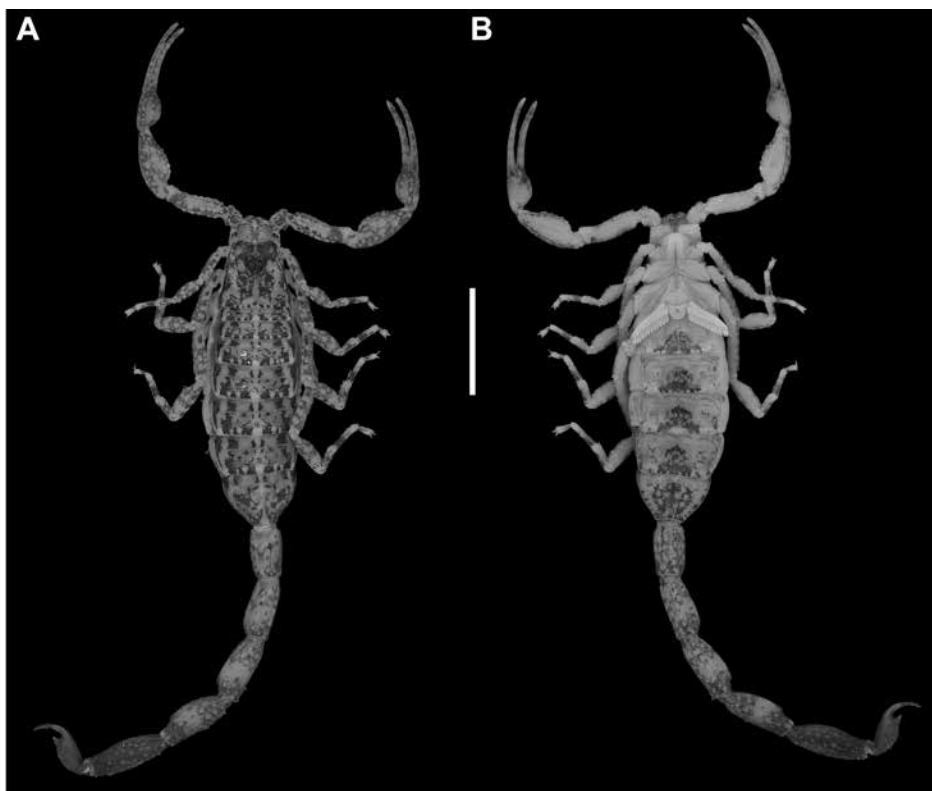


FIGURE 29. *Centruroides cuauhmapan*, sp. nov., ♀ (CNAN T01399), habitus. **A.** Dorsal aspect. **B.** Ventral aspect. Scale bars = 5 mm.

**DIAGNOSIS:** *Centruroides rileyi* is most closely related to *C. cuauhmapan*, from which it differs as follows. The posterosubmedian carinae of the carapace are weakly developed in *C. rileyi* (fig. 5A, B), but absent in *C. cuauhmapan* (fig. 5C, D). The retrodorsal carina of the pedipalp chela manus is smooth, the dorsomedian carina weakly granular, and the prodorsal carina weakly granular and restricted to the distal half of the segment, in the male of *C. rileyi* (figs. 11, 12A) whereas the retrodorsal carina is finely granular, the dorsomedian carina distinct, granular, and the prodorsal carina distinct, granular and complete in the male of *C. cuauhmapan* (figs. 11, 12B). The ventrolateral and ventrosubmedian carinae of mesosomal sternite VII are obsolete to absent and the intercarinal surfaces smooth in *C. rileyi*, whereas the ventrolateral and ventrosubmedian carinae are distinct, granu-

lar and the intercarinal surfaces finely granular in *C. cuauhmapan*. The metasoma and telson are shorter in the male and slenderer, proportionally shorter and narrower, in the female of *C. rileyi* (figs. 17A, D, 18A, D, 19A, D, 20A, D, 21A, D, 22A, D, 23A, D, 24A, D, 25A, D, table 2) than *C. cuauhmapan* (figs. 17G, J, 18G, J, 19G, J, 20G, J, 21G, J, 22G, J, 23G, J, 24G, J, 25G, J, table 3). The ventral carinae are granular on metasomal segment I in the female, vestigial on segments I–III and smooth on IV and V in the male of *C. rileyi* (figs. 18A, D, 19A, D, 20A, D, 21A, D, 22A, D) but distinct, granular on segments I–V in the male and female of *C. cuauhmapan* (figs. 18G, J, 19G, J, 20G, J, 21G, J, 22G, J). The surfaces of the telson vesicle of the female are smooth in *C. rileyi* (figs. 24A, D, 25A, D) but granular in *C. cuauhmapan* (figs. 24G, J, 25G, J).

TABLE 9

**Meristic data for type material of *Centruroides chanae*, sp. nov., and *Centruroides yucatanensis*, sp. nov.**

Material deposited in the Colección Nacional de Arácnidos (CNAN), Universidad Nacional Autónoma de México, Mexico City. Measurements follow Stahnke (1970), Lamoral (1979), and Prendini (2001b).

	<i>Centruroides chanae</i>						<i>Centruroides yucatanensis</i>			
	Holotype		Paratypes		Paratypes		Holotype		Paratype	
	♂	♂	♂	♀	♀	♂	♂	♀	♂	♀
	CNAN	CNAN	CNAN	CNAN	CNAN	CNAN	CNAN	CNAN	T01418	T01419
	T01403	T01404	T01405	T01406	T01407	T01416	T01417	T01418	T01418	T01419
Total length <sup>1</sup>	42.4	42.6	38	34.4	33.2	48.7	29.9	27.8	27.8	24.8
Carapace	length	3.4	3.5	3.3	2.9	3.3	3.7	3.4	2.7	2.9
	ant. width	1.8	1.7	1.6	1.4	1.8	1.7	1.6	1.3	1.5
	post. width	3.8	3.8	3.4	3.0	3.8	3.7	3.5	2.8	3.1
Median ocelli	diameter	0.3	0.3	0.3	0.2	0.3	0.3	0.3	0.2	0.3
Interocular	length <sup>2</sup>	0.3	0.4	0.3	0.3	0.4	0.4	0.3	0.3	0.3
Pedipalp	length <sup>3</sup>	15.1	16.0	16.7	12.7	14.3	16.5	14.7	10.8	11.5
Trochanter	length	1.5	1.5	3.5	1.1	1.3	1.7	1.4	1.0	1.1
Femur	length	3.7	3.8	3.6	3.0	3.3	3.8	3.3	2.4	2.6
	width	0.7	0.6	0.6	0.5	0.8	0.7	0.8	0.5	0.9
	height	1.0	1.0	0.9	0.8	1.0	1.0	1.0	0.9	0.6
Patella	length	3.9	4.2	3.9	3.6	3.9	4.5	3.9	2.9	3.1
	width	0.9	1.0	0.9	0.8	0.8	1.0	1.0	0.8	0.9
	height	1.5	1.5	1.3	1.2	1.5	1.5	1.6	1.3	1.4
Chela	length <sup>4</sup>	6.0	6.5	5.7	5.0	5.8	6.5	6.1	4.6	4.8
Manus	length	2.9	2.7	3.5	3.0	3.5	3.6	3.7	1.6	1.8
	width	1.1	1.3	1.0	1.0	1.1	1.4	1.2	0.8	0.9
	height	1.0	1.0	1.0	0.9	0.8	1.3	1.2	0.9	0.9
Mov. finger	length	4.4	4.3	4.0	3.5	4.2	4.1	4.3	3.4	3.5
Leg I	length	6.1	6.6	6.2	5.5	6.0	6.6	6.1	4.6	5.1
Pectines	length	5.2	6.2	5.7	5.0	4.7	5.5	4.5	3.5	3.7
	tooth count	15/15	17/17	17/15	17/17	14/14	14/14	14/14	12/12	13/13
Mesosoma	length <sup>5</sup>	9.5	9.4	8.0	8.2	8.8	13.0	8.7	8.8	7.6
Sternite VII	length	3.5	2.7	2.6	2.5	3.0	2.8	2.2	2.3	2.0
	width	3.3	3.5	3.0	2.8	3.8	3.1	3.5	3.3	3.0
Metasoma	length <sup>6</sup>	29.5	29.7	26.7	23.3	21.1	32.0	17.8	16.3	17.1
Metasoma I	length	3.7	3.7	3.5	3.1	2.6	4.1	2.5	2.1	2.0
	width	1.6	1.5	1.3	1.3	1.6	1.5	1.7	1.4	1.5
	height	1.5	1.5	1.3	1.3	1.5	1.5	1.5	1.2	1.3

TABLE 9 *continued*

		<i>Centruroides chanae</i>						<i>Centruroides yucatanensis</i>			
		Holotype		Paratypes		Paratypes		Holotype		Paratype	
		♂	♂	♂	♀	♀	CNAN	♂	♀	juv.	♀
		CNAN	CNAN	T01404	T01405	T01406	T01407	T01416	T01417	T01418	T01419
Metasoma II	length	4.7	4.7	4.2	3.7	3.2		5.1	3.2	2.4	2.5
	width	1.4	1.3	1.2	1.2	1.4		1.2	1.4	1.1	1.3
	height	1.4	1.4	1.3	1.3	1.5		1.1	1.5	1.3	1.2
Metasoma III	length	5.5	5.2	4.8	4.1	3.5		5.8	3.6	2.7	2.7
	width	1.4	1.3	1.2	1.2	1.3		1.4	1.4	1.1	1.2
	height	1.5	1.4	1.3	1.1	1.5		1.3	1.6	1.2	1.3
Metasoma IV	length	5.8	5.7	5.3	4.5	4.0		6.1	4.0	3.1	3.2
	width	1.3	1.2	1.2	1.2	1.3		1.3	1.3	1.0	1.1
	height	1.4	1.4	1.2	1.1	1.5		1.3	1.5	1.1	1.2
Metasoma V	length	6.0	6.4	5.7	4.8	4.5		6.9	4.5	3.5	3.9
	width	1.4	1.3	1.2	1.1	1.3		1.4	1.3	1.0	1.0
	height	1.5	1.3	1.3	1.3	1.5		1.3	1.5	1.1	1.2
Telson	length	3.8	4.0	3.2	3.1	3.3		4.0	-	2.6	2.8
Vesicle	length	2.7	2.7	2.2	2.0	1.6		2.9	-	1.5	1.6
	width	1.3	1.1	1.0	0.9	0.9		1.2	-	0.7	0.7
	height	1.2	1.2	1.0	1.0	1.1		1.2	-	0.8	0.8
Aculeus	length	1.3	1.6	1.3	1.2	1.6		1.3	-	1.3	1.3

<sup>1</sup> Sum of carapace, tergites I–VII, metasomal segments I–V, and telson; <sup>2</sup> distance between median ocelli; <sup>3</sup> sum of trochanter, femur, patella, and chela; <sup>4</sup> measured from base of condyle to tip of fixed finger; <sup>5</sup> sum of tergites I–VII; <sup>6</sup> sum of metasomal segments I–V and telson.

**VARIATION:** Adult males and females differ as follows. The dorsomedian carinae of the pedipalp patella are absent, the mesosoma proportionally longer and slenderer, and the metasoma longer, in males (figs. 26A, B, 27A, B, 28A, B, 29A, B, table 2). The first pair of legs are longer in males and the metasomal carinae more pronounced and finely serrate in females (figs. 17A, D, 18A, D, 19A, D, 20A, D, 21A, D, 22A, D, table 2).

**DISTRIBUTION:** *Centruroides rileyi* is endemic to northern Mexico, east of the Sierra Madre Oriental. The species is fairly widespread, with records from the states of Puebla, Tamaulipas, San Luis Potosí, and Veracruz (fig. 3).

**ECOLOGY:** The localities at which *C. rileyi* has been recorded range in altitude from 100 to 2554

m. The habitat at these localities varies from subtropical and semi-deciduous forests near the El Cielo Biosphere Reserve, Tamaulipas, to tropical and subtropical moist broadleaf forest at La Sierra Gorda, San Luis Potosí, and tropical humid moist forest in Veracruz (Mendoza-Villa et al., 2018). The habitat and habitus are consistent with the arboreal, corticolous ecomorphotype (Prendini, 2001a).

**REMARKS:** *Centruroides rileyi* has never been confused with other species of the “thorellii” clade nor with *C. thorellii*, perhaps due to its occurrence in northern Mexico. Furthermore, the small size and distinctive mottling pattern contrast with other buthids, such as *Centruroides gracilis* (Latreille, 1804) and *Centruroides vittatus* (Say, 1821), that occur in sympatry (Shelley and Sissom, 1995).

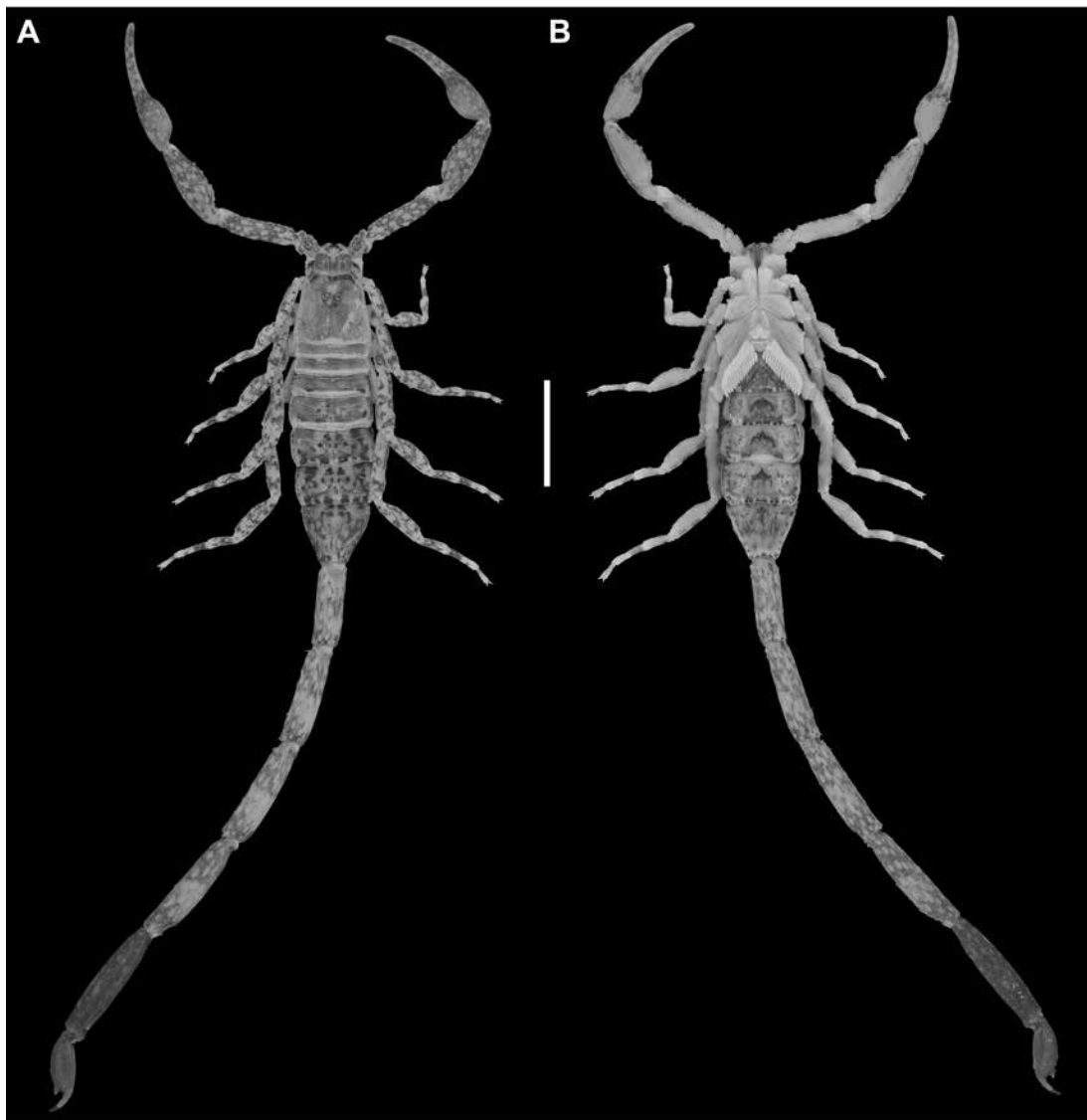


FIGURE 30. *Centruroides catemacoensis*, sp. nov., ♂ (CNAN T01424), habitus. A. Dorsal aspect. B. Ventral aspect. Scale bars = 5 mm.

MATERIAL EXAMINED: MEXICO: Puebla: Municipio Cuetzalan el Progreso: Cuetzalan, Santiago Yancuitlalpan, 18°54'42.2"N 98°35'15.3"W, 2554 m, 19.v.1995, G. Oclogaig Barrzia, juvs (CNAN SC3999). San Luis Potosí: Municipio Axtlan de Terrazas: Axtlan de Terrazas, 21°25'34.9"N 98°52'42"W, 100 m, 28.iv.2006, O.F. Francke, A. Valdez, G. Villegas and R. Pare-

des, 1 ♂ (AMNH [LP 6445]), 1 ♀, 2 juv. ♀ (CNAN SC4003). Veracruz: Municipio Papantla: Papantla, 20°27'24.1"N 97°18'56.1"W, 2197 m, iii.2000, J.L. Castelo, 1 ♂ (CNAN SC4000). Municipio Tamiahua: Moralillo, Cerro Azul, 21°11'03.8"N 97°44'49.6"W, 153 m, 27.ii.2007, E. Barrera and L. Cervantes, 2 ♀ (CNAN SC3985), 1 juv. ♀ (CNAN SC4002).

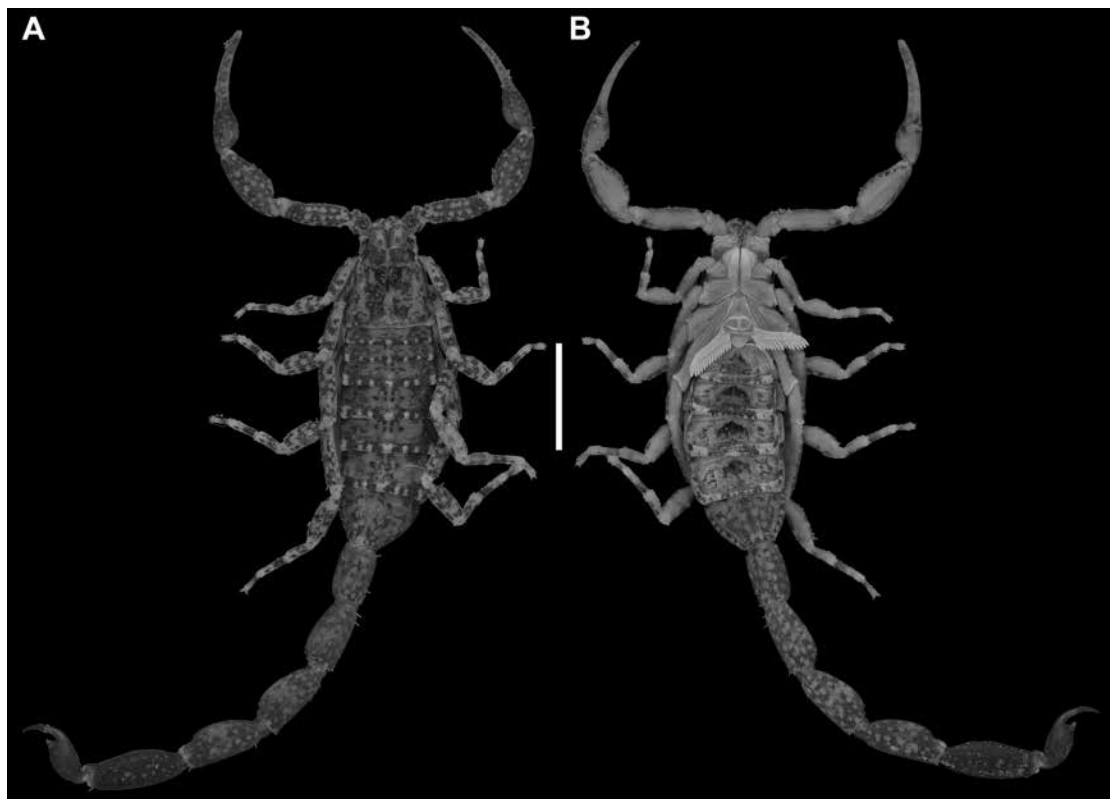


FIGURE 31. *Centruroides catemacoensis*, sp. nov., ♀ (CNAN T01423), habitus. **A.** Dorsal aspect. **B.** Ventral aspect. Scale bars = 5 mm.

*Centruroides schmidti* Sissom, 1995

Figures 1A, C, 2, 4, 6E, F, 9E, F, 13C, 14C, 17N, Q, 18N, Q, 19N, Q, 20N, Q, 21N, Q, 22N, Q, 23N, Q, 24N, Q, 25Q, B, 36, 37, tables 1, 7, 10

*Centruroides schmidti* Sissom, 1995: 94–96, 98, figs. 10–18; Armas, 1996: 22–24, table I (misidentification, part); 1999: 30; Vázquez, 1999: 53, 60–62, fig. 7 (misidentification, part); Armas and Maes, 2000: 27; 2001: 16; Fet and Lowe, 2000: 118; Armas et al., 2002: 169–171 (misidentification); Teruel and Stockwell, 2002: 111–127, figs. 6, 20, tables II, III; Armas et al., 2003: 95–96 (misidentification); Armas and Martín-Frías, 2003: 205, 209; 2008: 7–10, 12, 17, 19, 20, figs. 2–4, table XIV (misidentification); Armas and Trujillo, 2010: 235, 238, 240; Borges et

al., 2012: 131, table I; Teruel et al., 2015a: 7; Delfin-González et al., 2017: 284 (misidentification), table I; Esposito et al., 2018: 97, table 5; Esposito and Prendini, 2019: 4, fig. 2; Crews and Esposito, 2020: 14, fig. 11.

**TYPE MATERIAL:** **HONDURAS:** Departamento Cortés: Município Choloma: Holotype ♂ (FMNH), Coloma [Choloma], Lake Ticamaya 15°32'41.5"N 87°53'06.1"W, 26.iv.1923, K. Schmidt and L. Walters (Capt. Field Mus. Exped.), found on bones of crocodile skull. **GUATEMALA:** Departamento Izabal: Município Morales: Paratype ♀ (FMNH), Escobas, Izabal 15°24'12"N 89°08'24.5"W 27.xi.1933, K.P. and P.J. Schmidt, Leon Mandel Guatemala Exped.

**DIAGNOSIS:** *Centruroides schmidti* differs from the closely related species, *C. berstoni*, *C. catemacoensis*, *C. cuauhmapan*, *C. hamadryas*,



FIGURE 32. *Centruroides hamadryas*, sp. nov., ♂ (CNAN T01408), habitus. A. Dorsal aspect. B. Ventral aspect. Scale bars = 5 mm.

and *C. rileyi*, as follows. The pattern of infuscation of *C. schmidti* is unlike that of the other species and includes a pronounced pale stripe medially on the carapace and mesosomal tergites, flanked on the tergites by a pair of orange stripes, which

are more infuscate in females (figs. 36A, B, 37A, B). The cheliceral manus is entirely dark with reticulate infuscation in *C. schmidti*, whereas the infuscation is lighter and restricted to the distal half of the chelicerae in the other species. The

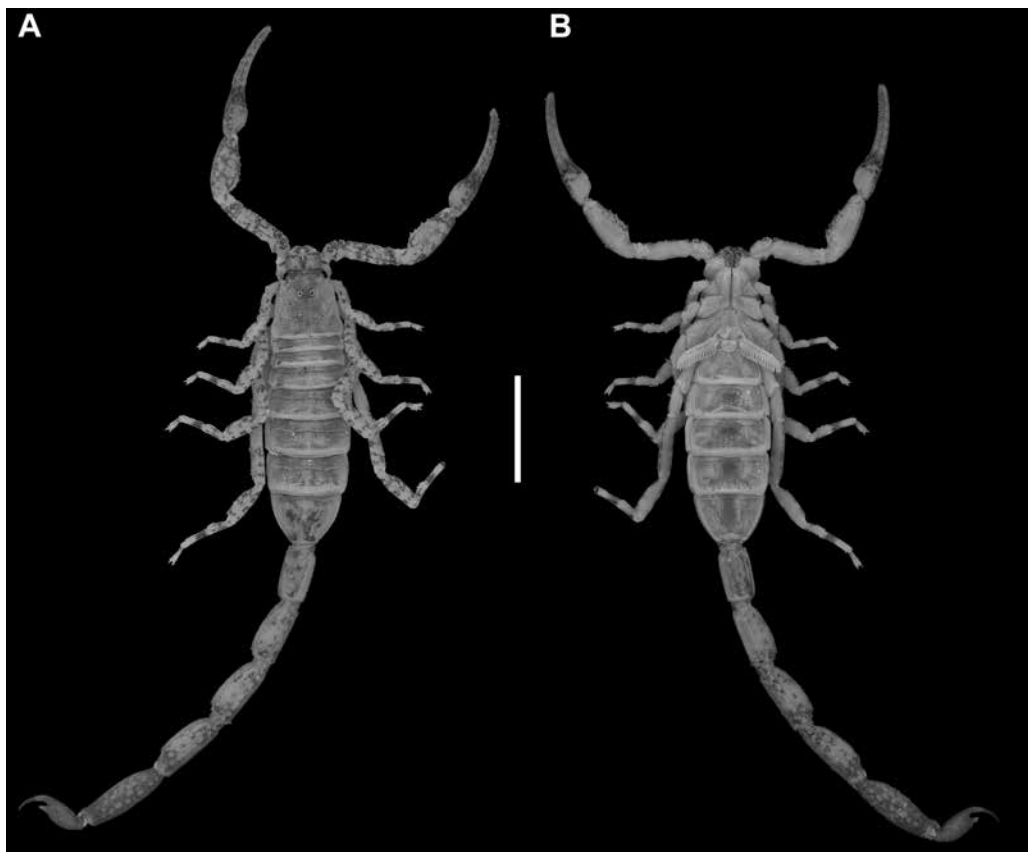


FIGURE 33. *Centruroides hamadryas*, sp. nov., ♀ (CNAN T01415), habitus. A. Dorsal aspect. B. Ventral aspect. Scale bars = 5 mm.

telotarsi of the first pair of legs possess short, dense setae in *C. schmidti*, unlike in *C. cuauhmapan* and *C. rileyi*. The posterosubmedian and lateral ocular carinae on the carapace are present in *C. schmidti* (fig. 6E, F) but reduced or absent in *C. catemacoensis* (fig. 5E, F) and absent in *C. berstoni* (fig. 6C, D), *C. cuauhmapan* (fig. 5C, D), and *C. hamadryas* (fig. 6A, B). The posterior margin of sternite III is pale and setose in *C. schmidti*, unlike in the other species. The dorsomedian carinae are restricted to the posterior two-thirds of tergites I–VI, and absent on VII in *C. schmidti*, whereas the dorsomedian carinae are vestigial on tergites I–VII in *C. catemacoensis* and weakly granular on I–VII in *C. berstoni*. Ventrosubmedian and ventrolateral carinae are present on sternite VII in *C. schmidti*, unlike in *C. catemacoensis* and *C. rileyi*.

Metasomal segment V is more than 2× the length of the carapace in *C. schmidti*, but less than 2× its length in the other species (table 7). The telson surfaces of the female are very granular and the ventromedian carina well developed in *C. schmidti* (figs. 23–25D), whereas the telson surfaces of females are smooth in *C. hamadryas* (figs. 23–25E) and *C. rileyi* (figs. 23–25Q). The subaculear tubercle is strongly angled toward the aculeus in *C. schmidti* (fig. 25N, Q).

*Centruroides schmidti* differs from *C. hoffmanni* as follows. The mottled infuscation of the carapace, pedipalps, tergites, and metasoma is less pronounced in *C. schmidti* than *C. hoffmanni*, but the carapace is more infuscate, with a darker border around the margins, in *C. schmidti*. The carapacial sulci are broad and shallow in *C. schmidti*

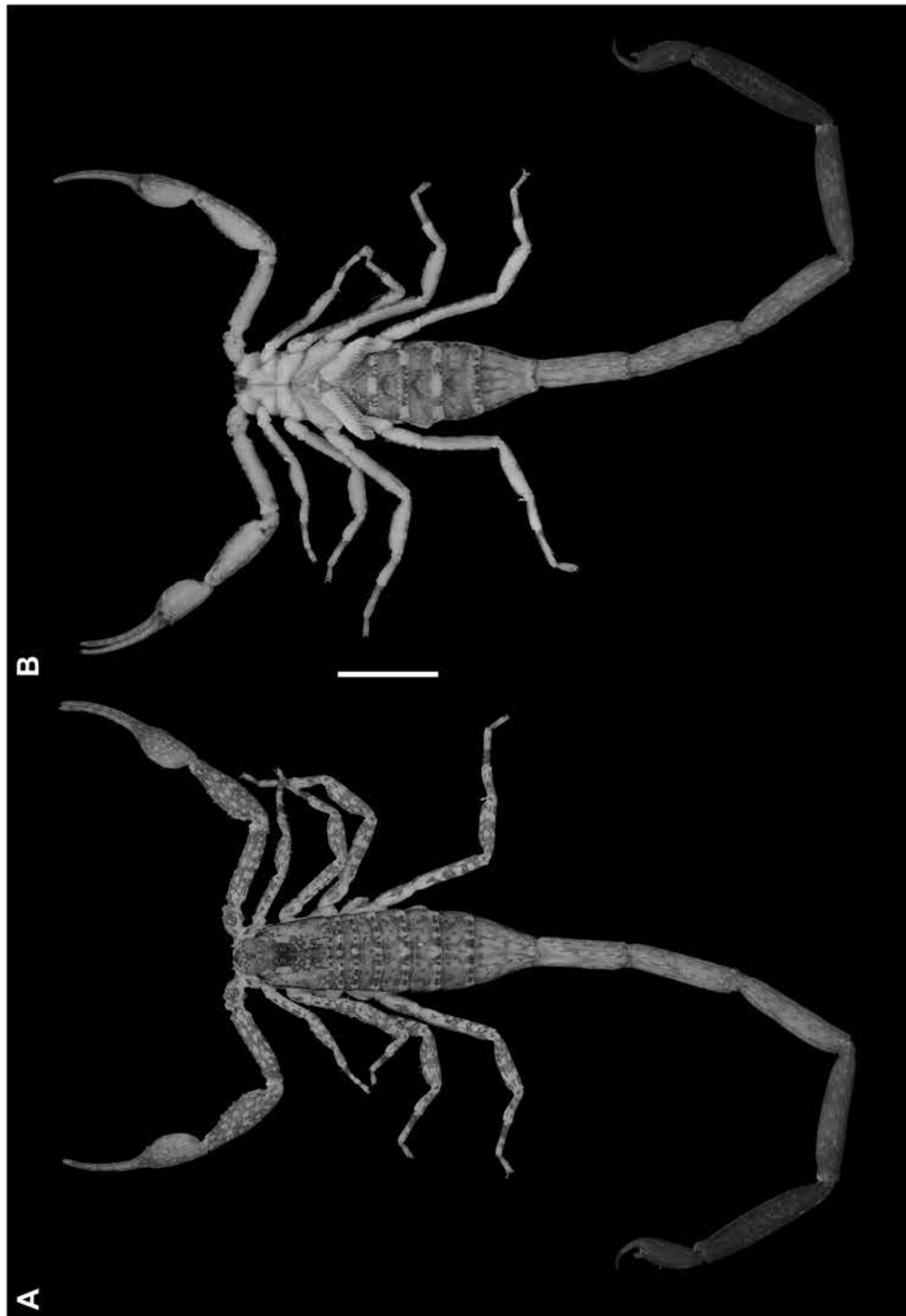


FIGURE 34. *Centruroides berstoni*, sp. nov., ♂ (CASENT 9073325), habitus. A. Dorsal aspect. B. Ventral aspect. Scale bars = 5 mm.



FIGURE 35. *Centruroides berstoni*, sp. nov., ♀ (CASENT 9073313), habitus. **A.** Dorsal aspect. **B.** Ventral aspect. Scale bars = 5 mm.

but narrow and deep in *C. hoffmanni*. The dorso-median carina is restricted to the posterior two-thirds of tergites I–VI, and absent on VII in *C. schmidti*, whereas the dorsomedian carina is complete on tergites I–VII in *C. hoffmanni*.

**VARIATION:** Carapace surface granulation varies from sparse granules to uniform, moderate granulation. Specimens from Honduras exhibit variation in granulation of the lateral ocular carinae (fig. 6E, F). The dorsomedian carina of the pedipalp chela manus of the male is well developed in material from Guatemala but weakly developed to absent in material from Honduras.

Adult males and females differ as follows. The pedipalp chela of the male is incrassate unlike the female. The prodorsal carina on the chela manus comprises a row of spiniform granules in the male but is finely granular in the female (fig. 13C, D). The mesosoma is proportionally longer and slenderer, the metasoma up to 3× longer, with segment V markedly longer, and the telson more elongate, with the vesicle more rounded, in males (figs. 17N, Q, 18N, Q, 19N, Q, 20N, Q, 21N, Q, 22N, Q, 23N, Q, 24N, Q, 25N, Q, table 2).

**DISTRIBUTION:** *Centruroides schmidti* is the most widespread species of the clade. It appears

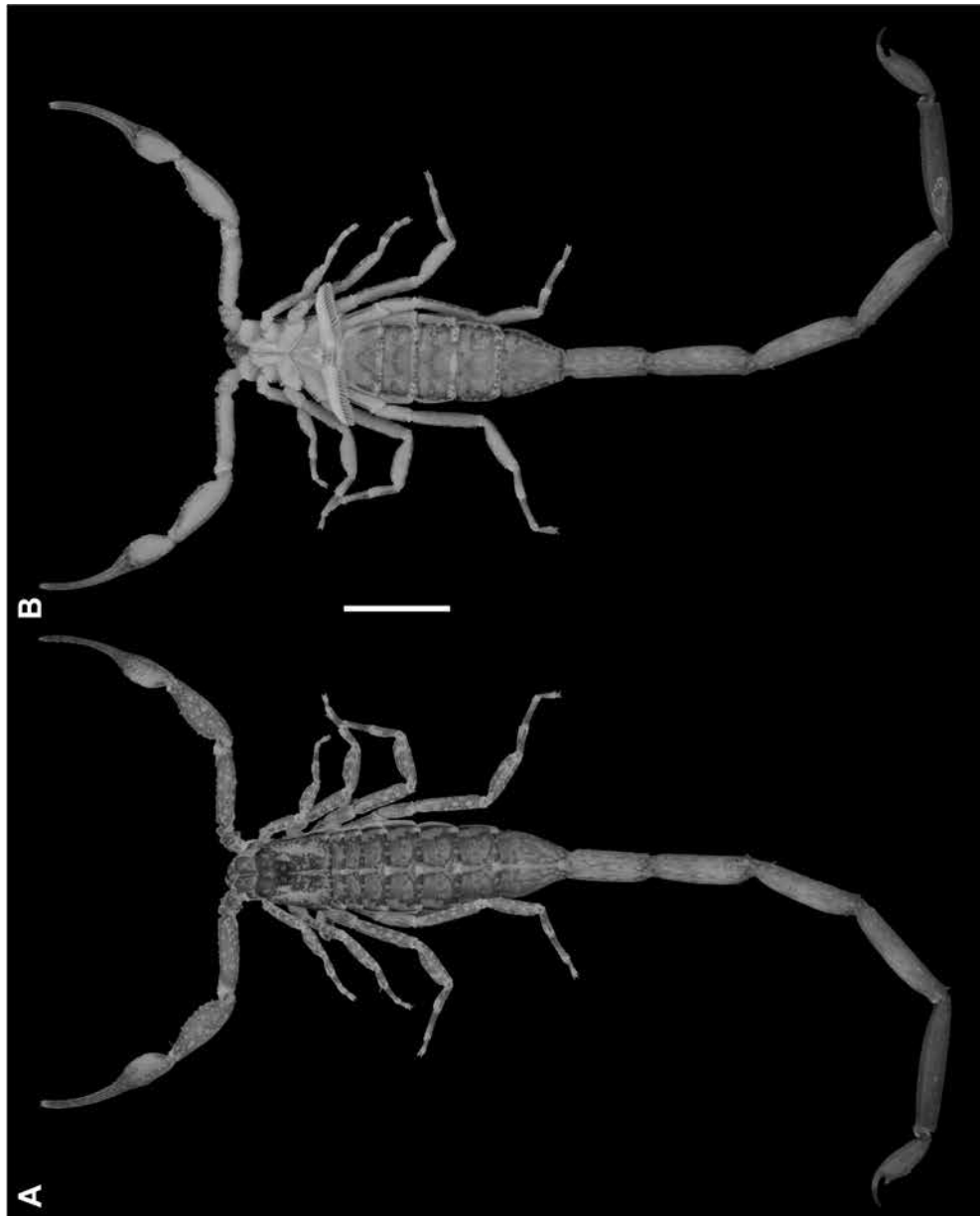


FIGURE 36. *Centruroides schmidti* Sissom 1995, ♂ (CASENT 9073278), habitus. A. Dorsal aspect. B. Ventral aspect. Scale bars = 5 mm.

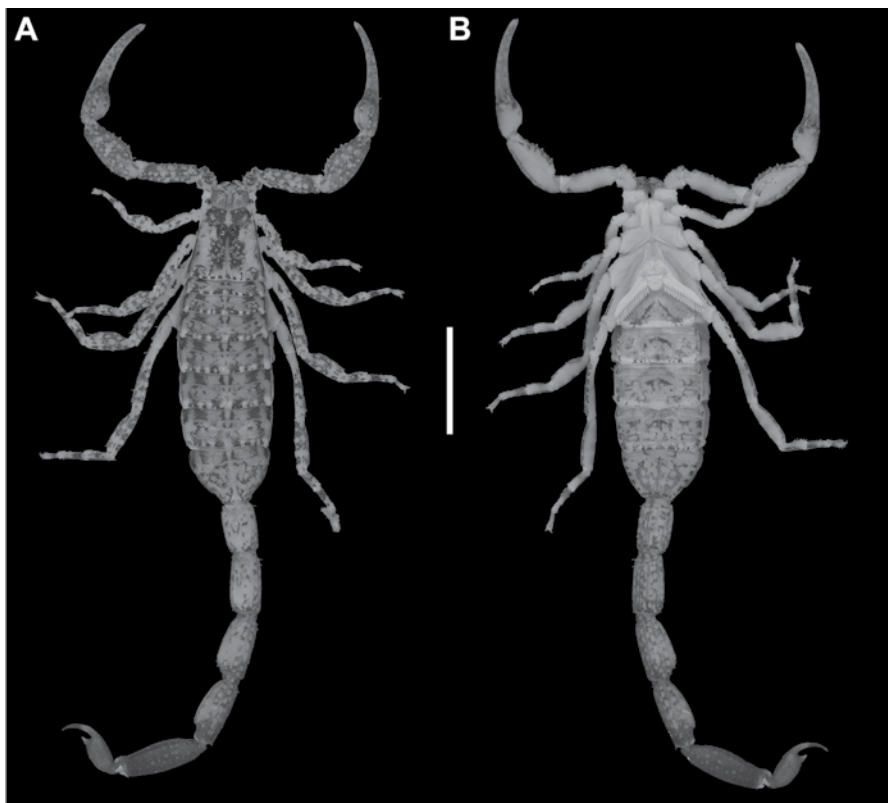


FIGURE 37. *Centruroides schmidti* Sissom 1995, ♀ (CASENT 9073317), habitus. **A.** Dorsal aspect. **B.** Ventral aspect. Scale bars = 5 mm

to be endemic to Guatemala, where it has been recorded from the Izabal and Zacapa departments, and Honduras, where it has been recorded from the Atlántida, Cortés, Francisco Morazán, and Islas de la Bahía departments. The known localities extend along the Caribbean coasts of both countries, including the Bay Islands of Honduras, and inland to the Sierra de Las Minas of Guatemala (fig. 4).

**ECOLOGY:** The localities at which *C. schmidti* has been recorded range in altitude from 12 to 773 m. This species occurs in a broader range of habitats than other species of the “*thorelli*” clade. The habitat at localities near Zacapa, Guatemala is semiarid savannah, dominated by scrub forest and cacti. In this area, specimens were found on the bark of large oaks at night. The habitat at San Antonio de Oriente, Honduras, is open deciduous broadleaf

forest/savannah, interspersed with grassland. The habitat near Las Minas, Guatemala, is moist montane subtropical pine-oak forest; specimens were collected on *Pinus oocarpa* Schiede ex Schltdl. and various oak species (fig. 2A, C). The habitat on the northern coast and Bay Islands of Honduras is lowland tropical rainforest. The habitat and habitus are consistent with the arboreal, corticolous ecomorphotype (Prendini, 2001a).

**REMARKS:** Previous records of *C. schmidti* from Costa Rica and the Mexican states of Chiapas, Quintana Roo, and Veracruz are misidentifications of other species, including some of those described herein. Armas (1996) included specimens from Quintana Roo, probably conspecific with *C. yucatanensis*, in a redescription of *C. schmidti*. Armas et al. (2002) described an individual from northern Costa Rica as *C. schmidti*,

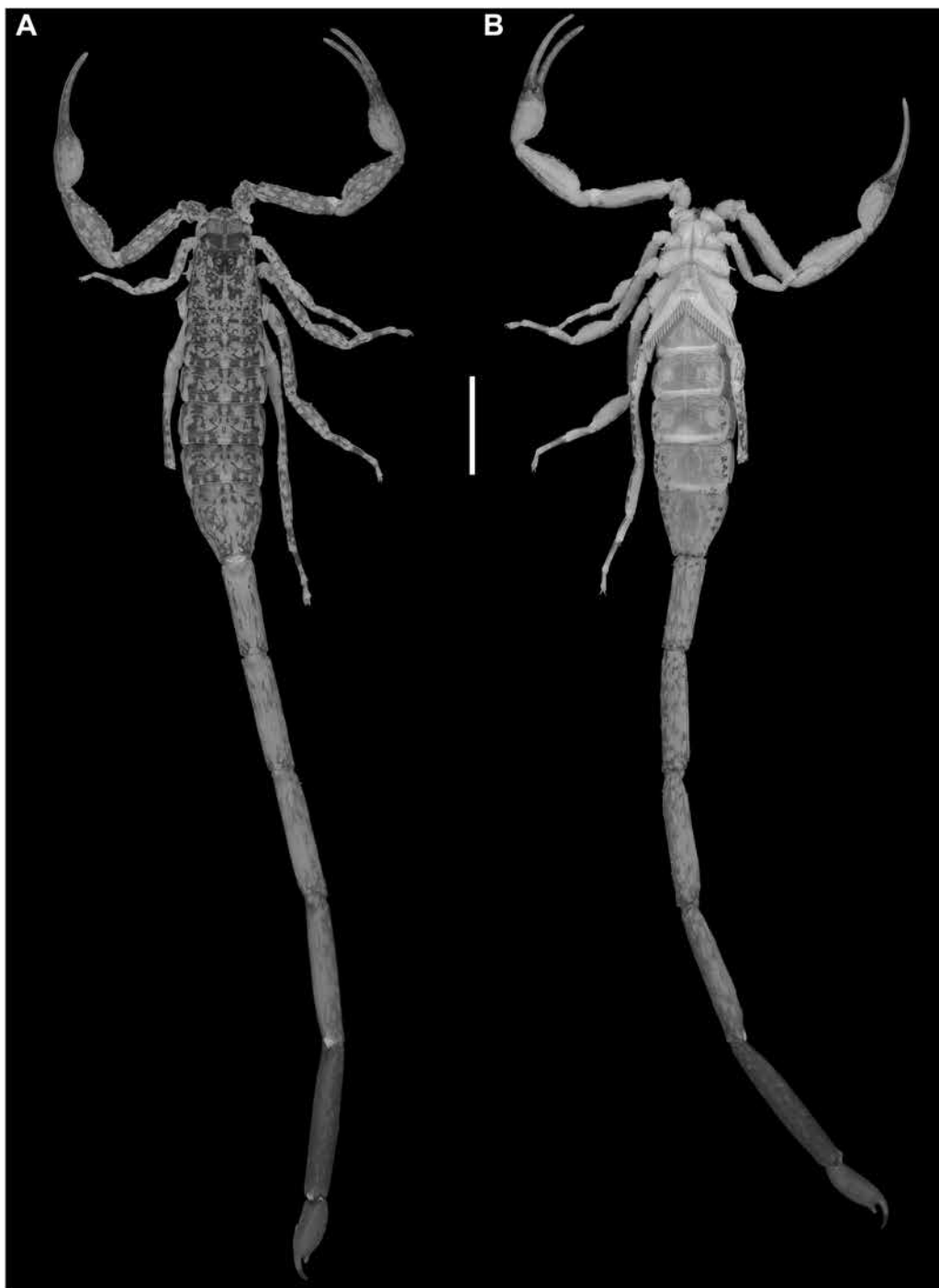


FIGURE 38. *Centruroides hoffmanni* Armas 1996, ♂ (CNAN SC3996), habitus. A. Dorsal aspect. B. Ventral aspect. Scale bars = 5 mm.

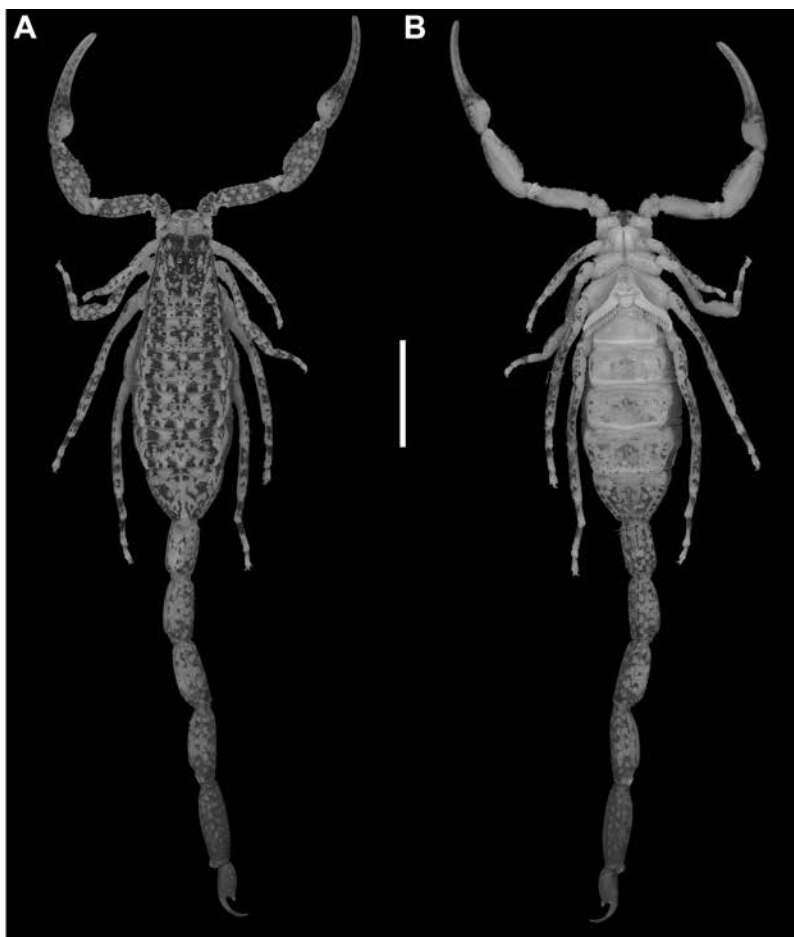


FIGURE 39. *Centruroides hoffmanni* Armas 1996, ♀ (CNAN SC3996), habitus. A. Dorsal aspect. B. Ventral aspect. Scale bars = 5 mm.

without differentiating it from *C. thorellii*, a species erroneously recorded from the country by Francke and Stockwell (1987). Armas et al. (2003) included Mexico (Chiapas, Quintana Roo, and Yucatán) in the distribution of *C. schmidti*. Vázquez (1999) again included *C. schmidti* in the fauna of Quintana Roo and erroneously suggested the species is endemic to the Yucatán Peninsula. Photographs and measurements of individuals identified as *C. schmidti* from the Sian Ka'an Biosphere Reserve, Quintana Roo, by Armas and Martín-Frías (2008), are consistent with the coloration and morphology of *C. yucatanensis*. Additionally, Armas and Martín-Frías (2008) listed *C.*

*schmidti* from Veracruz. Delfín-González et al. (2017) listed *C. schmidti* from Chiapas and Veracruz. Finally, Armas and Martín-Frías (2003) erroneously suggested that the distribution of *C. schmidti* extends from southeastern Mexico to Costa Rica, following Armas et al. (2002).

**MATERIAL EXAMINED: GUATEMALA:**  
*Departamento El Progreso: Municipio Rio Hondo: San Francisco Zapotitlan: Finca El Olvido, Las Minas, 15°02'04.8"N 89°52'26.7"W, 1214 m, 17.ix.2019, A.M. Goodman, UV hand collection, found on oak and pine trees, 2–3 m high, 4 ♀, 4 juv. ♀ (CASENT 9073317), 18.ix.2019, A.M. Goodman, L.A. Esposito, and*

L. Allen, 5 ♀, 1 juv. ♂, 1 juv. ♀ (CASENT 9073402). *Departamento Zacapa*: Município Rio Hondo: Bosque Pino, Guadalupe, Manta de Golpeo, 14°58'04.7"N 89°24'47"W, 751 m, 20.ix.2019, A.M. Goodman, M. Barrios, and M. van Dam, UV hand collection, found on oak and pine trees, 2–3 m high, 7 ♂, 1 ♀, 1 juv. ♂, 1 juv. ♀ (CASENT 9073278); Aldea Casas de Pinto, near turnoff for Zacapa at Rio Hondo, 15°01'38.2"N 89°36'57.2"W, 77 m, 13.vii.2006, J.H. Huff, semiarid region with scrub forest and cacti, collected under rocks in shaded areas and at night using UV, 1 ad. (AMNH [LP 5985]). **HONDURAS**: *Departamento Atlántida*: Município La Ceiba: Parque Nacional Pico Bonito, Pico Bonito, trails from Visitor Centre and park entrance, 14°43'30.6"N 86°44'11.5"W, 184 m, 30.viii.2013, S. Longhorn, dense wet lowland tropical forest near large river, sweeping and beating, may have been on or under wood, day search, 1 juv. ♂ (AMNH [LP 13416]). *Departamento Francisco Morazán*: Município San Antonio de Oriente: E.A.P. Zamorano, Monte Redondo, Acuacultura, 13°39'59.6"N 86°59'21"W, 773 m, 23.ix.2008, C. Víquez, UV at night, 1 ♀ (AMNH [LP 9172]). *Departamento Islas de la Bahía*: Município Roatán: Cayos Cochinos, Cayos Menor, forest trails, 15°57'26.9"N 86°30'03.3"W, 101 m, 2.viii.2012, S. Longhorn, scrub oak forest, 1 ♀ (AMNH [LP 13411]); Isla Utila, 16°06'22.1"N 86°54'08.1"W, 12 m, 21.vii.2012. S. Longhorn, scrub forest/wet Savannah, 1 ♀ (AMNH LP [13417]).

#### *Centruroides yucatanensis*, sp. nov.

Figures 2, 4, 7E, F, 10E, F, 15C, 16C, 17O, R, 18O, R, 19O, R, 20O, R, 21O, R, 22O, R, 23O, R, 24O, R, 25R, O, 42, 43, tables 1, 9, 10

*Centruroides schmidti*: Armas, 1996: 25–29, 98, figs. 1–4 (misidentification), table I.

*Centruroides sissoomi*: Vázquez, 1999: 53, 60–62, fig. 7 (misidentification); Armas et al., 2003: 95 (misidentification, part); Armas, 2006: 4, 7, fig. 5 (misidentification, part); Teruel et

al., 2015a: 8 (misidentification); Delfín-González et al., 2017: 283, 285, table 2 (misidentification); Esposito and Prendini, 2019: 4, fig. 2 (misidentification); Ponce-Saavedra and Francke, 2019: 3, table 1 (misidentification); Crews and Esposito, 2020: 14, fig. 11 (misidentification).

**TYPE MATERIAL: MEXICO:** *Quintana Roo*: Município Benito Juárez: Holotype ♂ (CNAN T01416), paratype ♀ (CNAN T01417), 2 juv. ♀ paratypes (CNAN T01418, T01419), Puerto Morelos, Jardín Botânico Alfredo Barrera, 20°50'42.1"N 86°54'12.9"W, 23 m, 4.vii.2007, G. Montiel, R. Paredes, M. Ramírez, D. Chibras, and G. Bonilla.

**ETYMOLOGY:** The species name refers to the Yucatán Peninsula of southeastern Mexico, where the species occurs.

**DIAGNOSIS:** *Centruroides yucatanensis* differs from the closely related species, *C. chanae* and *C. hoffmanni*, as follows. The carapace, pedipalps, tergites, and metasoma are less infuscate, creating a less mottled appearance, in *C. yucatanensis* than *C. chanae*. Less reticulate infuscation is present on the chelicerae of *C. yucatanensis* than *C. chanae*. The interocular triangle is less darkly infuscate in *C. yucatanensis* than *C. hoffmanni*. The carapace is shorter, its length and width similar, in *C. yucatanensis* (fig. 7E, F, table 10) but longer, its length greater than its width, in *C. hoffmanni* (fig. 7A, B, table 10). The carapace surfaces are more finely granular, the carinae less developed and the sulci broader and shallower in *C. yucatanensis* than *C. hoffmanni*. The pedipalp chela manus of the male is less incrassate in *C. yucatanensis* (fig. 15C) than *C. hoffmanni* (fig. 15B), with fewer spiniform granules on its pro-lateral surfaces than in *C. chanae* and *C. hoffmanni* (fig. 15A, B). The ventral surfaces of the telotarsi of leg I are more finely and sparsely setose in *C. yucatanensis* than *C. chanae*. The pectinal tooth count of the male is lower in *C. yucatanensis*, usually 13 or 14 (fig. 9E, table 10) than *C. chanae*, usually 17 (fig. 9A, table 10) and *C. hoffmanni*, usually 15 (fig. 9D, table 10), and

TABLE 10

**Diagnostic ratios (mean/median/mode) for species of the arboreal Neotropical “*thorelli*” clade of *Centruroides* Marx, 1890, bark scorpions**

	Leg I length: carapace length	Metasoma V length: mesosoma length	Metasoma V length: carapace length
<i>Centruroides berstoni</i> , sp. nov.	1.9/1.9/1.9	2.5/2.4/2.0	1.6/1.6/1.9
<i>Centruroides catemacoensis</i> , sp. nov.	1.9/1.9/1.9	2.3/2.2/2.2	1.5/1.5/1.7
<i>Centruroides chanae</i> , sp. nov.	1.9/1.9/1.9	3.0/3.1/3.1	1.7/1.8/1.8
<i>Centruroides cuauhmapan</i> , sp. nov.	1.8/2.1/1.9	2.2/2.1/1.8	1.5/2.1/1.7
<i>Centruroides hamadryas</i> , sp. nov.	1.8/1.9/1.8	1.8/2.8/2.8	1.6/1.7/1.8
<i>Centruroides hoffmanni</i> Armas, 1996	1.8/1.8/1.8	2.3/2.4/1.7	1.6/1.7/1.3
<i>Centruroides rileyi</i> Sissom, 1995	1.9/1.9/1.9	2.2/2.1/2.1	1.5/1.5/1.2
<i>Centruroides schmidti</i> Sissom, 1995	2.0/1.9/1.9	2.2/2.2/2.8	1.5/1.4/1.9
<i>Centruroides yucatanensis</i> , sp. nov.	1.8/1.8/1.8	2.1/2.1/2.0	1.5/1.4/1.3

the pectinal teeth are more ovoid. The ventrolateral and ventrosubmedian carinae of mesosomal sternite VII are vestigial, weakly granular in *C. yucatanensis*, whereas the ventrolateral carinae are distinct, granular, and the ventrosubmedian carinae weakly developed, granular in *C. chanae*, and the ventrolateral carinae granular, and the ventrosubmedian carinae weakly granular and restricted to the posterior half of the segment in *C. hoffmanni*. The ventrolateral and ventrosubmedian carinae of the metasomal segments are more pronounced in *C. yucatanensis*, being slightly serrate on segments I–IV, compared with finely granular to subserrate on I–III and obsolete, smooth on IV in *C. chanae*. The ventrosubmedian carinae of segments I and II are absent in *C. yucatanensis* (figs. 18O, R, 19O, R, 20O, R, 21O, R, 22O, R), absent or obsolete in *C. chanae* (figs. 18I, L, 19I, L, 20I, L, 21I, L, 22I, L), and very pronounced in *C. hoffmanni* (figs. 18C, F, 19C, F, 20C, F, 21C, F, 22C, F).

**DESCRIPTION:** The following description is based on the holotype male, with differences among other material noted in the section on variation.

**Coloration:** Base color yellow, with extensive infuscation, creating mottled or marbled pattern.

Carapace with uniformly infuscate marbling, more densely infuscate medially. Pedipalp chela fingers and manus, dorsal and retrolateral intercarinal surfaces with moderately infuscate marbling; prolateral and ventral intercarinal surfaces mostly immaculate. Legs retrolateral surfaces with infuscate marbling; prolateral surfaces pale, immaculate. Tergites with uniformly infuscate mottling, pale stripe medially, blackish spots submedially, and faint, narrow bands laterally. Sternites with faintly infuscate marbling. Metasomal segments uniformly, faintly marbled; segment V and telson markedly infuscate, noticeably darker than preceding segments.

**Carapace:** Shape trapezoidal; anterior width four-fifths of posterior width (table 10); antero-median sulcus moderately deep, oval; postero-median sulcus shallow anteriorly, deep posteriorly; median ocular tubercle weakly granular; carinae moderately developed, comprising small to medium-sized granules; lateral ocular and posterosubmedian carinae weakly developed; intercarinal surfaces finely and evenly granular (fig. 10E).

**Pedipalps:** Orthobothriotaxic, Type A; femur dorsal trichobothria with a configuration; pedipalp chela fixed finger, trichoboth-

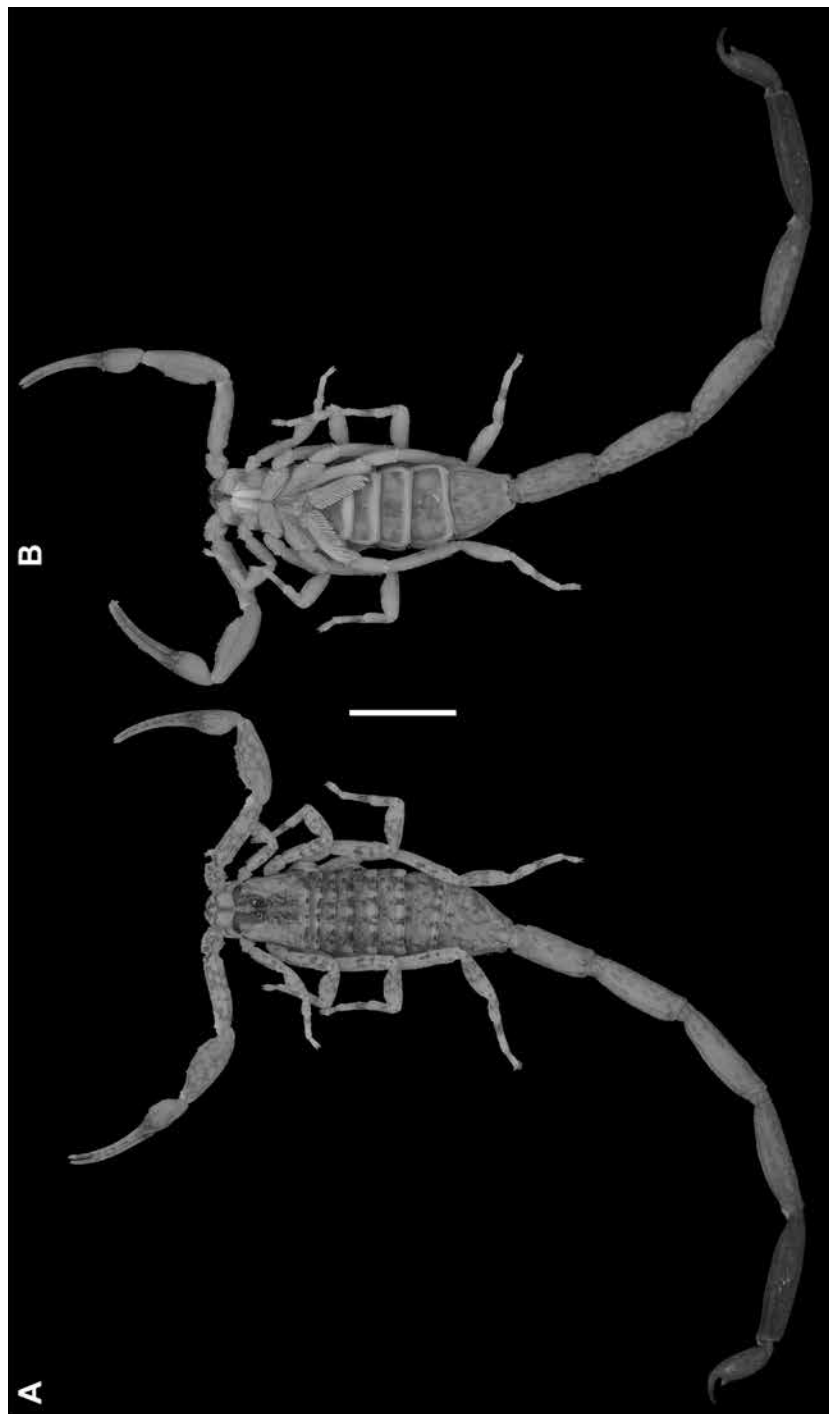


FIGURE 40. *Centruroides chanae*, sp. nov., ♂ (CNAN T01407), habitus. A. Dorsal aspect. B. Ventral aspect. Scale bars = 5 mm.



FIGURE 41. *Centruroides chanae*, sp. nov., ♀ (CNAN T01405), habitus. A. Dorsal aspect. B. Ventral aspect. Scale bars = 5 mm.

rium *db* situated slightly distal to *et*. Femoral carinae strongly developed, serrate; dorsal intercarinal surface moderately granular; pro-lateral intercarinal surface with series of large spiniform granules. Patella carinae strongly developed, granular; prolateral intercarinal surface with five or six large subspiniform granules. Chela manus dorsomedian and retrodorsal carinae complete, granular; prodorsal carina absent. Fixed finger, median denticle row comprising eight oblique subrows, each flanked by pro- and retrolateral supernumerary denticles. Movable finger, median denticle row with short terminal row comprising four denticles preceded by eight

oblique subrows, each flanked by pro- and retrolateral supernumerary denticles.

**Legs:** Leg I length 1.78× greater than carapace length (table 10). Telotarsi ventral surfaces sparsely covered with short setae; unguis markedly curved.

**Pectines:** Pectinal plate 1.61× wider than long; posterior margin distinctly rounded; pectinal tooth count 13/14 (♂) (fig. 8D, table 10).

**Mesosoma:** Tergites width similar to carapace posterior width; I and II slightly narrower (table 10). Pretergites surfaces smooth to finely granular. Posttergites surfaces weakly granular; I–VI with dorsomedian carinae absent on I and II, vestigial, granular on III–VI; VII surface weakly



FIGURE 42. *Centruroides yucatanensis*, sp. nov., ♂ (CNAN T01416), habitus. A. Dorsal aspect. B. Ventral aspect. Scale bars = 10 mm.

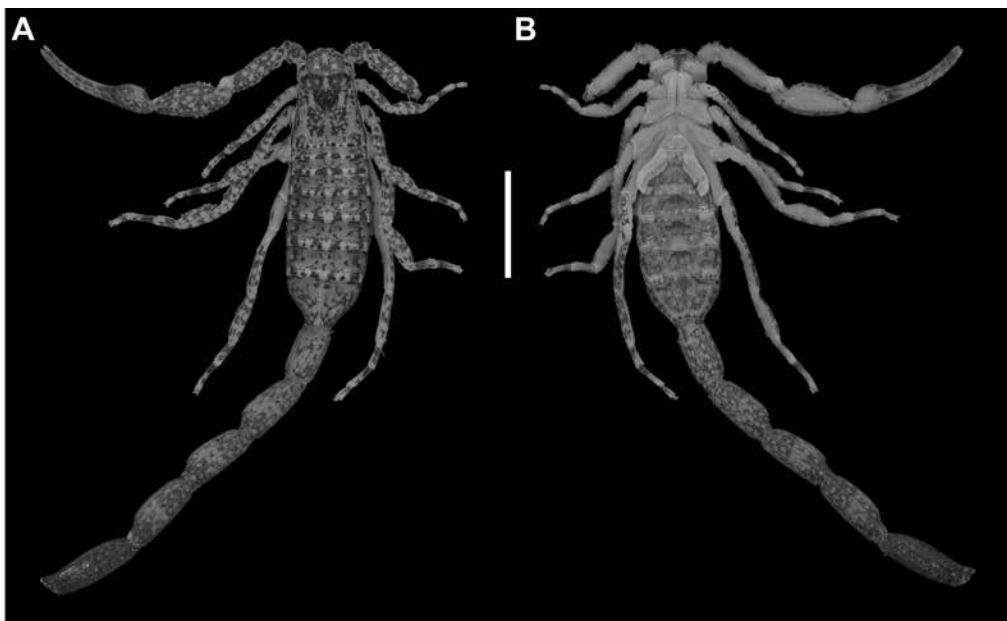


FIGURE 43. *Centruroides yucatanensis*, sp. nov., ♀ (CNAN T01417), habitus. **A.** Dorsal aspect. **B.** Ventral aspect. Scale bars = 10 mm.

granular, dorsomedian carina vestigial, granular, dorsosubmedian and dorsolateral carinae smooth. Sternites III–VI, surfaces smooth; VII surface smooth, ventrolateral and ventrosubmedian carinae smooth.

**Metasoma:** Metasoma length  $2.45 \times$  mesosoma length (table 10). Segments longer than wide; increasing in length posteriorly, segment V  $2 \times$  length of I; ventral carinae vestigial, weakly granular on segments I–IV, other carinae absent or obsolete; lateral intercarinal surfaces sparsely granular on segments I–III, other surfaces smooth (figs. 17–22O).

**Telson:** Vesicle elongate, ovoid; ventral surface shallowly convex; ventromedian carina granular, terminating at subaculear tubercle; subaculear tubercle narrow and angular in lateral aspect, directed toward midpoint of aculeus. Aculeus angled ventrally at slightly less than  $90^\circ$  (fig. 25O, R).

**Variation:** Base coloration varies from light yellow to orange. Adult males and females differ as follows. The pedipalp chela manus is incrassate, with the prodorsal carina spinose, the mesosoma

proportionally longer and slenderer, the metasoma  $2 \times$  longer, with segment V markedly longer ( $1.86 \times$  carapace length), and the telson more elongate, with the vesicle more rounded and bilobed posteriorly, in males (figs. 23O, R, 24O, R, 25O, R, table 10). The tegument is more densely infuscate, the prodorsal carina of the pedipalp chela manus finely granular, the pectinal plate produced into a rounded lobe posteriorly, which is punctate and slightly infuscate, metasomal segment V shorter ( $1.3 \times$  carapace length) and the telson shorter and narrower, with the vesicle surfaces less granular, in females (figs. 10E, F, 15–16C, 17O, R, 18O, R, 19O, R, 20O, R, 21O, R, 22O, R, 23O, R, 24O, R, 25O, R, table 10). The pectinal tooth count is similar in both sexes (table 9).

**DISTRIBUTION:** *Centruroides yucatanensis* is endemic to the Yucatán Peninsula. Although presently known from only three localities, two in the state of Yucatán in the north of the peninsula, and a third on the western coast, in the state of Quintana Roo, the distribution of this species was probably more extensive before much of its habitat was destroyed for agriculture and rangeland (fig. 4).

**ECOLOGY:** The localities at which *C. yucatanensis* has been recorded range in altitude from 23–38 m. The habitat at these localities varies from low or medium semideciduous broadleaf forest to tall, moist evergreen broadleaf forest, often with a dense understory. Much of the original habitat has been cleared for agriculture and rangeland across the Yucatán Peninsula, and this species appears to be confined to remnant patches of forest. The habitat and habitus are consistent with the arboreal, corticolous ecomorphotype (Prendini, 2001a).

**REMARKS:** Armas (1996) identified 11 individuals from the Jardín Botánico Alfredo Barrera, Puerto Morelos, Quintana Roo, as *C. schmidti*. Meristic data recorded by Armas (1996) for an adult male and three females differed greatly from comparative data for the holotype of *C. schmidti* collected at Lake Tickamaya, Honduras (Sissom, 1995). Armas (1996) also described *C. sissomi*, and assigned it to the *thorellii* group due to its small size. Illustrations and photographs of the holotype female of *C. sissomi* in the original description indicate that the pectinal plate is not lobed, and subsequent photographs of the holotype by Armas (2006) indicate a densely granular tegument, characters inconsistent with the “*thorellii*” clade. Material examined during the present study confirmed the presence of two sympatric species of *Centruroides* in the Jardín Botánico Alfredo Barrera, Puerto Morelos. One species, determined to be conspecific with the material previously misidentified as *C. schmidti* by Armas (1996), based on meristic data, is a hitherto undescribed species, described herein as *C. yucatanensis*. The other is presumed to be *C. sissomi*, based on the fact that the pectinal plate is not lobed and the tegument is densely granular, as well as its dark orange coloration and larger size (40 mm). Other records of *C. schmidti* and/or *C. sissomi* from the Yucatán Peninsula (Vázquez, 1999; Teruel et al., 2015a; Ponce-Saavedra and Francke, 2019) are misidentifications of *C. yucatanensis*.

**MATERIAL EXAMINED: MEXICO:** Quintana Roo: Municipio Benito Juárez: Puerto Morelos,

Jardín Botánico Alfredo Barrera, 20°50'42.1"N 86°54'12.9"W, 38 m, 4.vii.2007, G. Montiel, R. Paredes, M. Ramírez, D. Chibras, and G. Bonilla, 1 ♂ (AMNH [LP 7597]), 2 juv. ♂ (CNAN SC3984). Yucatán: Municipio Felipe Carrillo Puerto: Cenote Chac-ha, 3.5 km N and 3 km E of Kalacmul, 20°04'40.3"N 88°08'27.9"W, 23 m, 9.vii.2007, R. Paredes, D. Chibras, and G. Montiel, 1 ♀ (CNAN SC4004).

#### ACKNOWLEDGMENTS

We thank the following for assisting with fieldwork or donating material used in the study: L. Allen, A.J. Ballesteros, D. Barrales-Alcalá, M.A. Barrios-Izás, P. Berea, G. Bonilla, J.L. Castelo, D. Chibras, M. Cordóva, M. Escalante, T. Gearheart, E. González-Santillán, J. Gorneau, J.H. Huff, A. Jaimes, M.K. Lippey, S. Longhorn, R. Monjaraz-Ruedas, H. Montaño, G. Montiel-Parra, D. Ortiz, R. Paredes, J. Ponce-Saavedra, M. Ramírez, M.E. Soleglad, A. Tietz, A. Valdez, M. van Dam, G. Villegas, C. Víquez, and H. Yamaguti; R. Coates Lutes for use of the Los Tuxtlas Field Station; P. Sierwald and S. Ware (FMNH) for providing photographs of the holotype of *C. schmidti*; E.S. Volschenk for providing unpublished morphological characters; D. Casellato, P. Rubi, and T. Sharma for generating some of the DNA sequence data at the AMNH; A. Lam, M. van Dam, L. Bonomo, and S.F. Loria for assistance with DNA sequencing and phylogenetic analysis at the CAS; P. Colmenares for logistical support with collections at the AMNH; S. Thurston (AMNH) for assisting with UV digital photomicrography and preparation of the plates for this contribution; and two anonymous reviewers for constructive comments on a previous draft of the manuscript. Research presented herein comprised part of the M.S. thesis of A.M. at San Francisco State University and the CAS, partially supported by a grant from the Vincent Roth Fund for Systematic Research of the American Arachnological Society, and a Collections Study Grant from the AMNH. Some data presented herein emanated from the Ph.D. dissertation of L.A.E. at the City University of New York (CUNY) and the

AMNH, supported by a U.S. National Science Foundation (NSF) GK-12 Fellowship, a CUNY/NSF AGEP Grant, a CUNY Presidential Fellowship, a CUNY College Now Fellowship, and an NSF Postdoctoral Fellowship (1003087). Additional funding for this research was provided by a grant from the Theodore Roosevelt Memorial Fund of the AMNH to L.A.E., an Ernst Mayr Award from the Museum of Comparative Zoology, Harvard University, to L.A.E., an NSF Doctoral Dissertation Improvement Grant (DEB 0910147) to L.P. and L.A.E., NSF grant DEB 0413453 to L.P., and a grant from the Richard Lounsbery Foundation to L.P.

## REFERENCES

- Aguilar, F.P.G., and G.O. Meneses. 1970. Escorpiones y escorpionismo en el Perú. I. Nota preliminar sobre los Scorpionida peruanos. Anales Científicos de la Universidad Nacional Agraria 8: 1–5.
- Armas, L.F. de. 1974a. Escorpiones del archipiélago cubano. II. Hallazgo de género *Microtityus* (Scorpionida: Buthidae) con las descripciones de un nuevo subgénero y tres nuevas especies. Poeyana 132: 1–26.
- Armas, L.F. de. 1984. Tipos de Arachnida depositados en el Instituto de Zoológica de la Academia de Ciencias de Cuba. 1. Amblypygi, Opiliones, Ricinulei, Scorpiones, Schizomida e Uropygi. Poeyana 284: 1–11.
- Armas, L.F. de. 1988. Sinopsis de los escorpiones antillanos. Havana: Editorial Científico-Técnica, 102 pp.
- Armas, L.F. de. 1996. Presencia de *Centruroides schmidti* Sissom en el sureste de Mexico y descripción de dos especies nuevas (Scorpiones: Buthidae). Revista Nicaragüense de Entomología 36: 21–33.
- Armas, L.F. de. 1998. The Greater Antillean scorpions (Arachnida: Scorpiones). Abstract of the XIV International Congress of Arachnology/22nd Annual Meeting of the American Arachnological Society, Field Museum of Natural History, Chicago: 50.
- Armas, L.F. de. 1999. Nueva especie de *Centruroides* (Scorpiones: Buthidae) de Chiapas, Mexico. Novitates Caribaea 1: 47–52.
- Armas, L.F. de. 2006. Name-bearing types of scorpions deposited at the Institute of Ecology and Systematics, Havana, Cuba (Arachnida: Scorpiones). Euscorpius 33: 1–14.
- Armas, L.F. and A.F. Ávila. 2015. Arachnofauna (except Acari) del Archipiélago de Sabana-Camagüey, Cuba. Solenodon 12: 57–71.
- Armas, L.F. de, and J.M. Maes. 2000. Lista anotada de los alacranes (Arachnida: Scorpiones) de América Central, con algunas consideraciones biogeográficas. Revista Nicaragüense de Entomología 46: 23–38.
- Armas, L.F. de, and E. Martín-Frías. 2003. Nueva especie de *Centruroides* Marx, 1890 (Scorpiones: Buthidae) del estado de Veracruz, México. Revista Ibérica de Aracnología 7: 205–209.
- Armas, L.F. de, and E. Martín-Frías. 2008. El género *Centruroides* Marx, 1890 (Scorpiones: Buthidae) en el estado de Veracruz, México. Boletín de la Sociedad Entomológica Aragonesa 43: 7–22.
- Armas, L.F. de, and R.E. Trujillo. 2010. Nueva especie de *Centruroides* Marx, 1890 (Scorpiones: Buthidae) de Guatemala y Honduras. Boletín de la Sociedad Entomológica Aragonesa 47: 235–240.
- Armas, L.F., M. Montoya, and C. Víquez. 2002. *Centruroides schmidti* (Scorpiones: Buthidae) en Costa Rica. Revista de Biología Tropical 50: 169–171.
- Armas, L.F. de, E. Martín-Frías, and J.E. Ramírez. 2003. Lista anotada de las especies Mexicanas del género *Centruroides* Marx, 1890 (Scorpiones: Buthidae). Revista Ibérica de Aracnología 8: 93–98.
- Armas, L.F. de, E. Martín-Frías, and J.F. Paniagua-Solís. 2004. Taxonomic comments about some Mexican scorpions of the genus *Centruroides* (Scorpiones: Buthidae). Anales de la Escuela Nacional de Ciencias Biológicas 47: 167–171.
- Armas, L.F. de, D. Luna-Sarmiento, and E. Flórez. 2012. Composición del género *Centruroides* Marx, 1890 (Scorpiones: Buthidae) en Colombia, con la descripción de una nueva especie. Boletín de la Sociedad Entomológica Aragonesa 50: 105–114.
- Baldazo-Monsivaiz, J.G., et al. 2016. Los escorpiones (Arachnida: Scorpiones) del Municipio de Taxco de Alarcón, del Estado de Guerrero, México. Entomología Mexicana 3: 75–80.
- Baldazo-Monsivaiz, J.G., R. Teruel, A.J. Cortés-Guzmán, and I. Canché-Aguilar. 2017. Los escorpiones (Arachnida: Scorpiones) del Municipio de Chilpancingo de Los Bravo, Estado de Guerrero, México. Entomología Mexicana 3: 21–27.
- Banks, N. 1900. Synopses of North American invertebrates. IX. The scorpions, solpugids and Pedipalpi. American Naturalist 34: 421–427.
- Beutelspacher-Baigts, C.R. 2000. Catálogo de los alacranes de México. Morelia, Michoacan, Mexico:

- Universidad Michoacana de San Nicolás de Hidalgo, 175 pp.
- Birula, A.A. 1917a. Arachnoidea Arthrogaster Caucásica. Pars I. Scorpiones. Zapiski Kavkazskogo Muzeya [Mémoires du Musée du Caucase], Tiflis: Imprimerie de la Chancellerie du Comité pour la Transcaucasie A (5): 1–253. [in Russian; English translation: A.A. Byalynitskii-Birulya. 1964. Arthrogastri arachnids of Caucasia. 1. Scorpions. Jerusalem: Israel Program for Scientific Translations, 170 pp.]
- Birula, A.A. 1917b. Faune de la Russie et des pays limittrophes fondée principalement sur les collections de Musée Zoologique de l'Académie des Sciences de Russie. Arachnides (Arachnoidea). Petrograd 1 (1): xx, 1–227. [in Russian; English translation: Byalynitskii-Birulya, A.A. 1965. Fauna of Russia and adjacent countries. Arachnoidea. Vol. 1. Scorpions. Jerusalem: Israel Program for Scientific Translations, xix, 154 pp.]
- Borelli, A. 1909. Scorpioni raccolti dal Prof. F. Silvestri nell'America settentrionale e alle isole Hawaii. Bollettino del Laboratorio di Zoologia Generale e Agraria della Reale Scuola Superiore d'Agricoltura in Portici 3: 222–227.
- Borges, A., R.J. Miranda, and J.M. Pascale. 2012. Scorpionism in Central America, with special reference to the case of Panama. Journal of Venomous Animals and Toxins including Tropical Diseases 18: 130–143.
- Bücherl, W. 1964. Distribuição geográfica dos aracnídeos peçonhentos temíveis. Memórias do Instituto de Butantan 31: 55–66.
- Bücherl, W. 1967. Escorpiões, aranhas e escolopendromorfos da Amazônia. In H. Lent (editor), Atas do Simpósio sobre a Biota Amazônica 5 (Zoologia): 111–125.
- Bücherl, W. 1969. Giftige Arthropoden. In E.J. Fittkau, J. Illies, H. King, G.H. Schwabe, and H. Sioli (editors), Biogeography and ecology in South America. Monographiae Biologicae 19 (2): 764–793. Dordrecht: W. Junk.
- Bücherl, W. 1971. Classification, biology and venom extraction of scorpions. In W. Bücherl and E.R. Buckley (editors), Venomous animals and their venoms 3: 317–348. New York: Academic Press.
- Cancino, E.R., and J.M.C. Blanco. 2002. Artrópodos terrestres de los estados de Tamaulipas y Nuevo León, México (No. 4). Victoria, Tamaulipas, Mexico: Universidad Autónoma de Tamaulipas, Unidad Académica Multidisciplinaria Agronomía y Ciencias, Centro de Investigación y Desarrollo Agropecuario, Forestal y de la Fauna.
- Comstock, J.H. 1912. The spider book. New York: Doubleday, 729 pp.
- Comstock, J.H. 1940. The spider book. Revised and edited by W.J. Gertsch. New York: Doubleday, 729 pp.
- Crews, S.C., and L.A. Esposito. 2020. Towards a synthesis of the Caribbean biogeography of terrestrial arthropods. BMC Evolutionary Biology 20: 12.
- Cupitra Vergara, N.I., S. Cubides Cubillos, M.M. Saldaña-Córdoba, and E. Estrada-Gómez. 2014. Distribución de *Centruroides edwardsii* (Gervais, 1843) en el departamento de Antioquia, Colombia. Acta Biológica Colombiana 20: 207–215.
- Delfín-González, H., V.M. Ramírez, P.C. Manrique, A. Martín-Park, and C. Arisqueta-Chablé. 2017. Contribution to the knowledge of the arachnids in the Yucatan Peninsula, Mexico (excluding Araneae and Acari). Tropical and Subtropical Agroecosystems 20: 279–288.
- De los Santos, G., L.F. de Armas, and R. Teruel. 2016. Lista anotada de los escorpiones (Arachnida: Scorpiones) de la Española (República Dominicana y Haití). Novitates Caribea 10: 1–22.
- Díaz Nájera, A. 1966. Alacranes de la República Mexicana. Clave para identificar especies de *Centrurus*. Revista de Investigación de Salud Pública 26: 109–123.
- Díaz Nájera, A. 1970. Contribución al conocimiento de los alacranes de México (Scorpionida). Revista de Investigación de Salud Pública 30: 111–122.
- Esposito, L. 2011. Systematics and biogeography of the New World scorpion genus *Centruroides* Marx, 1890 (Scorpiones: Buthidae). Ph.D. dissertation, Department of Biology, City University of New York, New York.
- Esposito, L.A., and L. Prendini. 2019. Island ancestors and New World biogeography: a case study from the scorpions (Buthidae: Centruroidinae). Scientific Reports 9: 1–11.
- Esposito, L.A., H.Y. Yamaguti, C.A. Souza, R. Pinto-Da-Rocha, and L. Prendini. 2017. Systematic revision of the Neotropical club-tailed scorpions, *Physoctonus*, *Rhopalurus*, and *Troglorhopalurus*, revalidation of *Heteroctenus*, and descriptions of two new genera and three new species (Buthidae: Rhopalurusinae). Bulletin of the American Museum of Natural History 415: 1–136.
- Esposito, L.A., H.Y. Yamaguti, R. Pinto-da-Rocha, and L. Prendini. 2018. Plucking with the plectrum: phylogeny of the New World buthid scorpion subfamily Centruroidinae Kraus, 1955 (Scorpiones: Buthidae) reveals evolution of three pecten-sternite stridula-

- tion organs. *Arthropod Systematics and Phylogeny* 76: 87–122.
- Fet, V., and F. Kovařík. 2020. New scorpion taxa (Arachnida: Scorpiones) described in the journal *Euscorpius* in 2002–2020. *Euscorpius* 300: 1–31.
- Fet, V., and G. Lowe. 2000. Family Buthidae C.L. Koch, 1837. In V. Fet, W.D. Sissom, G. Lowe, and M.E. Braunwalder, Catalog of the scorpions of the world (1758–1998): 54–286. New York: New York Entomological Society.
- Francke, O.F. 1977. Escorpiones y escorpionismo en el Perú. VI: lista de especies y claves para identificar las familias y los géneros. *Revista Peruana de Entomología* 20: 73–76.
- Francke, O.F. 1985. Conspectus genericus scorpionorum 1758–1982 (Arachnida: Scorpiones). *Occasional Papers of the Museum, Texas Tech University* 98: 1–32.
- Francke, O.F. 2007. Alacranes (Arachnida: Scorpiones) de Frontera Corozal, en la selva Lacandona, Chiapas, México, con la descripción de una nueva especie de *Diplocentrus* (Diplocentridae). *Revista Mexicana de Biodiversidad* 78: 69–77.
- Francke, O.F., and S.A. Stockwell. 1987. Scorpions (Arachnida) from Costa Rica. *Special Publications of the Museum, Texas Tech University* 25: 1–64.
- Franganillo, P.B. 1936. Los arácnidos de Cuba hasta 1936. Havana: Imprenta Cultural, S.A, 179 pp.
- González-Santillán, E. 2001. Catálogo de escorpiones de la Colección Nacional de Arácnidos (CNAN). M.S. thesis, Facultad de Ciencias, Universidad Nacional Autónoma de México, México, DF.
- González-Sponga, M.A. 1984. Escorpiones de Venezuela. Caracas: Cuadernos Lagoven, 128 pp.
- González-Sponga, M.A. 1996. Guía para identificar escorpiones de Venezuela. Caracas: Cuadernos Lagoven, 204 pp.
- Goodman, A., and L.A. Esposito. 2020. Niche partitioning in congeneric scorpions. *Invertebrate Biology* 139: e12280.
- Goodman, A., L. Prendini, and L.A. Esposito. 2021. Systematics of the arboreal Neotropical “thorellii” clade of *Centruroides* Marx, 1890 bark scorpions (Buthidae C.L. Koch 1837), and the efficacy of mini-barcodes for museum specimens of variable age and preservation. *Diversity* 13.
- Hjelle, J.T. 1990. Anatomy and morphology. In G.A. Polis (editor), *The biology of scorpions*: 9–63. Stanford, CA: Stanford University Press.
- Hoffmann, C.C. 1932. Monografías para la entomología médica de México. Monografía N° 2, Los escorpiones de México. Segunda parte: Buthidae. *Anales del Instituto de Biología, Universidad Nacional Autónoma de México* 2: 291–408.
- Hoffmann, C.C. 1937. Nota acerca de los alacranes del Valle del Mesquital, Hidalgo. *Anales del Instituto de Biología, Universidad Nacional Autónoma de México* 8: 201–206.
- Howard, R.J., G.D. Edgecombe, D.A. Legg, D. Pisani, and J. Lozano-Fernandez. 2019. Exploring the evolution and terrestrialization of scorpions (Arachnida: Scorpiones) with rocks and clocks. *Organisms Diversity and Evolution* 19: 71–86.
- Kamenz, C., and L. Prendini. 2008. An atlas of book lung fine structure in the order Scorpiones (Arachnida). *Bulletin of the American Museum of Natural History* 316: 1–359.
- Karsch, F. 1879a. *Scorpionologische Beiträge*. Part I. *Mitteilungen des Münchener Entomologischen Vereins* 3: 6–22.
- Karsch, F. 1879b. *Skorpionologische Beiträge*. Part II. *Mitteilungen des Münchener Entomologischen Vereins* 3: 97–136.
- Kearse, M., et al. 2012. Geneious Basic: an integrated and extendable desktop software platform for the organization and analysis of sequence data. *Bioinformatics* 28: 1647–1649.
- Kovařík , F. 1998. *Štíři [Scorpions]*. Jihlava, Czech Republic: Madagaskar, 175 pp. [in Czech]
- Kovařík, F., and R. Teruel. 2014. Three new scorpion species from the Dominican Republic, Greater Antilles (Scorpiones: Buthidae, Scorpionidae). *Euscorpius* 187: 1–27.
- Kovařík, F., G. Lowe, J. Plíšková, and F. Štáhlavský. 2016a. *Scorpions of the Horn of Africa (Arachnida: Scorpiones)*. Part VII. *Parabuthus* Pocock, 1890 (Buthidae), with description of *P. hamar* sp. nov. and *P. kajibu* sp. nov. from Ethiopia. *Euscorpius* 228: 1–58.
- Kovařík, F., R. Teruel, and G. Lowe. 2016b. Two new scorpions of the genus *Chaneke* Francke, Teruel et Santibáñez-López, 2014 (Scorpiones: Buthidae) from southern Mexico. *Euscorpius* 218: 1–20.
- Kraepelin, K. 1891. Revision der Skorpione. I. Die Familie Androctonidae. *Beiheft zum Jahrbuch der Hamburgischen Wissenschaftlichen Anstalten* 8: 1–144.
- Kraepelin, K. 1899. Scorpiones und Pedipalpi. In F. Dahl (editor), *Das Tierreich*. Berlin: R. Friedländer und Sohn Verlag, 265 pp.
- Kraepelin, K. 1912 (“1911”). Neue Beiträge zur Systematik der Gliederspinnen. II. Chactinae (Scorpiones). Mitteilungen aus dem Naturhistorischen Museum (2. Beiheft zum Jahrbuch der Hamburgischen Wissenschaftlichen Anstalten) 29: 43–88.

- Lamoral, B.H. 1978. Systematics and bionomics of the scorpions of South West Africa. Ph.D. dissertation, Department of Zoology, University of Natal, Pietermaritzburg, South Africa.
- Lamoral, B.H. 1979. The scorpions of Namibia (Arachnida: Scorpionida). Annals of the Natal Museum 23: 497–784.
- Lamoral, B. H. 1980. Two new psammophile species and new records of scorpions from the northern Cape Province of South Africa (Arachnida: Scorpionida). Annals of the Natal Museum 24: 201–210.
- Larkin, M.A., et al. 2007. Clustal W and Clustal X version 2.0. Journal of Bioinformatics 23: 2947–2948.
- Laurie, M. 1896. Further notes on the anatomy and development of scorpions, and their bearing on the classification of the order. Annals and Magazine of Natural History (Ser. 6) 18: 121–133.
- Lönnberg, E. 1897. Om skorpionernas och pedipalpernas geografiska utbredning. Entomologisk Tidskrift 18: 193–211.
- Loria, S.F., and L. Prendini. 2014. Homology of the lateral eyes of Scorpiones: a six-ocellus model. PLoS One 9: e112913.
- Lourenço, W.R. 1979. A propos de la véritable identité des genres *Rhopalurus* Thorell, 1879 et *Centruroides* Marx, 1889 (Scorpiones, Buthidae). Revue Arachnologique 2: 213–219.
- Lourenço, W. R. 2014. A new species of scorpion from Chiapas Mexican amber (Scorpiones: Buthidae). Revista Ibérica de Aracnología 24: 59–63.
- Lourenço, W.R., and V.R.D. von Eickstedt. 1988. Considerações sobre a sistemática de *Tityus costatus* (Karsch 1879) provável espécie polimórfica de escorpião da floresta atlântica do Brasil (Scorpiones, Buthidae). Iheringia (Sér. Zool.) 68: 3–11.
- Lourenço, W. R., and J. Velten. 2016. A new species of *Rhopalurus* Thorell, 1876 from Dominican amber (Scorpiones, Buthidae). Revista Ibérica de Aracnología 29: 61–66.
- Maddison, W. P., and D.R. Maddison. 2018. Mesquite: a modular system for evolutionary analysis. Version 3.4. Available from: <http://mesquiteproject.org>
- Martín-Frías, E., L.F. de Armas, and J.F. Paniagua-Solís. 2005. Redescription of the Mexican scorpion *Centruroides hoffmanni* Armas, 1996 (Scorpiones: Buthidae). Euscorpius 22: 1–7.
- Marx, G. 1890 (“1889”). Arachnida. In L.O. Howard (editor), Scientific results of the explorations by the U.S. Fish Commission Steamer Albatross, No. V. Annotated catalogue of the insects collected in 1887–’88. Proceedings of the United States National Museum 12: 207–211.
- Masters, B.C., V. Fan, and H.A. Ross. 2011. Species delimitation—a Geneious plugin for the exploration of species boundaries. Molecular Ecology Resources 11: 154–157.
- McWest, K.J., Z.J. Valois, and W.D. Sissom. 2015. Scorpions (Arachnida) of the high plains and adjacent canyonlands of northwestern Texas. Texas Journal of Science 67: 3–38.
- Mello-Campos, O. de. 1924a. Os escorpiões brasileiros. Memórias do Instituto Oswaldo Cruz 17: 237–369.
- Mello-Campos, O. de. 1924b. Scorpions of Brazil. Memórias do Instituto Oswaldo Cruz 17 (2): 303–363. [English translation of Mello-Campos (1924a)]
- Mello-Leitão, C.F. de. 1932. Notas sobre escorpiões sulamericanos. Arquivos do Museu Nacional 34: 9–46.
- Mello-Leitão, C. de. 1934 (“1933”). Estudo monográfico dos escorpiões da Republica Argentina. Octava Reunión de la Sociedad Argentina, Santiago del Estero 1933: 1–97.
- Mello-Leitão, C.F. de. 1942. Los alacranes y la zoogeografía de Sudamérica. Revista Argentina de Zoogeografía 2: 125–131.
- Mello-Leitão, C.F. de. 1945. Escorpiões sul americanos. Arquivos do Museu Nacional 40: 1–468.
- Mendoza-Villa, O.N., V.H. Sandoval, J. Cerano-Paredes, R. Cervantes-Martínez, and J.C. Soto-Correa. 2018. Reconstruction of historical precipitation (1877–2014) for the southwestern of the Sierra Gorda Biosphere Reserve, Querétaro, Mexico. Revista Chapingo Serie Ciencias Forestales 23: 371–386.
- Meusnier, I., et al. 2008. A universal DNA mini-barcode for biodiversity analysis. BMC Genomics 9: 214.
- Miller, A.L., R.A., Makowsky, D.R., Formanowicz, L. Prendini, and C.L. Cox. 2014. Cryptic genetic diversity and complex phylogeography of the boreal North American scorpion, *Paruroctonus boreus* (Vaejovidae). Molecular Phylogenetics and Evolution 71: 298–307.
- Miller, M.A., W. Pfeiffer, and T. Schwartz. 2009. Creating the CIPRES Science Gateway for inference of large phylogenetic trees. In Proceedings of the Gateway Computing Environments Workshop (GCE), 14 Nov. 2010, New Orleans, LA, 8 pp.
- Millot, J., and M. Vachon. 1949. Ordre des scorpions. In P.-P. Grassé (editor), Traité de zoologie, vol. 6: 387–437. Paris: Masson et Cie.
- Miranda, R.J., and L.F. de Armas, L. F. 2020. A new species of *Ananteris* (Scorpiones: Buthidae) from Panama. Euscorpius 297: 1–7.

- Moreno, A. 1939. Contribución al estudio de los escorpiónidos cubanos. Parte II. Superfamilia Buthoidea. Memorias de la Sociedad Cubana de Historia Natural 13: 63–75.
- Moreno, A. 1940. Contribución al estudio de los escorpiónidos cubanos. Parte III. Familia “Buthidae.” Addendum. Memorias de la Sociedad Cubana de Historia Natural 14: 161–164.
- Muma, M.H. 1967. Scorpions, whip-scorpions and wind scorpions of Florida. Arthropods of Florida and Neighbouring Land Areas, Florida Department of Agriculture 4: 1–28.
- Nenilin, A.B., and V. Fet. 1992. Zoogeographical analysis of the world scorpion fauna (Arachnida: Scorpiones). Arthropoda Selecta 1: 3–31. [in Russian; English summary]
- Ochoterena, I. 1920. El alacrán de Durango (*Centrurus exilicauda* Wood). Memorias y Revista de la Sociedad Científica ‘Antonio Alzate’ 37: 215–226
- Pocock, R.I. 1890. A revision of the genera of scorpions of the family Buthidae, with descriptions of some South-African species. Proceedings of the Zoological Society 1890: 114–141.
- Pocock, R.I. 1893. Contribution to our knowledge of the arthropod fauna of the West Indies. Part I. Scorpiones and Pedipalpi, with a supplementary note upon freshwater Decapoda of St. Vincent. Journal of the Linnean Society 24: 374–409.
- Pocock, R.I. 1898. Descriptions of some new scorpions from Central and South America. Journal of Natural History 1: 384–394.
- Pocock, R.I. 1902a. Arachnida. Scorpiones, Pedipalpi, and Solifugae. In R.H. Porter, Biologia Centrali-Americana. London: Taylor and Francis, 71 pp.
- Pocock, R.I. 1902b. A contribution to the systematics of scorpions. I. Some corrections in nomenclature. II. Notes on some species of *Parabuthus* contained in the British Museum. III. Descriptions of some new and old species. Annals and Magazine of Natural History (Ser. 7) 10: 364–380.
- Ponce-Saavedra J., and O.F. Francke. 2014. Clave para la identificación de especies de alacranes del género *Centruroides* Marx 1890 (Scorpiones: Buthidae) en el centro occidente de México. Biológicas Revista de la DES Ciencias Biológico Agropecuarias Universidad Michoacana de San Nicolás de Hidalgo 15: 52–62.
- Ponce-Saavedra, J., and O.F. Francke. 2019. Una especie nueva de alacrán del género *Centruroides* (Scorpiones: Buthidae) del noroeste de México. Revista Mexicana de Biodiversidad 90: 1–17.
- Ponce-Saavedra J., and R.J. Moreno-Barajas. 2005. El género *Centruroides* Marx 1890 (Scorpiones: Buthidae) en México. Biológicas 7: 42–51.
- Ponce-Saavedra, J., A.F. Quijano-Ravell, R. Teruel, and O.F. Francke. 2015. Redescription of *Centruroides ornatus* Pocock, 1902 (Scorpiones Buthidae), a montane scorpion from central Mexico. Revista Ibérica de Aracnología 15: 81–89.
- Prendini, L. 2000a. Phylogeny and classification of the superfamily Scorpinoidea Latreille 1802 (Chelicerata, Scorpiones): an exemplar approach. Cladistics 16: 1–78.
- Prendini, L. 2000b. A new species of *Parabuthus* Pocock (Scorpiones: Buthidae), and new records of *Parabuthus capensis* (Ehrenberg), from Namibia and South Africa. Cimbebasia 16: 201–214.
- Prendini, L. 2001a. Substratum specialization and speciation in southern African scorpions: the Effect Hypothesis revisited. In V. Fet, and P.A. Selden (editors), Scorpions 2001: in memoriam Gary A. Polis: 113–138. Burnham Beeches, Bucks, U.K.: British Arachnological Society.
- Prendini, L. 2001b. Phylogeny of *Parabuthus* (Scorpiones, Buthidae). Zoologica Scripta 30: 13–35.
- Prendini, L. 2003. A new genus and species of bothriurid scorpion from the Brandberg Massif, Namibia, with a reanalysis of bothriurid phylogeny and a discussion of the phylogenetic position of *Lisposoma* Lawrence. Systematic Entomology 28: 149–172.
- Prendini, L. 2004. The systematics of southern African *Parabuthus* Pocock (Scorpiones, Buthidae): revisions to the taxonomy and key to the species. Journal of Arachnology 32: 109–187.
- Prendini, L., and W.C. Wheeler. 2005. Scorpion higher phylogeny and classification, taxonomic anarchy, and standards for peer review in online publishing. Cladistics 21: 446–494.
- Quijano-Ravell, A.F., and J. Ponce-Saavedra. 2015. Estructura poblacional de *Centruroides ornatus* (Scorpiones: Buthidae) en la cuenca de Cuitzeo, Michoacán, México. Revista Ibérica de Aracnología 27: 35–44.
- Quijano-Ravell, A.F., and J. Ponce-Saavedra. 2016a. Uso del hábitat por *Centruroides ornatus* Pocock 1902 (Scorpiones: Buthidae) en el cerro “El Águila” Morelia, Michoacán, México. Entomologica Mexicana 3: 85–90.
- Quijano-Ravell, A.F., and J. Ponce-Saavedra, J. 2016b. A new species of scorpion of the genus *Centruroides* (Scorpiones: Buthidae) from the state of Michoacán, Mexico. Revista Mexicana de Biodiversidad 87: 49–61.

- Quijano-Ravell, A.F., L.F. de Armas, O.F. Francke, and J. Ponce-Saavedra. 2019. A new species of the genus *Centruroides* Marx (Scorpiones, Buthidae) from western Michoacán state, México, using molecular and morphological evidence. *ZooKeys* 859: 31–48.
- Quintero Arias, D., and L.A. Esposito. 2014. A new species of *Centruroides* Marx (Scorpiones: Buthidae) from Panama and new distribution records for *Centruroides bicolor* (Pocock, 1898) and *Centruroides granosus* (Thorell, 1876). *Zootaxa* 3795: 373–382.
- Reyes-García, A., and M. Sousa 1995. Una nueva localidad para la familia Lacandoniaceae y nuevos registros para la Reserva de Montes Azules, Chiapas, México. *Botanical Sciences* 57: 117–119.
- Riquelme, F., et al. 2015. New fossil scorpion from the Chiapas amber Lagerstätte. *PLoS One* 10: e0133396.
- Rodrigo, A., et al. 2008. The perils of plenty: what are we going to do with all these genes? *Philosophical Transactions of the Royal Society B* 363: 3893–3902.
- Ronquist, F., and J.P. Huelsenbeck. 2003. MrBayes 3: Bayesian phylogenetic inference under mixed models. *Journal of Bioinformatics* 19: 1572–1574.
- Rosenberg, N.A. 2007. Statistical tests for taxonomic distinctiveness from observations of monophyly. *Journal of Evolution* 61: 317–323.
- Santibáñez-López, C.E., and G.A. Contreras-Félix. 2013. Two new species of *Centruroides* Marx 1890 (Scorpiones: Buthidae) from Oaxaca, Mexico. *Zootaxa* 3734: 130–140.
- Santibáñez-López, C.E., and J. Ponce-Saavedra. 2009. Una especie nueva de *Centruroides* (Scorpiones: Buthidae) de la Sierra Norte de Oaxaca, México. *Revista Mexicana de Biodiversidad* 80: 321–331.
- Scorza, J.V. 1954. Sistemática, distribución geográfica y observaciones ecológicas de algunos alacranes encontrados en Venezuela. *Memória de la Sociedad de Ciencias Naturales “La Salle”* 14: 179–214.
- Shelley, M., and W.D. Sissom. 1995. Distributions of the scorpions *Centruroides vittatus* (Say) and *Centruroides hentzi* (Banks) in the United States and Mexico (Scorpiones, Buthidae). *Journal of Arachnology* 2: 100–110.
- Sissom, W.D. 1990. Systematics, biogeography and paleontology. In G.A. Polis (editor), *The biology of scorpions*: 64–160. Stanford, CA: Stanford University Press.
- Sissom, W.D. 1995. Redescription of the scorpion *Centruroides thorelli* Kraepelin (Buthidae) and description of two new species. *Journal of Arachnology* 23: 91–99.
- Sissom, W.D., and B.E. Hendrixson. 2005. Scorpion biodiversity and patterns of endemism in northern Mexico. In J.E. Cartron, G. Ceballos, and R.S. Felger (editors), *Biodiversity, ecosystems, and conservation in northern Mexico*: 122–137. New York: Oxford University Press.
- Soleglad, M. E., and V. Fet. 2003. High-level systematics and phylogeny of the extant scorpions (Scorpiones: Orthosterni). *Euscorpius* 11: 1–56.
- Stahnke, H.L. 1970. Scorpion nomenclature and mensuration. *Entomological News* 81: 297–31.
- Stahnke, H.L. 1971. Some observations of the genus *Centruroides* Marx (Buthidae, Scorpionida) and *C. sculpturatus* Ewing. *Entomological News* 82: 281–307.
- Stahnke, H.L. 1972. A key to the genera of Buthidae (Scorpionida). *Entomological News* 83: 121–133.
- Stahnke, H.L., and M. Calos. 1977. A key to the species of the genus *Centruroides* Marx (Buthidae, Scorpionida). *Entomological News* 88: 111–120.
- Stamatakis, A. 2014. RAxML version 8: a tool for phylogenetic analysis and post-analysis of large phylogenies. *Journal of Bioinformatics* 30: 1312–1313.
- Stockwell, S.A. 1988. A key and checklist to the families and genera of North American scorpions. University of California, Berkeley [published by the author], 10 pp.
- Stockwell, S.A. 1989. Revision of the phylogeny and higher classification of scorpions (Chelicerata). Ph.D. dissertation, Department of Integrative Biology, University of California, Berkeley.
- Stockwell, S.A. 1992. Systematic observations on North American Scorpionida with a key and checklist of the families and genera. *Journal of Medical Entomology* 29: 407–422.
- Teruel, R. 2016. The true taxonomic identity of *Centruroides tenuis* (Thorell, 1876) and *Centruroides zayasi* Armas, 1976 (Scorpiones: Buthidae). *Revista Ibérica de Aracnología* 29: 91–93.
- Teruel, R., and B. Myers. 2017. A new island species of *Centruroides* Marx, 1890 (Scorpiones: Buthidae) from the southwestern Caribbean. *Euscorpius* 252: 1–14.
- Teruel, R., and K. Questel. 2020. A new Lesser Antillean scorpion of the genus *Didymocentrus* Kraepelin, 1905 (Scorpiones: Diplocentridae). *Euscorpius* 313: 1–15.
- Teruel, R., and T.M. Rodríguez-Cabrera. 2014. On the westernmost occurrence of the genus *Microtityus* Kjellesvig-Waering, 1966 in Cuba (Scorpiones: Buthidae). *Revista Ibérica de Aracnología* 24: 131–133.
- Teruel, R., and S.A. Stockwell. 2002. A revision of the scorpion fauna of Honduras, with the description of

- a new species (Scorpiones: Buthidae, Diplocentriidae). Revista Ibérica de Aracnología 6: 111–127.
- Teruel, R., V. Fet, and M.R. Graham. 2006. The first mitochondrial DNA phylogeny of Cuban Buthidae (Scorpiones: Buthoidea). Boletín de la Sociedad Entomológica Aragonesa 39: 219–226.
- Teruel, R., F. Kovařík, J.G. Baldazo Monsivais, and D. Hoferek. 2015a. A new species of *Centruroides* of the “*nigrovariatus*” group (Scorpiones: Buthidae) from southern Mexico. Revista Ibérica de Aracnología 26: 3–14.
- Teruel, R., L.F. de Armas, and F. Kovařík. 2015b. A new species of *Centruroides* Marx, 1890 (Scorpiones: Buthidae) from southern Hispaniola, Greater Antilles. Euscorpius 198: 1–18.
- Teruel, R., L.F. de Armas, and F. Kovařík. 2015c. Two new species of scorpions (Scorpiones: Buthidae, Scorpionidae) from Dominican Republic, Greater Antilles. Revista Ibérica de Aracnología 27: 13–33.
- Teruel, R., F. Kovařík, G. Lowe, and S. Friedrich. 2017. Complements to the taxonomy of some Amazonian scorpions (Scorpiones: Buthidae). Euscorpius 245: 1–7.
- Thompson, J.D., D.G. Higgins, and T.J. Gibson. 1994. CLUSTAL W: improving the sensitivity of progressive multiple sequence alignment through sequence weighting, position-specific gap penalties and weight matrix choice. Nucleic Acids Research 22: 4673–4680.
- Thorell, T. 1876a. On the classification of scorpions. Annals and Magazine of Natural History (Ser. 4) 17: 1–15.
- Thorell, T. 1876b. Études scorpiologiques. Atti della Società Italiana di Scienze Naturali 19: 75–272.
- Towler, W.I., J. Ponce Saavedra, B. Gantenbein, and V. Fet. 2001. Mitochondrial DNA reveals a divergent phylogeny in tropical *Centruroides* (Scorpiones: Buthidae) from Mexico. Biogeographica 77: 157–172.
- Trujillo, R.E., and L.F. de Armas. 2020. A new species of *Centruroides* (Scorpiones: Buthidae) from Quiché, northwestern Guatemala. Euscorpius 233: 1–8.
- Ubinski, C.V., L.S. Carvalho, and M.C. Schneider. 2018. Mechanisms of karyotype evolution in the Brazilian scorpions of the subfamily Centruroidinae (Buthidae). Genetica 146: 475–486.
- Vachon, M. 1952. Études sur les scorpions. Algiers: Institut Pasteur d'Algérie, 482 pp.
- Vachon, M. 1974 (“1973”). Étude des caractères utilisés pour classer les familles et les genres de scorpions (Arachnides). 1. La trichobothriotaxie en arachnologie. Sigles trichobothriaux et types de trichobothriotaxie chez les scorpions. Bulletin du Muséum National d'Histoire Naturelle, Paris, Ser. 3 (Zoologie) 140: 857–958.
- Vachon, M. 1975. Sur l'utilisation de la trichobothriotaxie du bras des pédipalpes des scorpions (Arachnides) dans le classement des genres de famille des Buthidae Simon. Comptes Rendus Hebdomadaires des Séances de l'Académie des Sciences D 281: 1597–1599.
- Vachon, M. 1977. Contribution à l'étude des scorpions Buthidae du nouveau monde. 1. Complément à la connaissance de *Microtityus rickyi* Kj.-W. 1956 de l'île de la Trinité. 2. Description d'un nouvelle espèce et d'un nouveau genre mexicains: *Darchenia bernadettiae*. 3. Clé de détermination des genres de Buthidae du nouveau monde. Acta Biológica Venezolica 9: 283–302.
- Vázquez, M.M. 1999. Fauna edáfica de las selvas tropicales de Quintana Roo. Chetumal, Quintana Roo, Mexico: Universidad de Quintana Roo, UQRoo-Conacyt.
- Volschenk, E.S., C.I. Mattoni, and L. Prendini. 2008. Comparative anatomy of the mesosomal organs of scorpions (Chelicerata, Scorpiones), with implications for the phylogeny of the order. Zoological Journal of the Linnean Society 154: 651–675.
- Wendruff, A. J., L.E. Babcock, C.S. Wirkner, J. Kluesendorf, and D.G. Mikulic. 2020. A Silurian ancestral scorpion with fossilised internal anatomy illustrating a pathway to arachnid terrestrialisation. Scientific Reports 10: 1–6.
- Werner, F. 1934. Scorpiones, Pedipalpi. In H.G. Bronn (editor), Klassen und Ordnungen des Tierreichs: 5, IV, 8, Lief. 1, 2 (Scorpiones): 1–316. Leipzig: Akademische Verlagsgesellschaft.
- Williams, S.C. 1980. Scorpions of Baja California, Mexico and adjacent islands. Occasional Papers of the California Academy of Sciences 135: 1–127.
- Wood, H.C. 1863. On the Pedipalpi of North America. Journal of the Academy of Natural Sciences of Philadelphia 5: 358–376.

## APPENDIX 1

Tissue samples, base-pair lengths, localities, and GenBank accession codes of DNA sequences from the mitochondrial cytochrome *c* oxidase subunit I gene used for phylogenetic analysis of the arboreal Neotropical “*thorellii*” clade of *Centruroides* Marx, 1890, bark scorpions (Buthidae C.L. Koch, 1837) and outgroup species of *Centruroides* and *Heteroctenus junceus* (Herbst, 1800). Material deposited in the following collections: Ambrose Monell Cryocollection (AMCC) at the American Museum of Natural History, New York; Colección Nacional de Arácnidos, Instituto de Biología (CNAN), Universidad Nacional Autónoma de México, Mexico City; California Academy of Sciences (CASENT), San Francisco. Oxford University Museum of Natural History (OUMNH), U.K. Sequences less than 150 base pairs in length deposited in the Dryad digital repository (doi: 10.5061/dryad.fttdz08t2).

Species	Collection	Locality	Length	GenBank Code
<b>Outgroup</b>				
<i>H. junceus</i>	AMCC [LP 12613]	Cuba: Guantánamo: Humboldt N. P.	1078	KY982192.1
<i>C. bani</i>	AMCC [LP 3302]	Puerto Rico: Isla Mona	1078	MK479164.1
<i>C. exilicauda</i>	AMCC [LP 1692]	Mexico: Baja California Sur: Cabo San Lucas	1078	KY982179.1
<i>C. gracilis</i>	AMCC [LP 1550]	Mexico: Veracruz: Los Idolos	1078	MK479175.1
<i>C. hentzi</i>	AMCC [LP 1673]	United States of America: Florida	1078	MK479177.1
<i>C. infamatus</i>	AMCC [LP 1822]	Mexico: Guanajuato: Acámbaro	1078	KY982181.1
<i>C. ochraceus</i>	AMCC [LP 7666]	Mexico: Morelos: Puerto Morelos Bot. Gard.	1078	MK479194.1
<i>C. thorellii</i>	AMCC [LP 5983]	Guatemala: Sacatepéquez: Parque Alux	1078	MK479208.1
	OUMNH [MID166]	Honduras: Cortés: San Pedro Sula	642	MZ366335
			658	MZ366336
<i>C. tuxtla</i>	AMCC [LP 3709]	Mexico: Chiapas: La Vuelta de alacran	1078	MK479209.1
<b>Ingroup</b>				
<i>C. berstoni</i>	CASENT 9073271	Guatemala: Izabal: Biotopo Chocón Machacas	430	MZ366346
	CASENT 9073272	Guatemala: Izabal: Hotel Tijax	621	MZ366345
	CNAN SC3968	Guatemala: Izabal: Morelos	658	MZ366344
<i>C. catemacoensis</i>	AMCC [LP 2070]	Mexico: Veracruz: Los Tuxtlas	1078	MZ429054
	AMCC [LP 5231]		1078	MZ429055
	CASENT 9073270		659	MZ366343
	CASENT 9073408		648	MZ366342
	CASENT 9073410		658	MZ366341
	CASENT 9073427		659	MZ366340
	CASENT 9073428		648	MZ366339
<i>C. chanae</i>	AMCC [LP 2009]	Mexico: Michoacán: Faro de Bucerias	1078	MZ429056
	AMCC [LP 7032]		1078	MZ429057
	AMCC [LP 8582]	Mexico: Guerrero: Microondas Fogos	1078	MZ429058

APPENDIX 1 *continued*

Species	Collection	Locality	Length	GenBank Code
<i>C. cuauhmapan</i>	AMCC [LP 2073]	Mexico: Veracruz: Cañada Blanca	1078	MZ429059
	CNAN SC4001	Mexico: Oaxaca: Cerro del Oro	40	–
	CNAN T01397	Mexico: Veracruz: Los Idolos	127	–
<i>C. hamadryas</i>	AMCC [LP 2948]	Mexico: Chiapas: La Galleta	1078	MZ429060
	CNAN SC3986		127	–
	CNAN SC3988		127	–
<i>C. hoffmanni</i>	AMCC [LP 5224]	Mexico: Chiapas: Las Delicias	1078	MZ429061
	AMCC [LP 5249]	Mexico: Chiapas: Santa Rosa	1078	MZ429062
	AMCC [LP 5350]	Mexico: Chiapas: Res. Biosfera Sepultura	1078	MK479178.1
	CNAN SC3990	Mexico: Chiapas: Siltepec	134	–
	CNAN SC3992	Mexico: Chiapas: P. N. Lagunas de Montebelo	137	–
	CNAN SC3997	Mexico: Chiapas: Gutierrez	134	–
	CNAN SC3998	Mexico: Chiapas: Villa Corzo	138	–
<i>C. rileyi</i>	AMCC [LP 6445]	Mexico: San Luis Potosí: Axtlan de Terrazas	1078	KY982183.1
	CNAN SC3985	Mexico: Veracruz: Cerro Azul	127	–
	CNAN SC3999	Mexico: Puebla: Cuetzalan	127	–
	CNAN SC4000	Mexico: Veracruz: Papantla	127	–
	CNAN SC4002	Mexico: Veracruz: Cerro Azul	127	–
<i>C. schmidti</i>	AMCC [LP 13416]	Honduras: Atlántida: Pico Bonito	127	–
	AMCC [LP 13411]	Honduras: Isla del Bahía: Cayos Menor	1078	MZ429064
	AMCC [LP 13417]		1078	MZ429065
	AMCC [LP 5985]	Guatemala: Zacapa: Aldea casas de Pinto	1078	MZ429063
	AMCC [LP 9172]	Honduras: Francisco Morazán: E.A.P. Zamorano	1078	KY982184.1
	CASENT 9073316	Guatemala: Zacapa: Guadalupe	606	MZ366338
	CASENT 9073402	Guatemala: Zacapa: Las Minas	620	MZ366337
<i>C. yucatanensis</i>	AMCC [LP 7597]	Mexico: Quintana Roo: Puerto Morelos	1078	MK479201.1
	CNAN SC3984		127	–
	CNAN SC4004	Mexico: Yucatán: Cenote Chac-ha	127	–

## APPENDIX 2

Morphological characters and character states used in phylogenetic analysis of the arboreal Neotropical “*thorellii*” clade of *Centruroides* Marx, 1890, bark scorpions (Buthidae C.L. Koch, 1837) and outgroup species of *Centruroides*, and *Heteroctenus junceus* (Herbst, 1800). Morphological terminology follows Hjelle (1990) and Sissom (1990), except for carapace and metasomal carination, which follows Vachon (1952), trichobothria, which follows Vachon (1974), tergite and pedipalp carination, which follows Prendini (2000a), book lung structure, which follows Kamenz and Prendini (2008), and ovariuterine anatomy, which follows Volschenk et al. (2008).

**Carapace**

1. Lateral ocular carinae: **0**, present, distinct; **1**, reduced to several granules; **2**, absent (E.S. Volschenk and L. Prendini, unpublished data; Esposito et al., 2017, 2018).
2. Centrolateral carinae: **0**, present; **1**, absent (E.S. Volschenk and L. Prendini, unpublished data; Esposito et al., 2017, 2018).
3. Anterior centrosubmedian carinae: **0**, present; **1**, absent (E.S. Volschenk and L. Prendini, unpublished data; Esposito et al., 2017, 2018).
4. Posterior centrosubmedian carinae: **0**, present; **1**, absent (E.S. Volschenk and L. Prendini, unpublished data; Esposito et al., 2017, 2018).
5. Anteromedian notch: **0**, present; **1**, absent (Esposito, 2011).
6. Surface granulation density: **0**, smooth; **1**, sparsely granular; **2**, densely granular medially; **3**, densely granular throughout (Esposito, 2011).
7. Surface granulation texture: **0**, weakly granular, shagreened; **1**, large, rounded granules; **2**, large, conical granules (Esposito, 2011).
8. Anterior median ocular sulcus: **0**, absent; **1**, wide; **2**, narrow, deep (Esposito, 2011).
9. Median ocular sulcus: **0**, absent; **1**, wide; **2**, narrow, deep (Esposito, 2011).
10. Posteromedian sulcus: **0**, absent; **1**, wide; **2**, narrow, deep (Esposito, 2011).
11. Posteromarginal sulci: **0**, absent; **1**, present (Esposito, 2011).
12. Posterolateral sulci: **0**, absent; **1**, present (Esposito, 2011).
13. Anterior margin, carina: **0**, absent; **1**, smooth; **2**, granular (Esposito, 2011).
14. Lateral margins, carina: **0**, absent; **1**, smooth; **2**, granular (Esposito, 2011).
15. Posterior margin, carina between posterior centrosubmedian carinae: **0**, absent; **1**, smooth; **2**, granular (Esposito, 2011).

**Pedipalps**

16. Chela prodorsal carina: **0**, granular; **1**, smooth; **2**, absent (E.S. Volschenk and L. Prendini, unpublished data; Esposito, 2011; Esposito et al., 2017, 2018).
17. Chela retrodorsal carina: **0**, granular; **1**, smooth; **2**, absent (E.S. Volschenk and L. Prendini, unpublished data; Esposito, 2011).
18. Chela retromedian carinae: **0**, granular; **1**, smooth; **2**, absent; **3**, vestigial, reduced to several sparse granules; **?**, unknown (E.S. Volschenk and L. Prendini, unpublished data; Esposito, 2011; Esposito et al., 2017, 2018).
19. Chela retroventral accessory carina: **0**, complete; **1**, reduced; **2**, absent (E.S. Volschenk and L. Prendini, unpublished data; Esposito, 2011).
20. Chela retroventral carinae: **0**, granular; **1**, smooth; **?**, unknown (Esposito, 2011; Esposito et al., 2017, 2018).

21. Chela retrodorsal accessory carinae: **0**, present; **1**, absent (Esposito, 2011; Esposito et al., 2017, 2018).
22. Chela prodorsal accessory carinae: **0**, present; **1**, absent (Esposito, 2011; Esposito et al., 2017, 2018).
23. Patella dorsomedian carina: **0**, present; **1**, absent (Esposito, 2011).
24. Femur retromedian carinae: **0**, small granules; **1**, large, conical granules (Esposito, 2011).
25. Fixed finger, number of median denticle subrows: **0**, eight; **1**, nine; **2**, 10 or more; **3**, seven plus fused proximal subrow; **4**, six plus fused proximal subrow (Esposito, 2011; Esposito et al., 2017, 2018).
26. Fixed and movable fingers, supernumerary granules: **0**, absent; **1**, present (Soleglad and Fet, 2003; Esposito, 2011; Esposito et al., 2017, 2018).
27. Movable finger, number of median denticle subrows: **0**, eight; **1**, nine; **2**, eleven; **3**, thirteen or more; **4**, seven plus fused proximal subrow (Soleglad and Fet, 2003; Prendini, 2004; Esposito, 2011; Esposito et al., 2017, 2018).
28. Chela shape (♂): **0**, incrassate (bulbous or swollen); **1**, slender (Prendini, 2001b, 2004; Esposito, 2011; Esposito et al., 2017, 2018).
29. Chela shape (♀): **0**, incrassate (bulbous or swollen); **1**, slender (Prendini, 2001b; Esposito, 2011; Esposito et al., 2017, 2018).
30. Chela movable finger, proximal lobe (♂): **0**, present; **1**, absent (Prendini, 2001b; Esposito, 2011; Esposito et al., 2017, 2018).
31. Patella prolateral surface, setation: **0**, long, dense setae; **1**, short, sparse setae (E.S. Volschenk and L. Prendini, unpublished data; Esposito, 2011).

### Legs

32. Leg I, tarsal setation: **0**, short, dense setae; **1**, long, dense setae; **2**, sparse setae (E.S. Volschenk and L. Prendini, unpublished data; Esposito, 2011; Esposito et al., 2017, 2018).
33. Leg IV, tarsal setation: **0**, short, dense setae; **1**, long, dense setae; **2**, sparse setae (Esposito, 2011; Esposito et al., 2017, 2018).
34. Legs I–IV, trochanter lateral margin carina: **0**, absent; **1**, smooth; **2**, granular (Esposito, 2011).
35. Telotarsal unguis: **0**, long, slightly curved; **1**, hooked (Esposito, 2011).

### Pectines

36. Pectinal tooth shape: **0**, elongate; **1**, rounded, spadelike (Esposito, 2011; Esposito et al., 2017, 2018).
37. Proximal teeth, nodules on dorsal surface: **0**, one; **1**, multiple; **2**, absent (Esposito, 2011; Esposito et al., 2017, 2018).
38. Dorsal fulcra: **0**, present; **1**, reduced (Esposito, 2011).
39. Tympanumlike expansion between lamellae and teeth: **0**, absent; **1**, present (Esposito, 2011).
40. Proximal fulcra, setal count: **0**, one; **1**, two; **2**, three; **3**, four; **4**, six or more; **5**, none; **?**, unknown. (Esposito, 2011; Esposito et al., 2017, 2018).
41. Pectinal plate anterior margin, sulcus (♂): **0**, present; **1**, absent (Esposito, 2011; Esposito et al., 2017, 2018).
42. Pectinal plate, posterior margin (♂): **0**, straight; **1**, convex; **2**, concave (Esposito, 2011; Esposito et al., 2017, 2018).
43. Median pectinal plate depression (♂): **0**, present; **1**, absent (Esposito, 2011; Esposito et al. 2017, 2018).

44. Lateral pectinal plate depression ( $\delta$ ): **0**, present; **1**, absent (Esposito, 2011).
45. Pectinal plate shape ( $\delta$ ): **0**, square; **1**, rectangular; **2**, trapezoidal (Esposito, 2011).
46. Pectinal plate anterior margin, sulcus ( $\varphi$ ): **0**, present; **1**, absent; **?**, unknown (Esposito, 2011).
47. Pectinal plate posterior margin ( $\varphi$ ): **0**, straight; **1**, slightly convex; **2**, prominently rounded; **3**, concave; **?**, unknown (Esposito, 2011).
48. Pectinal plate depressions ( $\varphi$ ): **0**, absent; **1**, single wide median depression; **2**, paired lateral depressions; **3**, single small, deep median depression (pinhole); **?**, unknown (Esposito, 2011).

### Sternites

49. Sternite VI, ventromedian carina: **0**, absent; **1**, granular; **2**, smooth (E.S. Volschenk and L. Prendini, unpublished data; Esposito, 2011; Esposito et al., 2017, 2018).
50. Sternite V, setation ( $\delta$ ): **0**, absent; **1**, present, setal base not situated in pits (surface smooth); **2**, present, setal base situated in pits (surface punctate) (Esposito, 2011).
51. Sternite VI, ventrolateral carinae: **0**, absent; **1**, reduced to single granule; **2**, present, more than one granule (E.S. Volschenk and L. Prendini, unpublished data; Esposito, 2011; Esposito et al., 2017, 2018).

### Tergites

52. Tergites III–VI, dorsolateral carinae: **0**, present; **1**, absent (E.S. Volschenk and L. Prendini, unpublished data; Esposito, 2011; Esposito et al., 2017, 2018).
53. Tergites III–VI, dorsosubmedian carinae: **0**, absent; **1**, vestigial; **2**, distinct (Prendini, 2004; Esposito, 2011; Esposito et al., 2017, 2018).
54. Tergite VII, median carina: **0**, narrow, granular carina; **1**, broad, granular carina; **2**, broad, smooth carina; **3**, vestigial (E.S. Volschenk and L. Prendini, unpublished data; Esposito, 2011; Esposito et al., 2017, 2018).

### Metasoma

55. Segment II, median lateral carinae: **0**, complete; **1**, posteriorly restricted; **2**, absent (Esposito, 2011; Esposito et al., 2017, 2018).
56. Segment III, median lateral carinae: **0**, complete; **1**, posteriorly restricted; **2**, absent (Esposito, 2011; Esposito et al., 2017, 2018).
57. Segment III, dorsolateral carinae, posterior granules: **0**, similar to preceding granules; **1**, larger than preceding granules, acuminate (E.S. Volschenk and L. Prendini, unpublished data; Esposito, 2011; Esposito et al., 2017, 2018).
58. Segment IV, median lateral carinae: **0**, absent or obsolete; **1**, present (Esposito, 2011; Esposito et al., 2017, 2018).
59. Segment V, posterior margin (anal rim) granulation: **0**, present; **1**, absent (Esposito, 2011; Esposito et al., 2017, 2018).
60. Segment V, dorsolateral carinae: **0**, present; **1**, absent (Esposito, 2011; Esposito et al., 2017, 2018).
61. Segment V, median lateral carinae: **0**, present; **1**, absent (Esposito 2011; Esposito et al., 2017, 2018).
62. Segment V, ventrolateral carinae: **0**, present; **1**, absent; **?**, unknown (Esposito, 2011).
63. Segment V, ventromedian carinae: **0**, absent or obsolete; **1**, present (Esposito, 2011; Esposito et al., 2017, 2018).
64. Segment V, ventrosubmedian carinae: **0**, absent or obsolete; **1**, present (Esposito, 2011; Esposito et al., 2017, 2018).
65. Segment V, ratio of segment length to width ( $\delta$ ): **0**, slightly elongated, length less than  $2 \times$  width; **1**, moderately elongated, length  $2.5\text{--}3 \times$  width; **2**, markedly elongated, length more than  $3 \times$  width (Esposito, 2011; Esposito et al., 2017, 2018).

66. Segments I–IV, width: **0**, narrowing posteriorly, segment I slightly wider than IV; **1**, slightly widening posteriorly, segment I slightly narrower than IV; **2**, markedly widening posteriorly, segment I much narrower than IV (Esposito, 2011; Esposito et al., 2017, 2018).
67. Metasoma length relative to length of prosoma and mesosoma ( $\delta$ ): **0**, similar or slightly greater; **1**, 1.5–2×; **2**, more than 2× (Esposito, 2011; Esposito et al., 2017, 2018).
68. Metasoma length relative to length of prosoma and mesosoma ( $\varphi$ ): **0**, similar or slightly greater; **1**, 1.5–2×; **2**, more than 2×; **?**, unknown (Lamoral, 1978; Prendini 2001b, 2003; Esposito, 2011; Esposito et al., 2017, 2018).

### Telson

69. Telson shape and length ( $\delta$ ): **0**, spherical, length similar to width; **1**, slightly ovate, length approximately 1.5× width; **2**, ovate, length more than 2× width (Esposito, 2011; Esposito et al., 2017, 2018).
70. Telson vesicle, width in relation to width of metasomal segment V ( $\delta$ ): **0**, similar; **1**, narrower; **2**, much narrower, less than half (Lamoral, 1978; Prendini 2001b, 2003; Esposito, 2011; Esposito et al., 2017, 2018).
71. Telson vesicle, ventromedian carinae: **0**, present; **1**, absent (E.S. Volschenk and L. Prendini, unpublished data; Esposito, 2011; Esposito et al., 2017, 2018).
72. Telson vesicle, ventrolateral carinae: **0**, present; **1**, absent (E.S. Volschenk and L. Prendini, unpublished data; Esposito, 2011; Esposito et al., 2017, 2018).
73. Telson aculeus angle: **0**, angled approximately 90° to vesicle; **1**, angled less than 90° to vesicle (Esposito, 2011).
74. Telson vesicle, proximal margin, notch: **0**, absent; **1**, present, unmodified; **2**, present, projecting vertically (Esposito, 2011).
75. Telson vesicle, lateral lobes: **0**, absent; **1**, present (Esposito, 2011).
76. Telson ventral surface: **0**, granular; **1**, smooth (Esposito, 2011).
77. Telson subaculear tubercle: **0**, distinct, singular; **1**, distinct, bifurcate; **2**, obsolete, slight protuberance; **3**, absent (Lamoral, 1980; Stockwell, 1989; Prendini, 2001b, 2003; Esposito, 2011; Esposito et al., 2017, 2018).

### Total length

78. Total length, sexual dimorphism: **0**, male shorter than or similar to female; **1**, male much longer than female; **?**, unknown (Esposito, 2011; Esposito et al., 2017, 2018).

### Ovariuterus

79. Number of loops (“cells”): **0**, eight; **1**, nine; **?**, unknown (Volschenk et al., 2008; Esposito, 2011; Esposito et al., 2017, 2018).
80. Loop shape: **0**, simple; **1**, complex bridged; **?**, unknown (Volschenk et al., 2008; Esposito, 2011; Esposito et al., 2017, 2018).

### Book lungs

81. Lamellar surface: **0**, slender venation; **1**, ribbed venation; **?**, unknown (Kamenz and Prendini, 2008; Esposito, 2011; Esposito et al., 2017, 2018).
82. Lamellar edge: **0**, thorns; **1**, smooth or wrinkled; **?**, unknown (Kamenz and Prendini, 2008; Esposito, 2011; Esposito et al., 2017, 2018).
83. Spiracle, posterior margin: **0**, hilocks; **1**, subconical; **?**, unknown (Kamenz and Prendini, 2008; Esposito, 2011; Esposito et al., 2017, 2018).

### Color and infuscation

84. Cheliceral manus, reticulate infuscation: **0**, present; **1**, laterally restricted; **2**, absent (Esposito, 2011).
85. Pedipalp segments, color pattern: **0**, chela manus and patella similar to femur; **1**, chela manus darker than femur; **2**, chela manus and patella darker than femur; **3**, chela manus paler than femur (Esposito, 2011).
86. Pedipalp femur, mottled infuscation: **0**, present; **1**, absent (Esposito, 2011).
87. Pedipalp patella, mottled infuscation: **0**, present; **1**, absent (Esposito, 2011).
88. Pedipalp chela manus, mottled infuscation: **0**, present; **1**, absent (Esposito, 2011).
89. Pedipalp chela fingers, mottled infuscation: **0**, present; **1**, absent (Esposito, 2011).
90. Tergites I–VI, mottled infuscation: **0**, present; **1**, absent (Esposito, 2011).
91. Tergites I–VI, lateral band of infuscation, shape: **0**, absent; **1**, narrow; **2**, distinct, rectangular; **3**, wide, almost touching lateral margins (Esposito, 2011).
92. Tergites I–VI, lateral band of infuscation, intensity: **0**, absent; **1**, faint; **2**, mottled; **3**, distinct (Esposito, 2011).
93. Tergites I–VI, infuscation: **0**, eye-shaped pattern; **1**, absent (Esposito, 2011).
94. Tergites I–VI, lateral margins infuscation: **0**, distinct black line; **1**, absent; **?**, unknown (Esposito, 2011).
95. Tergites I–VI, median stripe of infuscation: **0**, absent; **1**, present (Esposito, 2011).
96. Tergite VII, color pattern: **0**, similar to other tergites; **1**, paler than other tergites (Esposito, 2011).
97. Carapace, mottled infuscation: **0**, present; **1**, absent (Esposito, 2011).
98. Carapace, bands of infuscation: **0**, absent; **1**, two broad bands; **2**, four narrow lines (Esposito, 2011).
99. Carapace, interocular triangle infuscation: **0**, present; **1**, absent (Esposito, 2011).
100. Metasomal segments I–V, ventral surfaces, mottled infuscation: **0**, present; **1**, absent (Esposito, 2011).
101. Metasomal segments I–V, lateral surfaces, mottled infuscation: **0**, present; **1**, absent (Esposito, 2011).
102. Metasomal segments I–V, ventromedian stripe of infuscation: **0**, present; **1**, absent (Esposito, 2011).
103. Metasomal segment V, color pattern: **0**, similar to preceding segments; **1**, darker than preceding segments (Esposito, 2011; Esposito et al., 2017, 2018).
104. Telson, lateral bands of infuscation: **0**, present; **1**, absent (Esposito, 2011).
105. Telson, median stripe of infuscation: **0**, complete; **1**, posteriorly confined; **2**, absent (Esposito, 2011).
106. Telson, mottled infuscation: **0**, present; **1**, absent (Esposito, 2011).
107. Sternites III–VI, mottled infuscation: **0**, present; **1**, absent (Esposito, 2011).
108. Sternite V, pale surface (♂): **0**, present; **1**, absent; **?**, unknown (Esposito, 2011).
109. Sternite V, pale surface (♀): **0**, present; **1**, absent; **?**, unknown (Esposito, 2011).
110. Sternite VII, color pattern: **0**, similar to other sternites; **0**, paler than preceding sternites; **2**, darker than preceding sternites (Esposito, 2011).
111. Legs I–IV, dorsal surfaces, mottled infuscation: **0**, present; **1**, absent (Esposito, 2011).
112. Legs I–IV, ventral surfaces, mottled infuscation: **0**, present; **1**, absent (Esposito, 2011).

## APPENDIX 3

Distribution of 112 morphological characters scored for phylogenetic analysis of the arboreal Neotropical "*thorellii*" clade of *Centruroides* Marx, 1890, bark scorpions (Buthidae C.L. Koch, 1837) and outgroup species of *Centruroides* and *Heteroctenus junceus* (Herbst, 1800). Character states scored 0–5, unknown (?), or polymorphic [ ].

**Outgroup***Heteroctenus junceus*

2101131122	1120211321	0100011011	1212101013	0001112120	2000121000
0111020011	01120021??	0101021011	1011001001	1111211110	11

*Centruroides arctimanus*

1010010011	0120221221	0000010?1?	111111210?	00111???20	2121000010
0110102?10	01110000???	???1100000	1210000100	0110011110	00

*Centruroides bani*

0110021222	1120011121	0001010001	1011112000	0110011222	2112110000
0110101010	01110031??	???1101001	1[01]10000	0011001111	11201

*Centruroides exilicauda*

0100030202	1120200010	0000010111	0000200000	0010113110	2110220011
0000201010	11110130??	0111021111	1011101010	1101211110	11

*Centruroides gracilis*

1000011112	1120201321	0100111111	1212202000	0110003120	2120220011
0110201020	1102100100	0111001111	101?001011	1110011012	11

*Centruroides hentzi*

2010030122	0120200020	0000014110	1010102000	0101101112	2111010010
0111202020	00110000???	???1101011	1210000000	1101211000	01

*Centruroides infamatus*

1000031212	1120200011	0000010111	1010102000	0010111111	2110121010
0110100010	01010020???	???1001111	1210101011	1101011?12	11

*Centruroides ochraceus*

0000031202	1100211111	01000101?1	0000102000	00102????22	2110221011
0110101?21	01010100???	???1101111	1010011011	1101211110	11

*Centruroides thorelli*

0000021101	1120200000	0100010110	0101102000	0010112301	2100120011
0110201020	01011001???	???1100011	1301100010	0110000002	01

*Centruroides tuxtlae*

0100131222	1120100021	0000010111	1011102005	0110202322	2111120011
0101102010	1112010????	???1000011	1210100110	0010000012	01

**Ingroup***Centruroides berstoni*

1110010111	1000000010	00010101?0	1010012115	0110002111	2112220011
0?00202?10	01110100???	???1100000	0110000000	01110101?0	01

*Centruroides catemacoensis*

1110010222	1021200010	0001010110	1010010115	0010202111	2110020010
0110202120	00100100???	???1100000	0110000000	0111210000	01

*Centruroides chanae*

1110010111 1021200000 0001314110 1111010005 00112???12 2102220011  
0?10202120 0111010??? ???110000 0010000000 0111211010 01

*Centruroides cuauhmapan*

1110010110 1120200010 0000314110 1010012010 0111202121 2103120011  
0?10202010 01110100?? ???1100000 0010000000 0111010000 01

*Centruroides hamadryas*

1110010111 1000000010 00010101?0 1010012115 0110002111 2112220011  
0?00202?10 01110100?? ???1100000 0110000000 01110101?0 01

*Centruroides hoffmanni*

0100010111 1121000010 0000010110 1111012005 1110112110 2103220011  
0?00202020 01110100?? ???1100000 0210000010 0110211010 01

*Centruroides rileyi*

1110010110 1120200010 0000314110 1010012010 0111202121 2103120011  
0?10202010 01110100?? ???1100000 0010000000 0111010000 01

*Centruroides schmidti*

1110010111 0120200010 0101010110 1010012010 0100012122 2102220011  
0000202120 11110101?? 0111100000 0010000000 0101211010 00

*Centruroides yucatanensis*

1110010111 1120000010 0001014110 1010012105 0010012021 2103020011  
0?10201120 0111010??? ???1100000 0010000000 0110010112 01

**SCIENTIFIC PUBLICATIONS OF THE AMERICAN MUSEUM OF NATURAL HISTORY**

*AMERICAN MUSEUM NOVITATES*

*BULLETIN OF THE AMERICAN MUSEUM OF NATURAL HISTORY*

*ANTHROPOLOGICAL PAPERS OF THE AMERICAN MUSEUM OF NATURAL HISTORY*

**PUBLICATIONS COMMITTEE**

ROBERT S. VOSS, CHAIR

**BOARD OF EDITORS**

JIN MENG, PALEONTOLOGY

LORENZO PRENDINI, INVERTEBRATE ZOOLOGY

ROBERT S. VOSS, VERTEBRATE ZOOLOGY

PETER M. WHITELEY, ANTHROPOLOGY

**MANAGING EDITOR**

MARY KNIGHT

Submission procedures can be found at <http://research.amnh.org/scipubs>

All issues of *Novitates* and *Bulletin* are available on the web (<http://digilibRARY.amnh.org/dspace>). Order printed copies on the web from:

<http://shop.amnh.org/a701/shop-by-category/books/scientific-publications.html>

or via standard mail from:

American Museum of Natural History—Scientific Publications

Central Park West at 79th Street

New York, NY 10024

∞ This paper meets the requirements of ANSI/NISO Z39.48-1992 (permanence of paper).

*ON THE COVER: CENTRUROIDES BERSTONI, SP. NOV., ♂, FROM THE TYPE LOCALITY, IZABAL, RIO DULCE, HOTEL TIJAX, GUATEMALA.*